

# The Late Cretaceous San Juan Thrust System, San Juan Islands, Washington

Mark T. Brandon  
Darrel S. Cowan  
and  
Joseph A. Vance



***SPECIAL PAPER***

221

*The Late Cretaceous San Juan thrust system,  
San Juan Islands, Washington*

**Mark T. Brandon\***  
Geological Survey of Canada  
Pacific Geoscience Centre  
P.O. Box 6000  
Sidney, British Columbia V8L 4B2  
Canada

**Darrel S. Cowan and Joseph A. Vance**  
Department of Geological Sciences  
University of Washington  
Seattle, Washington 98195

---

\*Present address: Department of Geology and Geophysics, Yale University,  
P.O. Box 6666, New Haven, Connecticut 06511-8130.



***SPECIAL PAPER***

**221**

© 1988 The Geological Society of America, Inc.  
All rights reserved.

Copyright is not claimed on any material prepared  
by government employees within the scope of their  
employment.

All materials subject to this copyright and included  
in this volume may be photocopied for the noncommercial  
purpose of scientific or educational advancement.

Published by The Geological Society of America, Inc.  
3300 Penrose Place, P.O. Box 9140, Boulder, Colorado 80301

GSA Books Science Editor Campbell Craddock

Printed in U.S.A.

#### **Library of Congress Cataloging-in-Publication Data**

Brandon, M. T. (Mark Thomas)

The late Cretaceous San Juan thrust system, San Juan Islands,  
Washington / Mark T. Brandon, Darrel S. Cowan, and Joseph A. Vance.  
p. cm.—(Special paper / Geological Society of America ;  
221)

Bibliography: p.

ISBN 0-8137-2221-7

1. Thrust faults (Geology)—Washington (State)—San Juan Islands.  
2. Geology, Stratigraphic—Cretaceous I. Cowan, Darrel S., 1945–  
II. Vance, Joseph A., 1930– III. Title. IV. Series: Special  
papers (Geological Society of America) ; 221.

QE606.5.U6B73 1988

551.770979774—dc19

88-4003

CIP

**Cover Photo:** Satellite image of the San Juan Islands, provided by  
Advanced Satellite Productions, Inc., Vancouver, B.C., Canada. Late  
Cretaceous thrust faults of the San Juan–Cascades system are shown in  
yellow. Early Tertiary faults, related to accretion of a more outboard set of  
terranes, are shown in red. The northwest-striking islands visible in the west  
central part of the image correspond to broad, northwest-trending folds in  
the Naniamo Group, a syn-orogenic basin that formed peripheral to the San  
Juan–Cascades thrust system. The metropolitan areas are Vancouver  
(northeast), Victoria (west central), Bellingham (east central), and Port  
Angeles (south central).

10 9 8 7 6 5 4 3 2

# Contents

<b>Acknowledgments</b> .....	v
<b>Abstract</b> .....	1
<b>Introduction</b> .....	2
Previous work .....	2
Use of stratigraphic and tectonostratigraphic terms .....	5
Regional setting .....	5
Overview of the San Juan Islands .....	7
<b>Paleozoic and lower Mesozoic rocks of the thrust system</b> .....	11
Turtleback terrane: Paleozoic plutonic and volcanic rocks .....	11
Composition and age of the Turtleback Complex .....	11
Stratigraphy and age of the East Sound Group .....	13
Origin of the Turtleback and East Sound units .....	14
Regional correlation of the Turtleback and East Sound units .....	15
Deadman Bay terrane: Permian-Lower Jurassic chert, basalt, and limestone .....	15
Stratigraphy and age of the Deadman Bay Volcanics .....	15
Stratigraphy and age of the Orcas Chert .....	18
Origin and tectonic setting .....	19
Regional correlation .....	20
Garrison terrane: Permo-Triassic mafic schist .....	21
Composition .....	21
Age .....	21
Structural relationships .....	21
Origin and tectonic setting .....	24
Regional correlation .....	24
<b>Upper Mesozoic rocks of the thrust system</b> .....	25
Constitution Formation: Upper Mesozoic clastic sequence .....	25
Stratigraphy .....	26
Age .....	27
Provenance of clastic rocks .....	27

Origin and tectonic setting .....	27
Regional correlation .....	29
López Structural Complex: Late Cretaceous imbricate fault zone .....	29
Rock units and ages .....	29
Internal structural relations .....	31
Decatur terrane: Upper Mesozoic ophiolite, arc, and clastic sequence .....	31
Composition and age of the Fidalgo Complex .....	31
Geochemistry and tectonic setting of the Fidalgo Complex .....	33
Stratigraphic and age of the Lummi Formation .....	34
Metamorphism of Decatur rocks .....	34
Regional correlation .....	35
<b><i>External units: Mesozoic units forward of, and below, the</i></b>	
<b><i>San Juan thrust system</i></b> .....	36
Haro terrane: Upper Triassic and Jura-Cretaceous	
volcaniclastic units .....	36
Haro Formation (Upper Triassic) .....	36
Spieden Group (Upper Jurassic and Lower Cretaceous) .....	37
Nanaimo Group: Upper Cretaceous syn-orogenic clastic	
sequence .....	37
<b><i>Post-orogenic unit: The Eocene Chuckanut Formation</i></b> .....	38
<b><i>High-pressure metamorphism and its relation to thrusting</i></b> .....	38
<b><i>Terrane accretion and Late Cretaceous thrusting</i></b> .....	42
<b><i>Concluding remarks</i></b> .....	45
<b><i>Appendices</i></b>	
A. Summary of fossil ages and isotopic dates .....	47
B. Summary of geochemical analyses .....	64
<b><i>References cited</i></b> .....	78

## *Acknowledgments*

We are grateful to E. H. Brown, S. Y. Johnson, D. L. Jones, J.W.H. Monger, and R. W. Tabor for critical and helpful reviews of this paper and an earlier version; to R. L. Armstrong, R. B. Forbes, C. W. Naeser, R. A. Zimmerman, and R. E. Zartman for providing unpublished isotopic dates; and to W. R. Danner, H. Igo, D. L. Jones, M. J. Orchard, E. A. Pessagno, Jr., N. M. Savage, and W. V. Sliter for providing and clarifying various paleontological ages. We thank J. T. Whetten for giving us access to unpublished geochemical data, and D. Mogk and M. A. Dungan for microprobe analyses of Garrison amphiboles. Our study has profited from discussions with: P. R. Carroll, A. Drinkhouse Dailey, S. Y. Johnson, J. I. Garver, P. Misch, S. A. Monsen, J. E. Muller, and J. T. Whetten. Cowan and Brandon acknowledge support from the National Science Foundation (grants EAR 76-13127 and EAR 79-10827), the Society of Sigma Xi, and the Corporation Fund of the Department of Geological Sciences, University of Washington. Field accommodations were kindly provided by the University of Washington Friday Harbor Laboratories. Brandon is grateful to the National Science and Engineering Research Council of Canada for a post-doctoral fellowship at Pacific Geoscience Centre during which this manuscript was completed. We also thank the Department of Geological Sciences at the University of Washington and the Pacific Geoscience Centre for clerical and drafting support.

## ABSTRACT

The San Juan Islands expose a thick and regionally extensive sequence of Late Cretaceous thrust faults and nappes, referred to as the San Juan thrust system. This thrust system, which straddles the southeastern edge of the Wrangellia terrane of Vancouver Island, contains important information on the accretionary history of Wrangellia and other, related, far-traveled terranes. Nappes of the thrust system contain a diverse group of rocks ranging from early Paleozoic to middle Cretaceous in age. Based on contrasts in stratigraphy, metamorphism, and geochemistry, we identify five terranes within, and peripheral to, the thrust system. These terranes were widely separated from each other, and also from Wrangellia, until the Late Jurassic: (1) the Haro terrane, an Upper Triassic arc-volcanic sequence; (2) the Turtleback terrane, a Paleozoic arc-plutonic and volcanic unit; (3) the Deadman Bay terrane, a Permian to Lower Jurassic oceanic-island sequence containing Tethyan-fusulinid limestones; (4) the Garrison terrane, a Permo-Triassic, high-pressure metamorphic unit; and (5) the Decatur terrane, a Middle to Upper Jurassic ophiolite and superimposed arc-volcanic sequence. Thick Jura-Cretaceous clastic units are linked to these older San Juan terranes and to Wrangellia, either as directly overlapping units or by the presence of clastic material derived from the terranes. The voluminous amount of clastic material in these Jura-Cretaceous units requires a large, subaerially exposed source region. We infer that this source region was a continent-like landmass, presumably part of continental America (North or Central?).

Late Cretaceous thrusting juxtaposed these older terranes and disrupted the Jura-Cretaceous clastic units. Very low-temperature high-pressure metamorphic assemblages, including lawsonite and aragonite, were developed during this event, and formed as a direct result of thrust-related burial to depths of about 20 km. Stratigraphic evidence indicates that structural burial, metamorphism, and subsequent uplift back to the surface all occurred during a very short time interval, between 100 and 84 Ma, with average vertical transport rates of about 2 km/m.y. The Upper Cretaceous Nanaimo Group, a syn-orogenic basin to the north of the San Juan system, contains cobbles of metamorphosed rocks from the San Juan nappes, and therefore records the erosional unroofing of the thrust system.

We envision the San Juan system to be a short-lived collision-like orogen, rather than a long-lived subduction complex. This conclusion is based primarily on the diversity of rock units involved and the punctuated nature of the deformation. What remains unclear is the cause of this orogenic deformation. The clastic-rich Jura-Cretaceous units imply that Wrangellia and the older San Juan terranes were adjacent to or part of the American continent by latest Jurassic time. Moreover, there is no evidence for the arrival and collision of an exotic terrane during the Cretaceous. As a result, the San Juan system is considered to be the product of distributed deformation within an active continental margin. Two tectonic settings are examined: (1) a convergent margin where orogenic deformation is driven by greater coupling across the subduction boundary resulting in extensive shortening within the overriding continental plate, and (2) an irregular transform margin where terranes and overlap sequences are transported northward within a system of coast-parallel faults. In the latter case, orogenic shortening occurs when these fault slices collide with a reentrant in the margin, perhaps like the modern collision of the Yakutat block in the Gulf of Alaska.

## INTRODUCTION

A ten-km-thick sequence of nappes and imbricate fault zone is exposed in the San Juan Islands (Fig. 1). These nappes and thrust faults, which we refer to as the San Juan thrust system, were formed during the Late Cretaceous, and involve a wide variety of rock units ranging in age from early Paleozoic to middle Cretaceous. Early workers considered these units to represent an internally faulted, but otherwise continuous stratigraphic sequence (Danner, 1966; Vance, 1975). In contrast, Whetten and others (1978) argued that the San Juan Islands are composed of a series of disparate terranes. Their study, based on a reconnaissance collection of fossils and isotopic dates, showed that many of the units used by previous workers were composite, and several overlapped in age. Furthermore, important differences in stratigraphy among coeval units suggested that some were far traveled. This conclusion is important in light of the fact that the San Juan thrust system lies along the southeastern edge of Wrangellia, another displaced terrane that underlies much of Vancouver Island (Fig. 1).

Fundamental problems in the San Juan Islands concern the original palinspastic relations among units within the thrust system, and the process by which these units were juxtaposed. For example, does each fault-bounded unit constitute a separate exotic terrane, unrelated to adjacent units, or were some of the units already assembled prior to thrusting? Whetten (1975) and Whetten and others (1978, 1980) suggested that the San Juan Islands were the locus of thousands of kilometers of Mesozoic plate subduction, which swept together a wide variety of exotic and unrelated terranes. They envisioned that the thrust system represented a subduction melange, similar in some respects to the Franciscan Complex of California. As a consequence, they subdivided San Juan geology into a series of accretionary packages, each distinguished by a distinctive association of rock types and ages, or a characteristic structural style.

A closer comparison with the Franciscan Complex shows several problems with this interpretation. First, an important characteristic of the San Juan thrust system is that it contains a wide variety of Paleozoic and Mesozoic units, with the oldest rocks occurring in the lowest thrust sheets. In contrast, most of the Franciscan consists of a restricted group of Upper Jurassic to lower Tertiary units, which are structurally stacked with the youngest rocks at the bottom. Second, the San Juan thrust system was formed during a very short time interval, probably no longer than 20 m.y., whereas the Franciscan was slowly accreted over a 100-m.y. interval, from Late Jurassic to early Tertiary. And third, Upper Jurassic–Lower Cretaceous clastic units in the San Juan Islands, Vancouver Island, and North Cascades indicate that older Mesozoic–Paleozoic terranes were in continental margin settings prior to Late Cretaceous thrusting. As a result, thrusting cannot be easily related to the successive arrival of these terranes as exotic elements at a convergent margin.

Based on our work, we interpret San Juan thrusting to have dismembered and telescoped a continental margin that was un-

derlain by an older assemblage of terranes and associated overlap sequences. We show that the thrust system resulted from a short-lived event, perhaps collisional in nature, rather than from long-term steady-state subduction. Instead of mapping presumably accretionary, lithotectonic packages like Whetten and others (1978) did, we have focused on the pre-thrusting stratigraphy of the San Juans in order to reconstruct terranes and clastic linking sequences as they existed prior to Late Cretaceous time. Our approach is similar to that used in stratigraphic studies of on-land thrust belts. Since stratigraphic continuity cannot be assumed in poorly exposed areas, we have mostly concentrated on coastal exposures, which provide long and relatively continuous sections (Fig. 2). Our mapping in these areas has allowed us to determine the larger structural framework of the thrust system, and also to study local stratigraphic relationships in regions where units are relatively undeformed.

In this paper, we review the stratigraphy and structure of the San Juan thrust system, especially in light of our more recent mapping. We also draw heavily on abundant fossil ages and isotopic dates, and on numerous geochemical analyses of volcanic and plutonic rocks. These data, many of which are new or unpublished, are compiled in Appendices A and B. We use this information to identify terranes in the San Juan Islands, and to compare these terranes with others in adjacent areas, such as the North Cascade Mountains and Vancouver Island (Fig. 1). We conclude with a discussion on the tectonic setting in which the San Juan thrust system formed. Our results are germane to the Cordillera-wide problem of how terranes are identified, where they originate, and how they are emplaced.

### *Previous work*

The San Juan Islands were originally mapped by McLellan (1927). Danner (1957, 1966, 1977) redefined several units on the basis of his studies of limestone deposits and their fossils. Vance (1968) first recognized the widespread presence of aragonite in San Juan rocks and described their low-grade metamorphism. Mulcahey (1975) mapped Fidalgo and Guemes Islands. Vance (1975, 1977) remapped Orcas Island and northern San Juan Island, and identified a major system of Mesozoic thrusts. Whetten (1975) remapped the southeastern San Juan Islands. Glassley and others (1976) discovered that metamorphic lawsonite is present in many San Juan rocks. Whetten and others (1978) introduced the concept that the San Juan Islands include several, unrelated, tectonically juxtaposed terranes. They also published new fossil ages and isotopic dates, which established a Mesozoic age for many of the rock units in the archipelago. Other recent contributions to the geology of the islands include: the stratigraphy of the Nanaimo Group (Ward, 1978; Johnson, 1978; Ward and Stanley, 1982; Pacht, 1984); the stratigraphy of the Spieden Group and Haro Formation (Johnson, 1978, 1981); and mapping of Lopez Island (Cowan and Miller, 1981), southern San Juan Island (Brandon, 1980), Lummi Island (Carroll, 1980), and Fidalgo Island (Brown, 1977; Gusey, 1978; Brown and others, 1979).

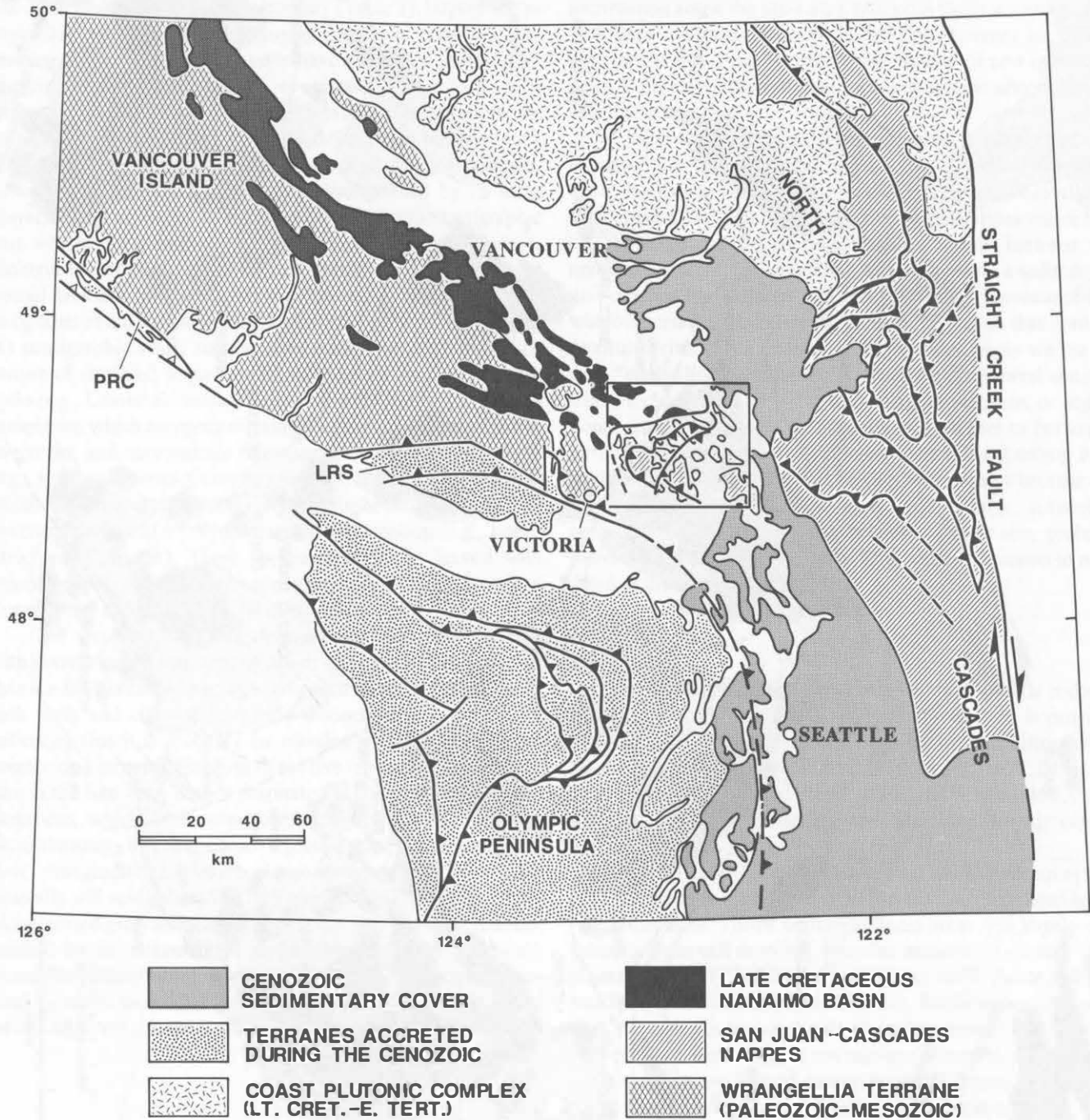
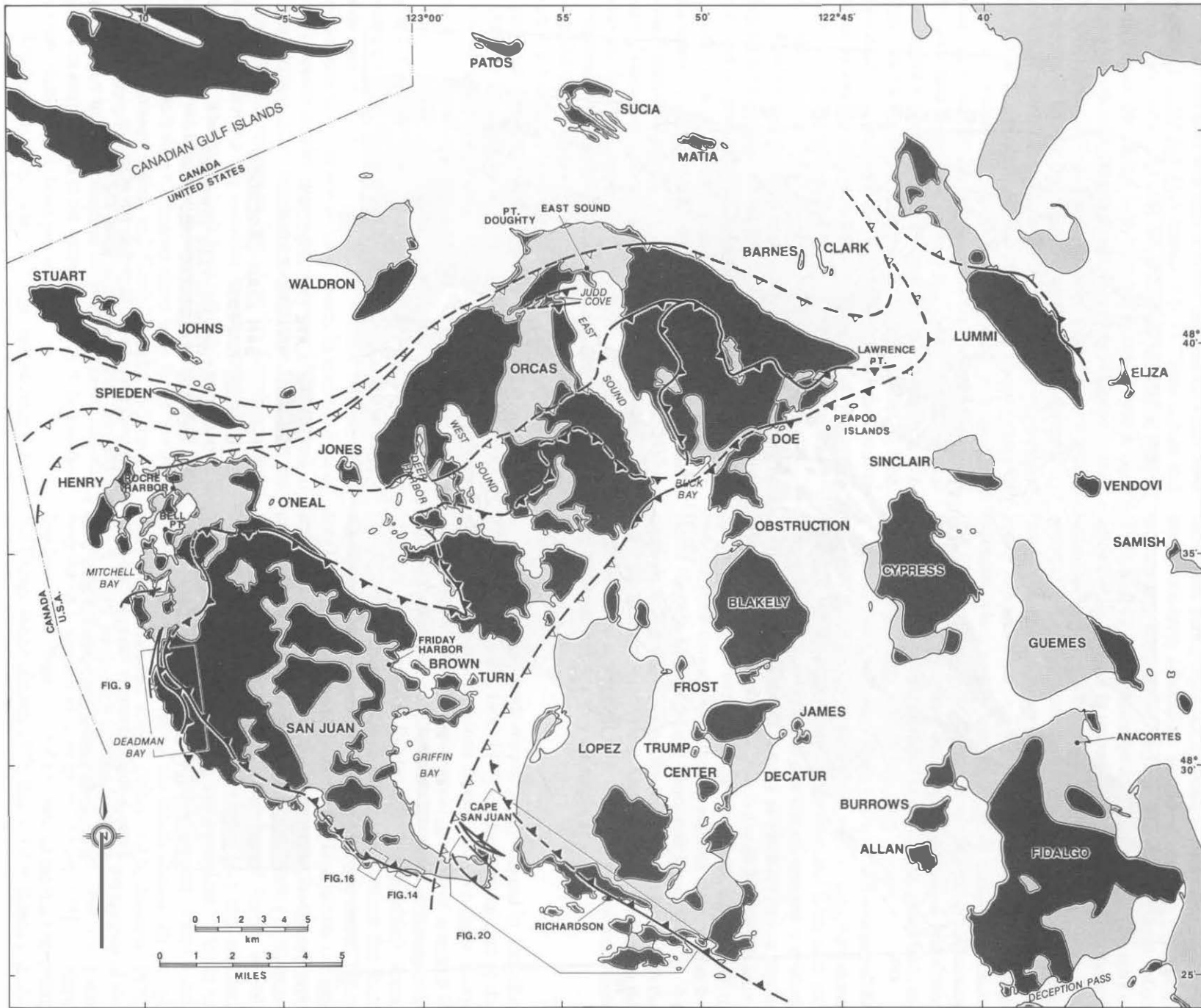


Figure 1. Regional tectonic setting of the San Juan Islands (enclosed in box). The geology east of the Straight Creek fault is not shown. PRC = Pacific Rim Complex. LRS = Leech River schist. The box indicates the location of the maps in Figures 2 and 3.



### *Use of stratigraphic and tectonostratigraphic terms*

During the last 60 years, stratigraphic nomenclature in the San Juan Islands has evolved tortuously (Table 1), largely due to improving age control and changing geological concepts. Depending on the authors, some units have been designated as formations, structural complexes, or terranes. Therefore, it is important to clarify the stratigraphic and tectonostratigraphic terminology used in this paper. We differentiate between rock units and tectonostratigraphic units. A rock unit is the fundamental unit of geologic mapping and is distinguished by its lithic characteristics and age. On the other hand, a tectonostratigraphic unit, which may consist of one or more mappable rock units, is distinguished not only by its internal stratigraphy, but also by its overall tectonic history (Jones and others, 1983). Rock units recognized in the San Juan Islands consist of three different types: (1) stratigraphic units, such as a formation or a group, which consist of stratified sequences of sedimentary and/or volcanic rocks (e.g., Lummi Formation or East Sound Group); (2) igneous complexes, which comprise related groups of intrusive and extrusive rocks, and may include minor amounts of other rock types (e.g., Fidalgo Igneous Complex); and (3) structural complexes, which are tectonic assemblages distinguished on the basis of structural style and a common age of deformation (e.g., Lopez Structural Complex). These designations are in accord with recommended stratigraphic nomenclature (North American Commission of Stratigraphic Nomenclature, 1983).

The tectonostratigraphic terminology used here follows, with several exceptions, that of Jones and others (1983). A terrane is a fault-bounded package composed of one or more related rock units and characterized by a distinctive geologic history indicating that it is probably far traveled with respect to other neighboring terranes. Four out of the five terranes that we recognize in the San Juan Islands originated as coherent stratigraphic sequences, which were subsequently disrupted by Late Cretaceous thrusting. We have chosen to define these terranes based on their stratigraphic attributes, since stratigraphic relations are generally still resolvable. The fifth terrane consists of thoroughly recrystallized greenschist and amphibolite, and therefore is distinguished by its metamorphic rather than stratigraphic history. Jones and others (1983) would probably define the Lopez Structural Complex as another terrane (i.e., a disrupted terrane) based on its distinctive structural style. We have decided to use the term

“structural complex” because our work indicates that the Lopez represents a thick imbricate fault zone that formed during San Juan thrusting. Thus, the Lopez does not provide any useful information about the pre-Late Cretaceous tectonic history of the rock units within it. Four of the San Juan terranes are defined here for the first time. To reduce the number of new names, we employ the convention of naming a new terrane after the oldest unit that it contains.

Clastic sedimentary sequences represent another important tectonostratigraphic element because they provide information about the timing of terrane amalgamation and continental collision. Jones and others (1983) describe two situations where clastic sequences can be used to establish a link between two unrelated terranes: (1) an overlap sequence where a sedimentary unit overlies two adjacent terranes, and (2) a provenance link where a terrane is overlain by a clastic sequence that contains detritus derived from another terrane. In this paper we use the term “clastic linking sequence” to describe the general situation where a clastic unit, by virtue of overlap, provenance, or depositional setting, indicates a tie between two terranes or between a terrane and a continental land mass. Depositional setting is included in this list of diagnostic linking relationships because certain types of marine clastic units require huge, subaerially exposed source regions, which because of their size, probably represent continental landmasses. This point is discussed in more detail at the end of the paper.

### *Regional setting*

Much of the significance of the San Juan Islands is due to their regional tectonic setting. A brief introduction is provided here. For a more regional discussion of the tectonic history of the Pacific Northwest, see: Dickinson, 1976; Muller, 1977; Davis and others, 1978; Monger and others, 1982; and Saleeby, 1983.

The geology surrounding the San Juan Islands can be broken into five main components (Fig. 1):

(1) San Juan–Cascades nappes: a Late Cretaceous system of thrust faults and nappes exposed in the San Juan Islands and North Cascades. Thrust faulting in these areas was largely contemporaneous and involved a similar assemblage of rock units (Misch, 1966, 1977; Whetten and others, 1978; Vance and others, 1980; Brandon and Cowan, 1985). Furthermore, nappes in both the San Juans and North Cascades contain a distinctive, high-pressure, metamorphic assemblage (lawsonite, prehnite, and aragonite) that was formed during thrusting (Vance, 1968; Misch, 1971; Glassley and others, 1976; Brown and others, 1981).

(2) Wrangellia: a large allochthonous terrane (Jones and others, 1977; Yole and Irving, 1980) that underlies most of Vancouver Island and parts of southern Alaska. On Vancouver Island, this terrane is characterized by a coherent Paleozoic to Lower Jurassic stratigraphic sequence, dominantly volcanic in nature, which is intruded by numerous Early to Middle Jurassic plutons (Muller, 1977). In contrast to the San Juan Islands and North Cascades, Late Cretaceous thrusts and high-pressure

---

Figure 2. Location map and distribution of bedrock exposure in the San Juan Islands (see Fig. 1 for location). The heavy and light patterns indicate areas with reasonably continuous bedrock exposure and areas covered by glacial sediments. Boxes show the outlines of detailed geologic maps presented in Figures 9, 14, 16, and 20. The names of islands are in large type and location names in smaller type. The distribution of bedrock was adapted from the map in Vance (1975) and Whetten (1975).

TABLE 1. EVOLUTION OF STRATIGRAPHIC NOMENCLATURE FOR ROCK UNITS IN THE SAN JUAN THRUST SYSTEM

McLellan (1924, 1927)	Danner (1966)	Vance (1975, 1977); Brown (1977)	Whetten and others (1978)	This paper Stratigraphic Names	Terrane Names
Turtleback Complex* (Jurassic intrusive)	Turtleback Complex* (pre-Devonian)	Turtleback Complex (early Paleozoic)	Roche Harbor and Eagle Cove terranes*	Turtleback Complex (early Paleozoic)	Turtleback terrane
Orcas Chert* and Leech River Group* (late Paleozoic)	Raccoon Pt. and President Channel units  Garrison Schist (pre-Devonian?)	Pennsylvanian and Devonian volcanics  Garrison Schist (Permian meta- morphism)		East Sound Group (late Paleozoic)	Garrison terrane
Eagle Cliff Porphyrite* (Jurassic)	Trafton sequence* (Permian)	Permian volcanics (Permian)		Garrison Schist (Permian-?Triassic metamorphic age)	Deadman Bay terrane
Orcas Chert* (Dev.-Miss.)		Orcas Chert (Triassic-E. Jurassic)	Deadman Bay Volcanics (Permian-Triassic)		
Leech River Group* (Penn.-Perm.)		Constitution Fm. (mid-Mesozoic?)	Friday Harbor terrane (L. Jur.-E. Cretaceous)	Constitution Formation (Jurassic-E. Cretaceous)	clastic link- ing sequence
		Lummi Formation (Cretaceous?)	López terrane (L. Jur.-middle Cret.)	Lopez Structural Complex (L. Jur.-middle Cret.)	imbricate fault zone
			Decatur and Sinclair terranes (M. Jur.-E. Cretaceous)	Lummi Formation (L. Jur.-E. Cret)	Decatur terrane
Eagle Cliff Porphyrite* Turtleback Complex* and Fidalgo Formation (Jurassic igneous rocks)	Turtleback Complex* (pre-Devonian)	Fidalgo ophiolite (M. Jurassic)	Fidalgo ophiolite (M. Jurassic—part of the Decatur terrane)	Fidalgo Igneous Complex (M. and L. Jurassic)	

Note: The ages shown above are those assigned by the various authors. Hyphenated age terms indicate the age range of the unit; e.g., Triassic-Permian indicates a Triassic and Permian age.

\*Composite units that were subdivided and redefined by later authors.

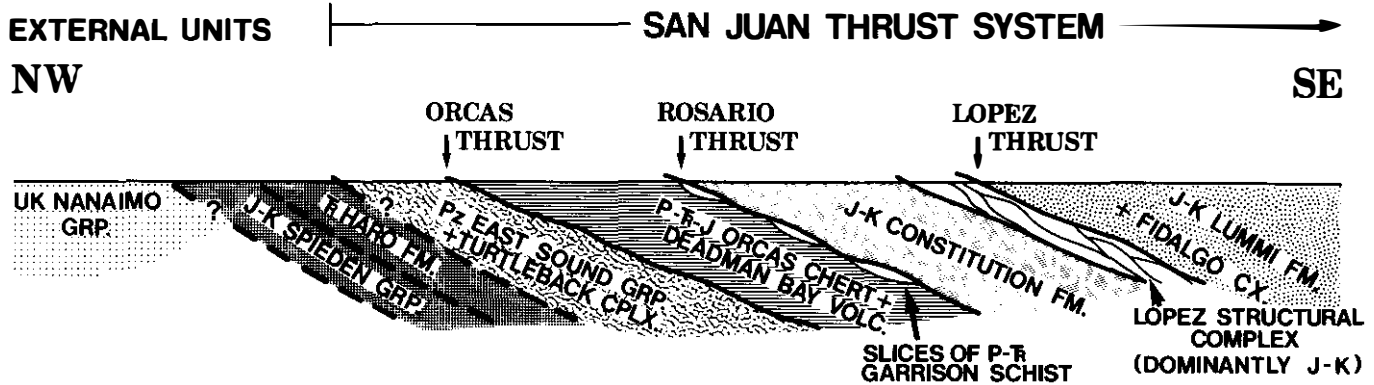


Figure 4. Schematic cross-section showing the general stacking order of nappes in the San Juan system. Patterns are the same as those used in Figure 3.

metamorphic assemblages are notably absent. Instead, the main structures are broad folds and moderate to steep faults. Since they involve Upper Cretaceous strata, these structures are, at least in part, Tertiary in age.

(3) Coast Plutonic Complex: a regionally extensive granitic complex that consists dominantly of Late Cretaceous and early Tertiary plutons (Tipper and others, 1981; Armstrong, 1987). Older plutonic rocks are also present, as well as screens and pendants of country rocks that correlate, at least in part, with the Wrangellia terrane and nappes of the North Cascades thrust system (Misch, 1966, 1977; Woodsworth, 1979; Tipper and others, 1981).

(4) Nanaimo Basin: a thick syn-orogenic sequence of Upper Cretaceous marine and nonmarine clastic strata that unconformably overlie Wrangellia. Provenance studies (Ward and Stanley, 1982; Pacht, 1984; Vance, 1975; Brandon, 1982) indicate that the source for Nanaimo conglomerates and sandstones included Wrangellia, the San Juan and Cascades nappes, and older rocks of the Coast Plutonic Complex. Thus, the Nanaimo Group represents a linking sequence that ties all of these various tectonic elements together by the Late Cretaceous. This relation is important because paleomagnetic data (Irving and others, 1985a, b) indicate that Wrangellia, the Coast Plutonic Complex, and by association, the San Juan and Cascades nappes were still at low latitudes during the Late Cretaceous, about 2,400 km south of their expected North American position.

(5) Terranes accreted during the Cenozoic: Cenozoic and minor Mesozoic rocks that were accreted or displaced during the Cenozoic. These terranes include Eocene basalts of the Olympic Peninsula and southern Vancouver Island, an Eocene and younger subduction complex exposed on the Olympic Peninsula (Tabor and Cady, 1978; Clowes and others, 1987; Massey, 1986), and displaced Mesozoic rocks of the Pacific Rim Complex (PRC) and the Leech River Schist (LRS) (Fairchild and Cowan, 1982; Rusmore and Cowan, 1985; Brandon, 1985). During earli-

est Tertiary time, a major transform fault apparently truncated and removed the western continuation of Wrangellia and the San Juan-Cascades nappes (Brandon, 1985; Johnson, 1984c). Mesozoic rocks, such as the Pacific Rim Complex and at least part of the Leech River Schist, were displaced 100 to 200 km northward along this transform fault (Brandon, 1985). Subsequent Cenozoic accretion occurred against this newly truncated margin. The point to be made here is that much of the Mesozoic geology that lay southwest of the San Juan Islands is now missing.

#### Overview of the San Juan Islands

The overall structure of the San Juan Islands (Fig. 3, in pocket inside back cover) is a folded sequence of sub-parallel thrust faults. The folds, which may be Tertiary in age, plunge gently to the southeast and have limbs that dip as steeply as 45° to 60°. This structural sequence can be divided into two main components (Table 2; Figs. 4 and 5): (1) the San Juan thrust system, consisting of those rocks that were affected by Late Cretaceous thrusting and high-pressure metamorphism; and (2) the external units, comprising all those units that are in front of and below the San Juan thrust system. The external units, which include the Upper Cretaceous Nanaimo Group and older Mesozoic rocks of the Spieden Group and Haro Formation, may have been affected by Late Cretaceous thrusting but were never subjected to high-pressure metamorphic conditions. The rationale behind this division is that the high-pressure metamorphic assemblages (lawsonite-prehnite-aragonite) that characterize the San Juan thrust system can be shown to have formed as a direct result of deep structural burial during thrusting (discussed below under the heading "High-pressure metamorphism and its relation to thrusting"). Therefore, the juxtaposition of the external units with the San Juan thrust system must have occurred in a structurally shallow setting, and probably postdated the more deeply seated San Juan thrusting.

TABLE 2. GEOLOGIC UNITS IN THE SAN JUAN ISLANDS

Name of Unit	Age	Lithologic description
<b>Post Orogenic Unit</b>		
Chuckanut Formation	Eocene	Nonmarine sandstone and conglomerate
<b>External Units: units forward of, and below, the San Juan thrust system</b>		
<b>Syn-Orogenic Clastic Sequence</b>		
Nanimo Group	Lt. Cretaceous	Basinal sequence containing marine and nonmarine sandstone, conglomerate, and shale.
<b>Haro Terrane</b> Spieden Group	Lt. Jurassic and E. Cretaceous	Marine sandstone and conglomerate derived from an arc-volcanic source.
Haro Formation	Lt. Triassic (Carnian or or Norian)	Marine volcanoclastic sandstone and conglomerate with minor silicic tuff and shelly interbeds.
<b>San Juan Thrust System: units shown in their relative structural position</b>		
<b>Decatur Terrane</b> Lummi Formation	latest Jurassic and E. Cretaceous	Clastic marine sequence overlying the Fidalgo Complex.
Fidalgo Igneous	M. and Lt. Jurassic	An ophiolite with a younger superimposed volcanic arc.
<b>Imbricate Fault Zone</b> Lopez Structural Complex	Lt. Cretaceous deformational age	An imbricate fault zone containing a variety of fault slices, including Jura-Cretaceous sandstone, pebbly mudstone, pillow lava, and chert; mid-Cretaceous pillow basalt and rare Turtleback tonalite.
<b>Clastic Linking Sequence</b> Constitution Formation	Jurassic or E. Cretaceous.	A clastic sequence containing massive volcanoclastic sandstone, with interbedded mudstone, ribbon chert, pillow lava, and green tuff.
<b>Garrison Terrane</b> Garrison Schist	Permian to E. Triassic metamorphism	High-pressure metamorphic rocks consisting of mafic schist with minor quartz-mica schist. Ranges from greenschist to albite-epidote amphibolite facies. Occurs only in small fault slices along the Rosario thrust.
<b>Deadman Bay Terrane</b> Orcas Chert	Triassic and E. Jurassic	Ribbon chert and minor pillow basalt and limestone. Inferred to be stratigraphically related to the Deadman Bay Volcanics. Locally imbricated with slices of Turtleback Complex.
Deadman Bay Volcanics	E. Permian to Triassic	Pillow basalt with minor interbedded Tethyan-fusulinid limestone and ribbon chert.
<b>Turtleback Terrane</b> East Sound Group	E. Devonian to E. Permian	An arc-volcanic sequence with minor interbedded limestone. Fusulinids from these limestones are non-Tethyan.
Turtleback Igneous Complex	probably Cambrian	A plutonic complex consisting of tonalite and subordinate gabbro. Inferred to be basement for the East Sound Group.

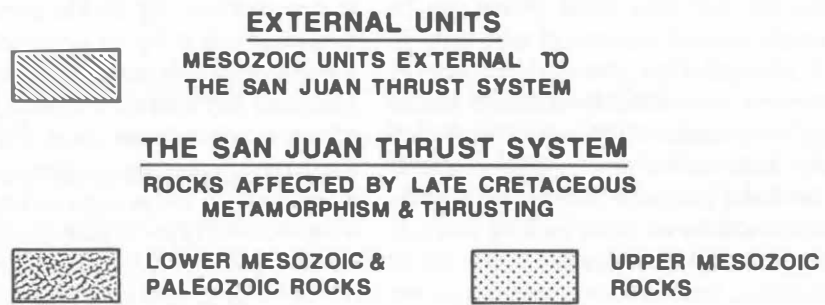
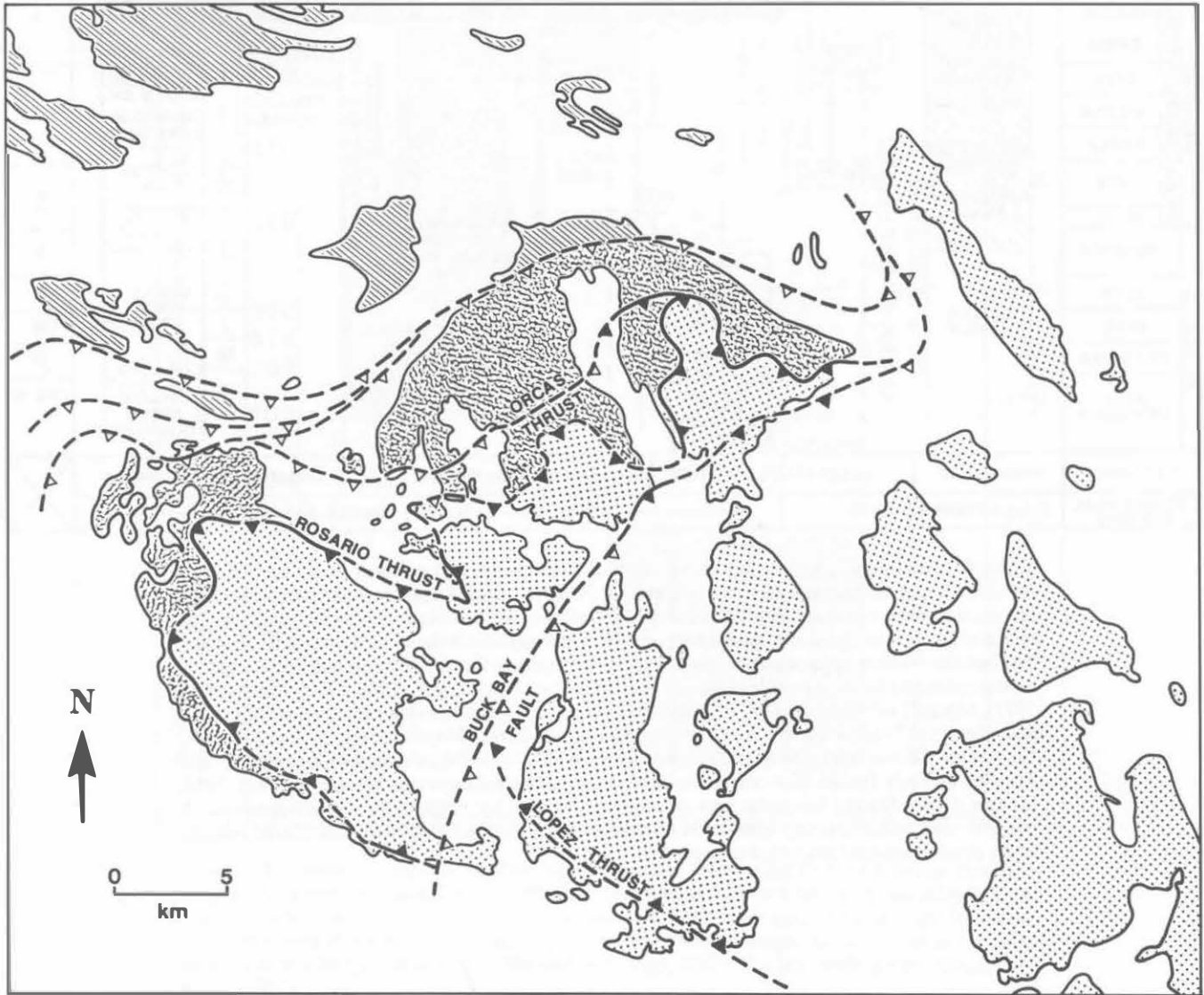


Figure 5. Major structural divisions in the San Juan Islands.



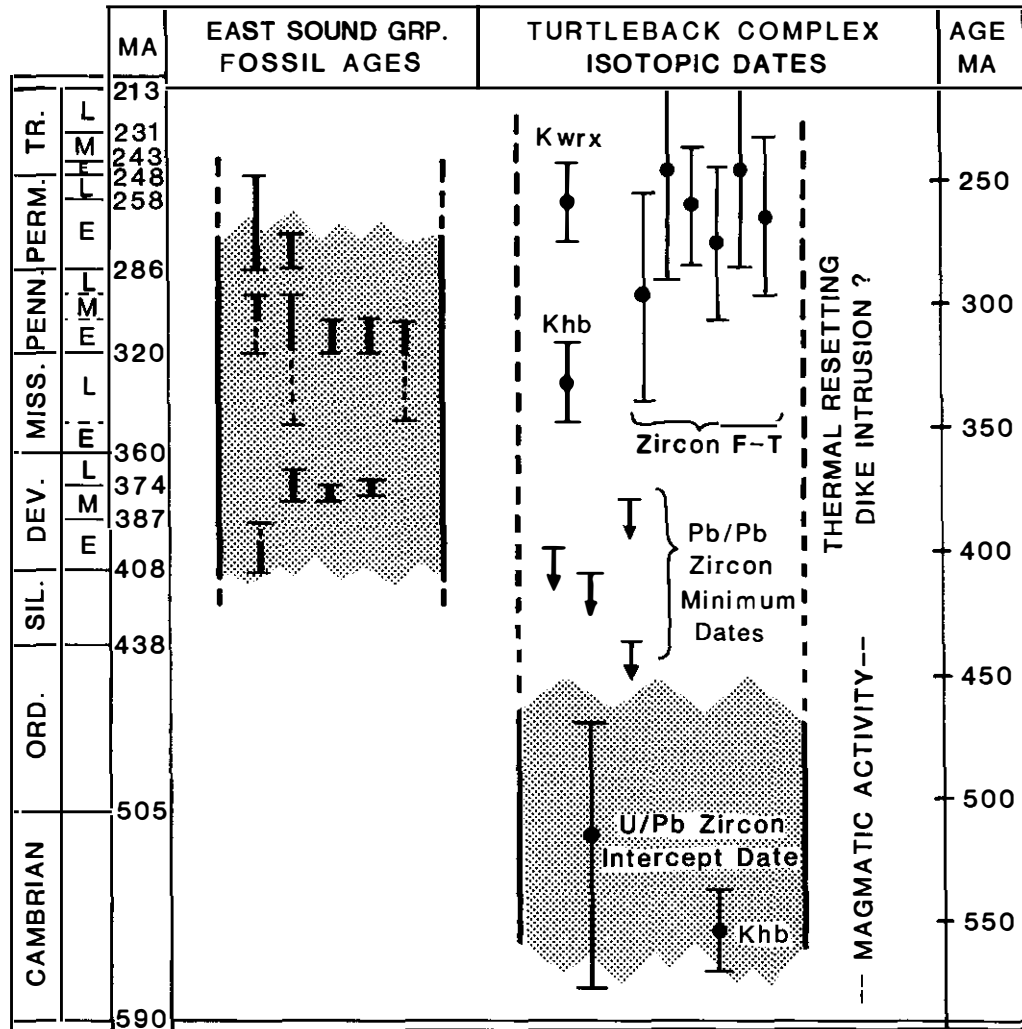


Figure 7. Stratigraphic compilation of fossil ages and isotopic dates for the Turtleback terrane. See Table A-1 and A-2 for original data. Isotopic dates are abbreviated as follows: Khb = K-Ar hornblende, KwrX = K-Ar whole rock, F-T = fission-track. These dates are shown with error brackets at the 95 percent confidence limit. Brackets for fossil ages indicate their possible age range. All isotopic dates are calculated using new decay constants (e.g., Harland and others, 1982). The time scale is from Harland and others (1982).

**PALEOZOIC AND LOWER MESOZOIC ROCKS OF THE THRUST SYSTEM**

*Turtleback terrane: Paleozoic plutonic and volcanic rocks*

The Turtleback terrane (new name) consists of an early Paleozoic plutonic suite called the Turtleback Complex and an upper Paleozoic arc-volcanic sequence called the East Sound Group (new name) (Fig. 6). This terrane occupies the structurally lowest position within the San Juan thrust system and is mostly restricted to a wide outcrop belt on northern Orcas Island and on several smaller islands to the southwest (Fig. 3). Outside this belt, small thrust slices of Turtleback plutonic rocks are also locally present in structurally higher positions within the Deadman Bay

terrane and the Lopez Structural Complex (Fig. 3). Isotopic dates indicate that the Turtleback Complex is probably largely early Paleozoic in age, while fossils from the East Sound Group indicate a late Paleozoic age (Fig. 7). In most places, these two units are now found interleaved as thrust slices. Evidence presented below suggests that the East Sound Group was originally deposited on the Turtleback Complex.

**Composition and age of the Turtleback Complex.** The Turtleback Complex is a heterogeneous plutonic suite consisting of an older gabbroic phase and a younger, cross-cutting, tonalitic phase (Table 3; plutonic rock names are according to IUGS [International Union of Geological Sciences] classification: Streckeisen, 1973). These plutonic rocks are in turn cut by basal-

TABLE 3. SUMMARY OF GEOCHEMICAL DATA FOR THE TURTLEBACK, DEADMAN BAY, AND GARRISON TERRANES

Rock unit	Interpreted tectonic setting†	SiO <sub>2</sub> %	TiO <sub>2</sub> %	Ti/V	Y/Nb	Zr (ppm)	Cr (ppm)	REE pattern‡
<b>Turtleback Terrane</b>								
Turtleback gabbroic phase	volcanic arc(?)	46.2 [1]	0.44 [1]	n.d.	n.d.	n.d.	n.d.	n.d.
Turtleback tonalitic phase	mature(?) volcanic arc	67.9 [5] (57.4-74.3)	0.76 [5] (0.29-1.95)	n.d.	n.d.	n.d.	8 [4] (2-13)	moderately LREE enriched, negative Eu anomaly [4]
East Sound Group andesite and dacite	mature(?) volcanic arc	64.2 [3] (61.3-68.3)	0.82 [3] (0.55-0.97)	n.d.	n.d.	n.d.	24 [2] (14-35)	slightly LREE enriched, negative Eu anomaly [2]
<b>Deadman Terrane</b>								
Orcas-Deadman Bay pillow basalts	oceanic-island basalt	51.8 [7] (48.7-55.7)	2.23 [7] (1.05-2.74)	69 [4] (53-84)	0.97 [6] (0.49-1.94)	239 [6] (150-352)	159 [9] (4-329)	strongly LREE enriched [9]
<b>Garrison Terrane</b>								
Garrison Schist meta-basalts	ocean-floor basalts	49.8 [6] (47.3-51.9)	1.90 [6] (1.35-2.23)	34 [6] (22-52)	6.6 [6] (1.4-13.8)	112 [6] (58-166)	416 [6] (133-803)	n.d.

Note: The data format is: mean [number of analyses]; (min.-max.); n.d. = not determined. All elements and oxides are relative to a volatile-free basis.

See Appendix B for total analyses and description of sample locations.

†See Table 4.

‡REE (rare earth element) patterns normalized to chondritic abundances; number of analyses in brackets; Eu = Europium; LREE = light REE.

tic to silicic dikes, which for reasons discussed below, are interpreted to be feeders for the East Sound Group.

McLellan (1927) originally defined the Turtleback Complex to include all plutonic rocks of the San Juan Islands. Further work (Mattinson, 1972; Whetten and others, 1978) has shown that McLellan's Turtleback Complex included both early Paleozoic and Jurassic plutonic rocks. We follow Whetten and others (1978) and restrict the name Turtleback Complex to the early Paleozoic plutonic rocks, which are mostly exposed on Orcas Island. The type area of the Turtleback is the Turtleback Range on western Orcas Island.

The intrusive history and age of the Turtleback Complex have been difficult to resolve, in part due to a widely developed static metamorphic event (Vance, 1975), which apparently reset many of the isotopic dates from the unit. This event, which culminated in upper greenschist and lower amphibolite conditions, affected all of the plutonic rocks of the Turtleback Complex and also some of the younger, cross-cutting dikes. Zircon fission-track dates and one whole-rock K-Ar date (Fig. 7; T4b, T5b, T8-10, and T7 in Table A-1) indicate that the Turtleback cooled during the Permian, presumably after being heated by a late Paleozoic thermal event.

We attribute this episode of static metamorphism and isotopic resetting to the emplacement of dike swarms in the Turtleback. These dikes are considered to be feeders for the volcanic rocks in the East Sound Group, based on the fact that the East Sound contains numerous dikes of similar composition. Furthermore, the Early Permian cessation of East Sound volcanism correlates well with Permian cooling of the Turtleback.

The older, gabbroic phase of the Turtleback Complex has been dated at two localities. A gabbro pegmatite yielded a K-Ar hornblende date of  $554 \pm 16$  Ma (T1 in Table A-1), which may represent its intrusive age. At the second locality, uraltic hornblende from an altered gabbro gave a younger K-Ar date of  $332 \pm 16$  Ma (T2 in Table A-1), which may have been partially reset during later static metamorphism.

The younger, tonalitic phase of the Turtleback Complex has been dated at four localities (T3-6 in Table A-1), all of which have yielded highly discordant dates (Mattinson, 1972; Whetten and others, 1978).  $^{207}\text{Pb}/^{206}\text{Pb}$  dates indicate a minimum age of Devonian (Fig. 7). When plotted on a U/Pb concordia diagram (Fig. 8), these discordant dates display a good linear array. Intercept dates indicate an intrusive age of  $507^{+60}_{-41}$  Ma with an episode of lead-loss at  $241^{+29}_{-41}$  Ma, perhaps related to late Paleozoic static metamorphism. Whetten and others (1978) and Mattinson (1972) suggested a younger intrusive age (460 to 471 Ma), but their interpretations were based on fewer U/Pb dates. Furthermore, they did not recognize the age and extent of Turtleback metamorphism. It is important to note that all of these interpretations of the U/Pb dates assume that the Turtleback tonalite represents a single coeval phase, even though the dated localities are widely separated and occur at different structural levels. More detailed dating of individual plutonic bodies is needed to better define the age of these intrusions.

**Stratigraphy and age of the East Sound Group.** Danner (1966, 1977) and Vance (1975) considered all upper Paleozoic rocks in the San Juan Islands to represent parts of a once-continuous stratigraphic sequence. Based on new fossil ages and further field work, we now recognize two unrelated upper Paleozoic units: (1) the East Sound Group, newly named here, and (2) the Orcas-Deadman Bay sequence. These two units are lithologically distinct and occur in different structural positions. The East Sound Group, which is Devonian to Early Permian in age, consists chiefly of intermediate arc-volcanic rocks and limestone, with little to no ribbon chert. Fusulinids in the limestones represent a cosmopolitan fauna, similar to that found in terranes farther east in the Cordillera (eastern assemblage in Monger and Ross, 1971). In contrast, the Orcas-Deadman Bay sequence ranges from Early Permian to Early Jurassic in age and consists of ribbon chert, basalt, and minor limestone. The fusulinid fauna in these limestones is Tethyan (Danner, 1966, 1977), a term that refers to Permian fusulinids that apparently were endemic to the paleo-Tethys seaway (Ross, 1967, 1979).

Another distinction is that the East Sound Group and Orcas-Deadman Bay sequence occur in different structural positions and are commonly separated from each other by fault slices of Turtleback Complex (Fig. 3). The only place where they occur in close proximity is in the Double Hill area on Orcas Island (located 1 km west of the town of East Sound), which has been described in detail by Danner (1966, p. 151-158). Unfortunately, exposures are poor in that area and are limited to several limestone quarries designated by Danner as Double Hill #1 through #4. Based on rock associations and fossils ages, we would place Danner's Double Hill #1 and #3 in the East Sound Group (E9 and E12 in Table A-2). Double Hill #4 (D1 in Table A-3), which lies about 300 m to the east of the other two quarries, is assigned to the Orcas-Deadman Bay sequence because limestone there has yielded Early Permian Tethyan fusulinids and is closely associated with ribbon chert.

Danner (1966) suggested that the Double Hill quarries exposed different parts of a single stratigraphic sequence. We, however, consider the East Sound Group and Orcas-Deadman Bay sequence to represent two unrelated terranes, each of which contains a different stratigraphy and fusulinid fauna. If our assignments are correct, then these two units are separated by a fault at Double Hill, which is consistent with the presence of numerous imbricate faults about half a kilometer to the south along the coast at the head of East Sound (Fig. 3).

We introduce the new name East Sound Group (after the town of East Sound) to distinguish this unit from the Orcas-Deadman Bay sequence. The unit is mainly exposed on Orcas Island, and also occurs on several small islands to the west (Danner, 1966, 1977; Vance, 1975, 1977). Following Danner (1957, 1966), the northwest side of Orcas Island is designated as the type area because a thick and relatively fossiliferous section is exposed there. The East Sound Group supersedes the following informal units: the Orcas Knob, Raccoon Point, and President Channel units of Danner (1957, 1966) and the Pennsylvanian

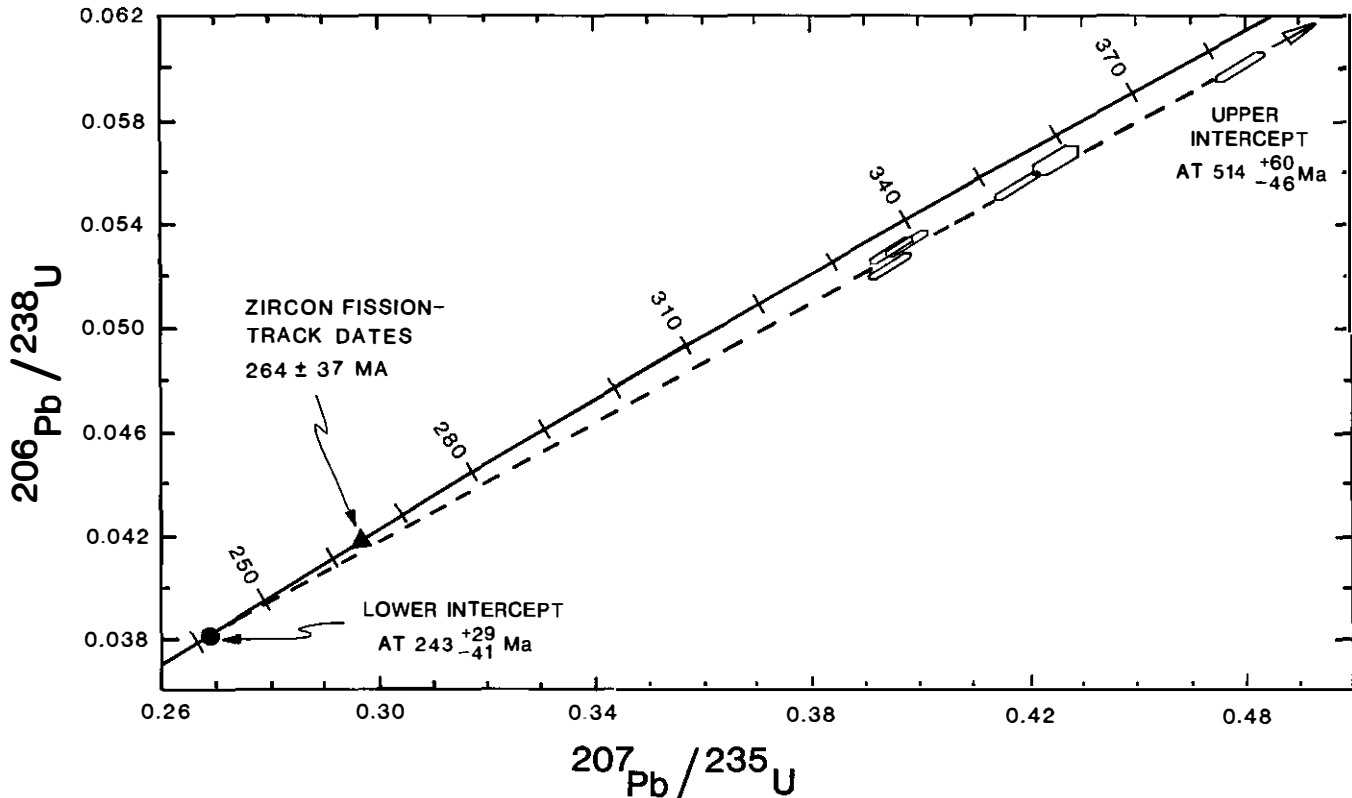


Figure 8. Concordia diagram for U/Pb zircon dates from the tonalitic phase of the Turtleback Complex (T3, T4a, T5a, T6 in Table A-1). The upper intercept date of 514 Ma is considered to be the intrusive age of the tonalite. The lower intercept date corresponds to Pb loss during a Late Paleozoic thermal event. The average of 6 zircon fission-track dates is plotted on the concordia curve and indicates the age of cooling after the thermal event (fission track dates: T4b, T5b, T8-10 in Table A-1). The discordia line and the concordia intercepts were calculated courtesy of R. L. Armstrong. All errors are at the 95 percent confidence level.

and Devonian volcanics of Vance (1975, 1977). These units may prove useful if further work can establish formational subdivisions within the East Sound Group.

The East Sound Group consists primarily of andesitic to dacitic pyroclastic rocks (see Table B-2 for some representative geochemical analyses), ranging from massive tuff-breccia to thin-bedded volcanic sandstone to very fine grained, laminated tuff. Subordinate lava flows are also present, some of which are pillowed. Dikes and hypabyssal intrusions that may have fed these volcanic rocks are widespread and range in composition from mafic to silicic. The East Sound also contains minor limestones, most of which can be demonstrated to be interbedded in the volcanic sequence (see notes in Table A-2). The age of the East Sound Group is based on fossils from these limestones, which indicate the presence of Lower Devonian, Middle Devonian, Pennsylvanian, and Lower Permian strata (Fig. 7).

The East Sound Group is generally in thrust contact with the Turtleback Complex and apparently lacks the static metamorphic

overprint that distinguishes the Turtleback. Both units, however, have experienced Late Cretaceous high-pressure metamorphism (Vance, 1968; Glassley and others, 1976). Plutonic rocks lithologically similar to the Turtleback locally intrude the East Sound Group (Sea Acres and Deer Harbor on Orcas Island; Muller, 1977; Danner, 1977). If these intrusions are indeed correlative with early Paleozoic tonalite of the Turtleback, then part of the East Sound Group must be older than late Paleozoic. Alternatively, these plutonic rocks may have been associated with and intruded during late Paleozoic East Sound volcanism, an interpretation that is compatible with the widespread occurrence of dikes and hypabyssal intrusions in the East Sound.

**Origin of the Turtleback and East Sound units.** We interpret the East Sound Group to originally have been deposited on the Turtleback Complex; together they represent a terrane that we call the Turtleback terrane. Although the evidence is not conclusive, there are several reasons why we favor this interpretation: (1) the presence of similar dikes and hypabyssal intrusions in

both units, (2) the similarity in timing of Turtleback metamorphism and East Sound volcanism, and (3) the close spatial association of the two units. Danner (1966; Fig. 4 in Danner, 1977) has described a possible unconformity between these two units, located on O'Neal Island where fossiliferous Devonian sedimentary beds (E5 in Table A-2) rest on Turtleback Complex. Parts of this contact do look depositional; however, faulting and limited exposure have obscured the nature of this relationship.

There is some evidence that could conflict with our stratigraphic interpretation. Based on differences in metamorphic grade, Vance (1977) suggested that Turtleback Complex and East Sound Group are separated by a major fault. Indeed, map evidence (Fig. 3) requires the presence of at least one major thrust fault because the bulk of the Turtleback Complex presently lies above the East Sound Group. The question becomes: Do these differences in metamorphic grade indicate that the two units are unrelated fault-bounded terranes? We think not. The higher metamorphic grade of the Turtleback is to be expected if, in fact, it did originally underlie the East Sound Group. In this interpretation, the emplacement of higher-grade Turtleback onto lower-grade East Sound Group would be attributed to Late Cretaceous thrusting within the Turtleback terrane.

As for the original tectonic setting of the East Sound Group and Turtleback Complex, they both were probably formed in arc-volcanic settings. This conclusion is supported by their probable calc-alkaline affinity (Tables 3 and A-1; compare with Table 4), and the predominance of intermediate and silicic plutonic and volcanic rocks (Pitcher, 1982; Gill, 1981). Therefore, the Turtleback terrane records an episodic history of Cambrian and late Paleozoic arc magmatism. The initial setting of this arc magmatic sequence, whether continental or oceanic, is not known.

**Regional correlation of the Turtleback and East Sound units.** Rocks that have been considered to be equivalent to the Turtleback Complex include (Fig. 6): (1) the Yellow Aster Complex in the Cascade Mountains (Misch, 1966), and (2) the Salt-spring Intrusions of southern Vancouver Island (Muller, 1980). The Yellow Aster shares many similarities with the Turtleback. It occurs in fault slices within the North Cascades thrust system and, like the Turtleback, includes a gabbroic phase and a tonalitic phase. Furthermore, discordant U/Pb zircon dates from the tonalite indicate a similar early Paleozoic age (older than 400 to 450 Ma; Mattinson, 1972). We, therefore, conclude that these units are probably equivalent.

The Salt-spring Intrusions, however, probably are not equivalent to the Turtleback Complex, based on significant differences in mode of occurrence, lithology, and age. This unit is a distinctive quartz-feldspar porphyry that occurs as small intrusive bodies within mafic volcanic rocks of the Sicker Group (Muller, 1980; Brandon and others, 1986). Two new, concordant U/Pb zircon dates (R. Parrish and M. Brandon, unpublished data) indicate intrusive ages of 362 and 366 Ma (two sigma errors of  $\pm 1$  m.y.), which are clearly much younger than the Turtleback Complex.

The Turtleback Complex has also been correlated with

other plutonic units on Vancouver Island: the Wark-Colquitz gneisses and the West Coast Complex (Muller, 1977). Yet, recent U/Pb dating of these units indicates that they are, in fact, Jurassic in age (Isachsen, 1984).

The East Sound Group has been correlated with the Sicker Group of Vancouver Island and the Chilliwack Group of the Cascade Mountains (Fig. 6), both of which are arc-volcanic sequences of broadly similar age. The Sicker is Silurian (and possibly older) to Early Permian in age (Brandon and others, 1986), whereas the Chilliwack is Devonian to Early Permian (Danner, 1977). Muller (1980) considers the East Sound Group to be equivalent to the Sicker, which would mean that Wrangellia extends into the San Juan Islands. Danner (1977) argues that major faunal differences preclude the equivalence of San Juan Paleozoic rocks with either the Chilliwack or the Sicker. His conclusion, however, is based on the Tethyan fusulinid fauna in the Orcas-Deadman Bay sequence, which we separate from the East Sound Group. Based on Danner's (1966, 1977) descriptions (also see Monger and Ross, 1971), the fauna of the East Sound Group is nearly identical to that of the Chilliwack Group, whereas the fauna of the Sicker Group is quite different. Another similarity between the East Sound and Chilliwack is that they both contain Devonian, Pennsylvanian, and Lower Permian limestone units that are interbedded within the volcanic sequences. In contrast, the Sicker Group contains only one limestone unit, the Pennsylvanian and Lower Permian Buttle Lake Formation, which caps the Sicker sequence (Brandon and others, 1986). These relationships suggest that the East Sound is equivalent to the Chilliwack and not to the Sicker.

***Deadman Bay terrane: Permian-Lower Jurassic chert, basalt, and limestone***

The Deadman Bay terrane comprises a disrupted stratigraphic sequence of Lower Permian to Lower Jurassic chert, basalt, and limestone. This sequence consists of two stratigraphic units: the Deadman Bay Volcanics (new name) and the Orcas Chert. Presently, these two units are separated by faults; however, similarities in age, lithology, and volcanic geochemistry indicate that they are related stratigraphic units. The bulk of the Deadman Bay terrane lies structurally above the Turtleback terrane, although there is a significant amount of structural interleaving between the two units. The Orcas thrust (Vance, 1977; Figs. 3 and 5), which we place at the top of the main outcrop of Turtleback Complex, represents an approximate boundary between these terranes.

***Stratigraphy and age of the Deadman Bay Volcanics.*** The Deadman Bay Volcanics is a new name for a unit that Vance (1975) informally called the Permian volcanics. This unit occurs in a number of discontinuous fault slices that are structurally interleaved with the Orcas Chert (Fig. 3). Stratigraphic relations in the Deadman Bay Volcanics are best displayed in a 4-km-long fault slice of the unit, north of Deadman Bay on the west side of San Juan Island (Fig. 9). We designate this as the type area of the unit.

TABLE 4. GENERAL GEOCHEMICAL CHARACTERISTICS OF SOME MODERN VOLCANIC SETTINGS

Tectonic Setting	Lithologic association	SiO <sub>2</sub> %	TiO <sub>2</sub> %	Ti/V	Y/Nb	Zr (ppm)	Cr (ppm)	REE pattern†
<b>Ocean-floor Basalts</b> mid-oceanic ridges and back-arc basins	tholeiitic basalts, commonly pillowed with rare pyroclastics	49 (47-62) [a,c]	1.4 (0.7-2.5) [a,b,g]	35 (20-50) [g]	6 (1.5-18) [b,d]	92 (45-140) [b]	310 (100-500) [c,e]	flat pattern with depleted LREE [a,e]
<b>Ocean-Island Basalts</b> hot spots and anomalous mantle plumes	tholeiitic and alkalic basalts	48 (40-70) [c,i]	2.5 (1.5-4.5) [b,d,f,g]	70 (40-110) [g]	0.9 (0.3-4.5) [b,d]	215 (80-350) [b,d,h]	280 (10-1000) [c,i]	moderate to strong LREE enrichment [e]
<b>Immature Island Arcs</b> young intraoceanic island arcs	low K tholeiite including mafic and silicic compositions	53 (45-70) [a,c,f]	0.8 (0.3-1.2) [b,e,f,g]	15‡ (10-20) [g]	13 (3-25) [b,f]	52‡ (20-150) [b,f]	160‡ (0-400) [c,e]	flat pattern with low abundances and variable LREE deple- tion or enrichment [a,e,f]
<b>Mature Arcs</b> continental arcs and older island arcs	moderate to high K calc-alkaline rocks, mainly intermediate compositions	59 (53-70) [a,f]	0.75 (0.5-1.2) [a,f,g]	30 (15-100) [g]	7 (3-15) [b,f]	106‡ (50-170) [b,f]	130‡ (0-400) [c,e]	moderate to strong LREE enrichment [a,e,f]

Note: Data format is: average, (min.-max.), with references in brackets.

†REE (rare earth element) patterns normalized to chondritic abundances; LREE = light REE.

‡For basaltic samples (SiO<sub>2</sub> <55-60%).

References: (a) Jakes and Gill (1970); (b) Pearce and Cann (1973); (c) Pearce (1975); (d) Floyd and Winchester (1975); (e) Garcia (1978); (f) Gill (1981); (g) Shervais (1982); (h) Pearce and Cann (1971); (i) Miyashiro (1975); Miyashiro and Shido (1975).

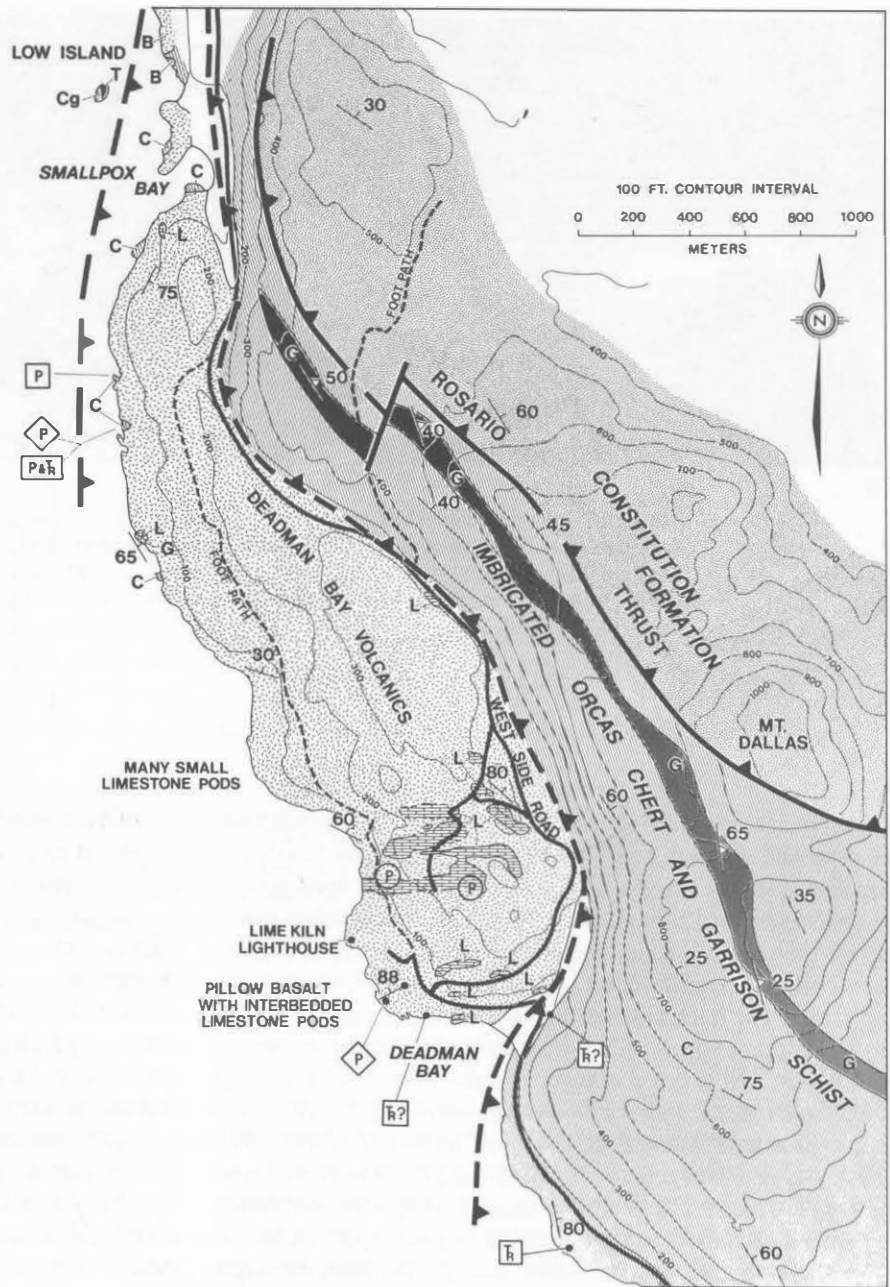


Figure 9. Geologic map of a fault slice of the Deadman Bay Volcanics on the west coast of San Juan Island (see Fig. 2 for location). Compiled from Danner (1966), Vance (1975) and Brandon and Cowan (unpublished mapping). Fossil localities are described in Tables A-3 and A-4.

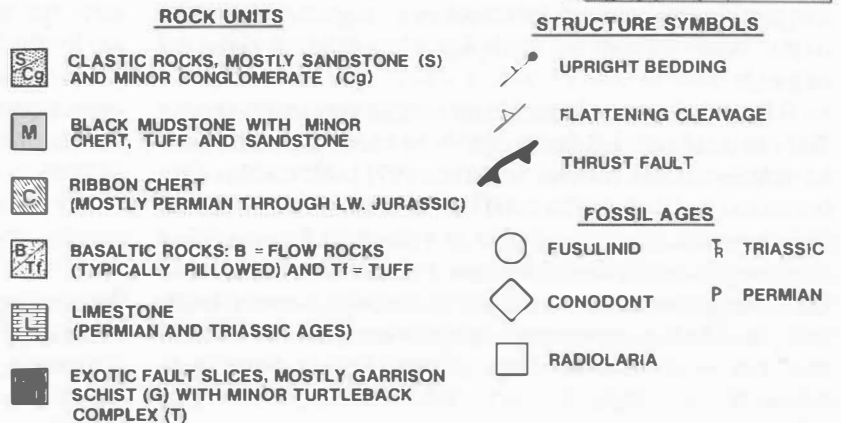




Figure 10. Limestones in pillow basalts of the Deadman Bay Volcanics. (a) Laminated pink limestone interbedded with pillow basalts. Conodonts from this limestone are Early Permian, late? Leonardian (D2b in Table A-3). Scale line is 20 cm. (b) Limestone in voids between pillow basalts. Limestones similar to these have yielded Tethyan fusulinids (see Table A-3 and Fig. 3 for distribution of Tethyan fusulinid localities).

The Deadman Bay unit, which internally is relatively undeformed, consists mostly of red and green pillow basalt and associated pillow breccia with minor interbeds of massive gray limestone and red ribbon chert. The limestone, which is extensively recrystallized to an aragonitic marble (Vance, 1968), occurs both as irregular bodies and also as tabular interbeds in the volcanics. The thickest limestones are tabular at map scale (Fig. 9) and appear to be roughly concordant to bedding in the volcanics. Where well exposed at outcrop scale, there is no doubt that these limestones are part of the volcanic sequence. Locally, laminated limestone is found draped over the top of pillows (Fig. 10a), and small irregular bodies containing fossil hash are found filling the voids between adjacent pillows (Fig. 10b). Moreover, small intercalations of green basaltic tuff are common in the larger limestone bodies. Where bedding is present in the larger irregular bodies, it is typically contorted, suggesting that these bodies were formed by slumping of unlithified carbonate material.

These limestones are important because they locally contain Tethyan fusulinids, a fauna thought to be exotic to North America (Danner, 1966; Monger and Ross, 1971). All the San Juan occurrences of Tethyan fusulinid limestones are restricted to the Deadman Bay unit (D1 and D3-7 in Table A-3). Fusulinids and conodonts from the limestones are Permian (Leonardian and Guadalupian) in age (Fig. 11; Table A-3). Conodonts and radiolaria from ribbon cherts interbedded in the volcanic sequence (e.g., Fig. 9) give a wider range of ages (Fig. 11; Table A-3), extending from Early Permian (late Wolfcampian) to Late Triassic.

**Stratigraphy and age of the Orcas Chert.** The Orcas Chert of Vance (1975) consists mainly of monotonous sequences of grayish ribbon chert, with subordinate mudstone, pillow basalt, basaltic tuff, and limestone. The unit has an average structural thickness of about 500 m, but its true thickness and internal stratigraphy are difficult to resolve due to deformation and the absence of distinctive marker beds. For instance, ribbon chert is commonly folded and contorted. Where interbedded black mudstone and green tuff are abundant, chert beds tend to be more chaotically disrupted. Small fault slices of Turtleback Complex are locally present in the Orcas Chert, providing further evidence of structural disruption and thrust duplication.

Radiolaria and conodonts from ribbon chert have been confidently identified from 27 localities (Fig. 11; Table A-4) and indicate that the Orcas Chert ranges from Triassic to Early Jurassic in age. Whetten and others (1978) reported one Mississippian age for the Orcas (013b in Table A-4), which would be the only pre-Permian radiolarian locality in the San Juan Islands. We suspect that this Mississippian age is incorrect since two other samples from the same locality yielded Triassic radiolaria (013a in Table A-4).

At several localities, dated chert is depositionally associated with Orcas pillow basalts (02, 04, 07, 021, 028, and 029 in Table A-4). Most of these cherts are Triassic, but some are Lower Jurassic, suggesting that basaltic volcanism continued into the Jurassic. We note, however, that in some areas there is clear evidence that the cherts represent condensed sequences. For instance, on northern San Juan Island a single outcrop of ribbon chert has yielded ages ranging from Triassic to at least latest Early

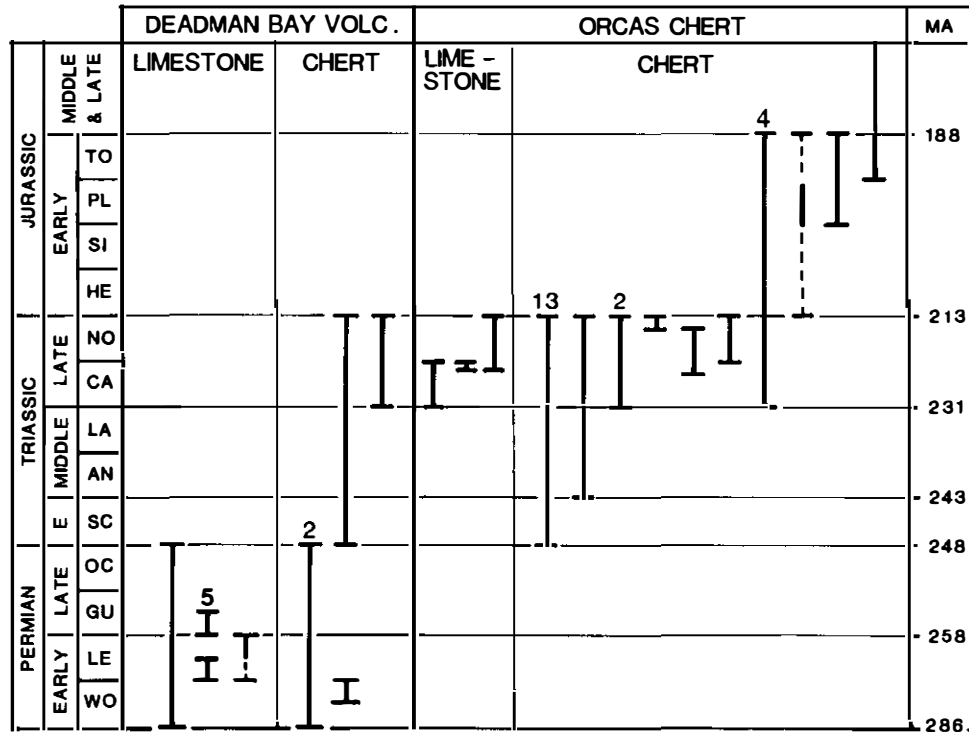


Figure 11. Fossil ages from the Deadman Bay terrane. Vertical bars represent the possible age range for each determination; numbers are the number of localities with that age range. Identified fossils are: radiolaria from chert, conodonts from chert or limestone, fusulinids from limestone. Only confidently determined fossil ages are included in this diagram (see Tables A-3 and A-4; Deadman Bay limestone: D1-D8; Deadman Bay chert: D6b, D9a-c, D10; Orcas limestone: 03, 012b, 030; Orcas chert: 04-6, 07a-c, 08-12, 013a, 014-18, 021-25, 028, 029, 031, 032).

Jurassic (07 in Table A-4). The Deadman Bay Volcanics contains another example (D8 in Table A-3) where a single outcrop of chert ranges from Early Permian (Wolfcampian) to Triassic. This problem of condensed sections, coupled with the possibility of significant hiatuses, makes it difficult to use chert ages to precisely resolve the timing of volcanism.

Field relations indicate that limestones in the Orcas are indigenous to the unit and are not exotic fault slices. Some of the limestones are clearly interbedded with the chert, whereas others appear to be submarine slide blocks, perhaps derived from shallow-water carbonate reefs (cf. p. 1846 in Monger, 1977; Wright, 1982). Originally, these limestones were thought to be upper Paleozoic, based in part on a tentative identification of macrofossils from limestone in the Roche Harbor area (Danner, 1966). Three of the Orcas limestone bodies, including the Roche Harbor body on northern San Juan Island, have since yielded Late Triassic conodonts (Fig. 11; 03, 012b, and 030 in Table A-4). Chert directly surrounding the Roche Harbor limestone bodies has yielded Late Triassic radiolaria (see 011, 012a, and 012b in Table A-4). The important conclusion is that there is no

longer any evidence indicating that the limestone blocks in the Orcas are older than the surrounding ribbon chert.

**Origin and tectonic setting.** Although not conclusive, indirect evidence indicates that the Orcas Chert and Deadman Bay Volcanics are related stratigraphic units, and that together they represent a discrete terrane which we call the Deadman Bay terrane. This conclusion is supported by two lines of evidence. First, pillow lavas in both units have a similar basaltic composition (Table 3). This similarity also extends to their immobile trace-element composition (Fig. 12; Table 3; see Appendix B for a description of sample localities), which indicates that the Orcas and Deadman Bay basalts erupted in the same type of tectonic setting. Based on their high  $TiO_2$  content and low  $Ti/V$  and  $Y/Nb$  ratios (Table 4), these basalts compare closely with tholeiitic and alkalic basalts at modern ocean islands. Other tectonic settings, such as volcanic-arc and ocean-floor, are ruled out by the relatively high  $TiO_2$ ,  $Zr$ , and  $Cr$  contents and the LREE-enriched character of the Deadman Bay and Orcas basalts (Table 4; compare Figure 12 with the OFB pattern in Figure 18b). The second line of evidence is that the Deadman Bay Volcanics and Orcas

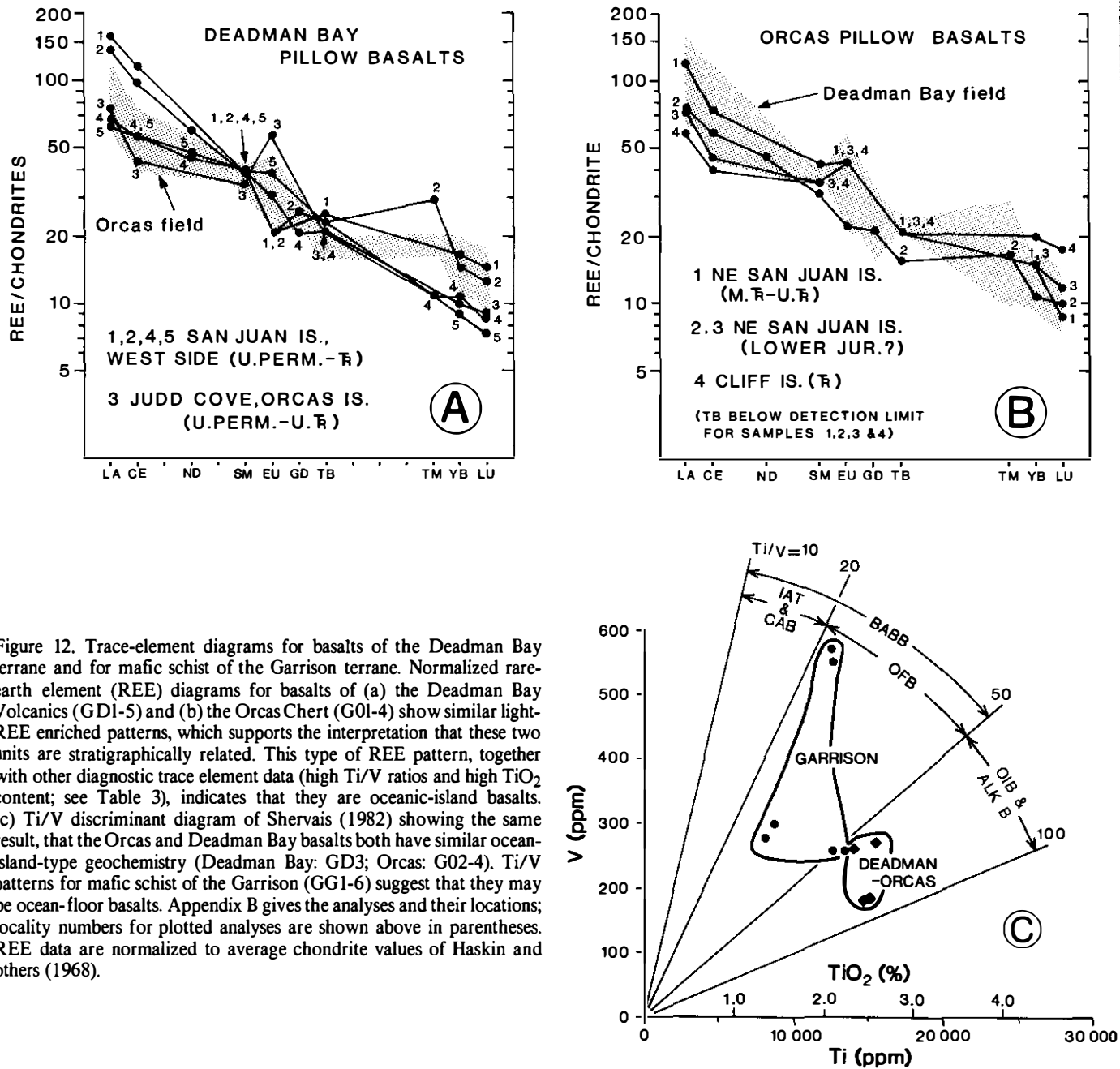


Figure 12. Trace-element diagrams for basalts of the Deadman Bay terrane and for mafic schist of the Garrison terrane. Normalized rare-earth element (REE) diagrams for basalts of (a) the Deadman Bay Volcanics (GD1-5) and (b) the Orcas Chert (G01-4) show similar light-REE enriched patterns, which supports the interpretation that these two units are stratigraphically related. This type of REE pattern, together with other diagnostic trace element data (high Ti/V ratios and high TiO<sub>2</sub> content; see Table 3), indicates that they are oceanic-island basalts. (c) Ti/V discriminant diagram of Shervais (1982) showing the same result, that the Orcas and Deadman Bay basalts both have similar oceanic-island-type geochemistry (Deadman Bay: GD3; Orcas: G02-4). Ti/V patterns for mafic schist of the Garrison (GG1-6) suggest that they may be ocean-floor basalts. Appendix B gives the analyses and their locations; locality numbers for plotted analyses are shown above in parentheses. REE data are normalized to average chondrite values of Haskin and others (1968).

Chert overlap in age and contain a similar association of chert and pillow basalt. Thus, the transition from the Deadman Bay to the Orcas can be viewed as due to a decline in the rate of volcanism during the Triassic. Finally, we note that the Orcas and Deadman Bay occur almost everywhere in direct proximity with each other, despite the fact that they are typically separated by faults.

The Deadman Bay terrane is probably far traveled, as indicated by the presence of Tethyan fusulinid limestones (Monger and Ross, 1971). Where these limestones came from, and when and how they were accreted to North America are important and

unanswered questions in Cordilleran geology. One interpretation is that they were deposited on oceanic islands or large seamounts located in the equatorial paleo-Pacific (e.g., Saleeby, 1983), which is compatible with the volcanic setting proposed here. Furthermore, the absence of continent-derived sediment and the predominance of siliceous biogenic deposits indicate that the Deadman Bay terrane probably formed in an open-ocean setting.

**Regional correlation.** The Deadman Bay terrane may be equivalent to several other upper Paleozoic-lower Mesozoic units of the western Cordillera based on a similar association of chert, basalt, and Tethyan fusulinid limestone. These units include:

(1) the Trafton Group of the western Cascade foothills (Danner, 1966), (2) the Cache Creek Group in central British Columbia (Monger, 1977), (3) parts of the Western Paleozoic and Triassic belt of the Klamath Mountains in northwest California and southwest Oregon (Irwin, 1981; Wright, 1982; Ando and others, 1983), and (4) possibly the Elkhorn Ridge argillite and related rocks in eastern Oregon (Vallier and others, 1977; Dickinson and Thayer, 1978). The Bridge River Complex of southern British Columbia and the Hozomeen Group of the North Cascades (Potter, 1983; Haugerud, 1985; Ray, 1986) may also be equivalent, based on similarities in age range and rock types, including the presence of oceanic island-type basalts. Tethyan fusulinid limestone, however, has not been found in these two units.

#### *Garrison terrane: Permo-Triassic mafic schist*

**Composition.** The metamorphic rocks referred to as the Garrison Schist were first recognized by Danner (1966) at Garrison Bay on northern San Juan Island (near Bell Point, see Fig. 2). Further work (Vance, 1975, 1977; Brandon, 1980; this paper) has shown that this unit occurs as a discontinuous sheet of fault slices at or near the contact between the Orcas Chert and overlying clastic sediments of the Constitution Formation (Figs. 13–16). At most outcrops, this exotic sheet is only 1 to 4 m thick and is nowhere thicker than a few tens of meters. The Garrison rocks are green, and less commonly black, fine-grained mafic schists with minor quartz-mica schist and rare lenses of recrystallized limestone. In the field, a well-developed schistosity distinguishes Garrison rocks from adjacent less-metamorphosed rocks of the Orcas and Constitution. This metamorphic fabric is commonly fractured and brecciated, and cut by veins of aragonite, calcite, and rare prehnite. We attribute these late-stage brittle structures to fault-zone deformation during the thrust emplacement of these exotic fault slices.

The Garrison includes two types of mafic schists that differ in metamorphic grade. The more common type is a very fine-grained greenschist with the assemblage: albite + epidote + chlorite ± actinolite ± calcite/aragonite (aragonite probably formed during the Late Cretaceous regional metamorphism). The second type is a fine-grained albite-epidote amphibolite. The amphibolite occurs with the greenschist but appears to be restricted to northwest San Juan Island (Mt. Dallas and Garrison Bay areas) and eastern Orcas Island (near the community of Rosario). Microprobe analyses show that the amphibole in the amphibolite is barrositic (D. Mogk and M. A. Dungan, written communication, 1983), indicating high-pressure metamorphic conditions.

**Age.** Two K-Ar hornblende dates for Garrison amphibolite indicate a Permian to Early Triassic metamorphic age ( $286 \pm 20$  Ma and  $242 \pm 14$  Ma; Table 5). This age range agrees well with that obtained from the Vedder Complex (Armstrong and others, 1983), an equivalent unit in the North Cascades that has been more extensively dated (discussed below). Another K-Ar determination on amphibole from Garrison greenschist yielded a younger Late Jurassic date ( $167 \pm 12$  Ma; Table 4). Since there is

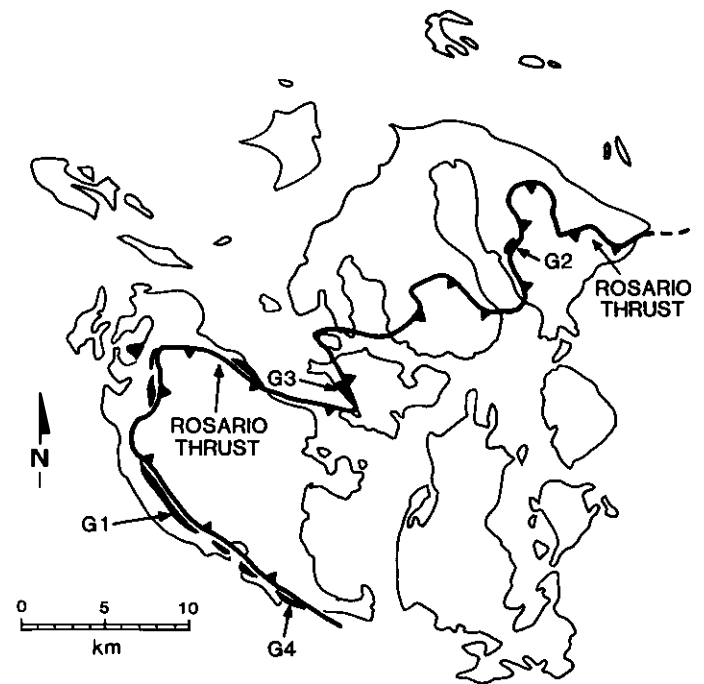


Figure 13. Map showing the distribution of the Garrison Schist, which occurs as exotic fault slices along the Rosario thrust. Solid pattern indicates areas, greatly exaggerated in size, containing one or more slices. See Figure 3 for overall geologic setting. Sample numbers refer to K-Ar dates and Rb-Sr whole-rock data listed in Tables 5 and 6.

no petrologic evidence for a separate and younger suite of Garrison metamorphic rocks, we conclude that this young date is due to argon loss, perhaps related to the very fine grain-size of the amphibole in this sample (about 0.1 mm) and its low potassium content (Table 5).

**Structural relationships.** The Garrison Schist is restricted to a major fault zone called the Rosario thrust (Fig. 13). We consider the Garrison to be slices of old metamorphic rock that were transported within this fault zone. In fact, the presence of the Garrison is the main evidence for a major thrust separating the Orcas Chert from the Constitution Formation. Several observations preclude the possibility that the Garrison was formed by local metamorphism along the thrust: (1) the metamorphism of the Garrison is older than either the Orcas Chert or the Constitution Formation; (2) there is a striking contrast between the higher grade, synkinematic metamorphism of the Garrison, and the very low grade, static Late Cretaceous metamorphism of the adjacent sedimentary rocks; and (3) clasts of the Garrison are present in conglomerates and sandstones of the overlying Constitution Formation (Vance, 1977; Brandon, 1980).

An important question is: How was the Garrison emplaced into its present structural position? We suggest that the Garrison

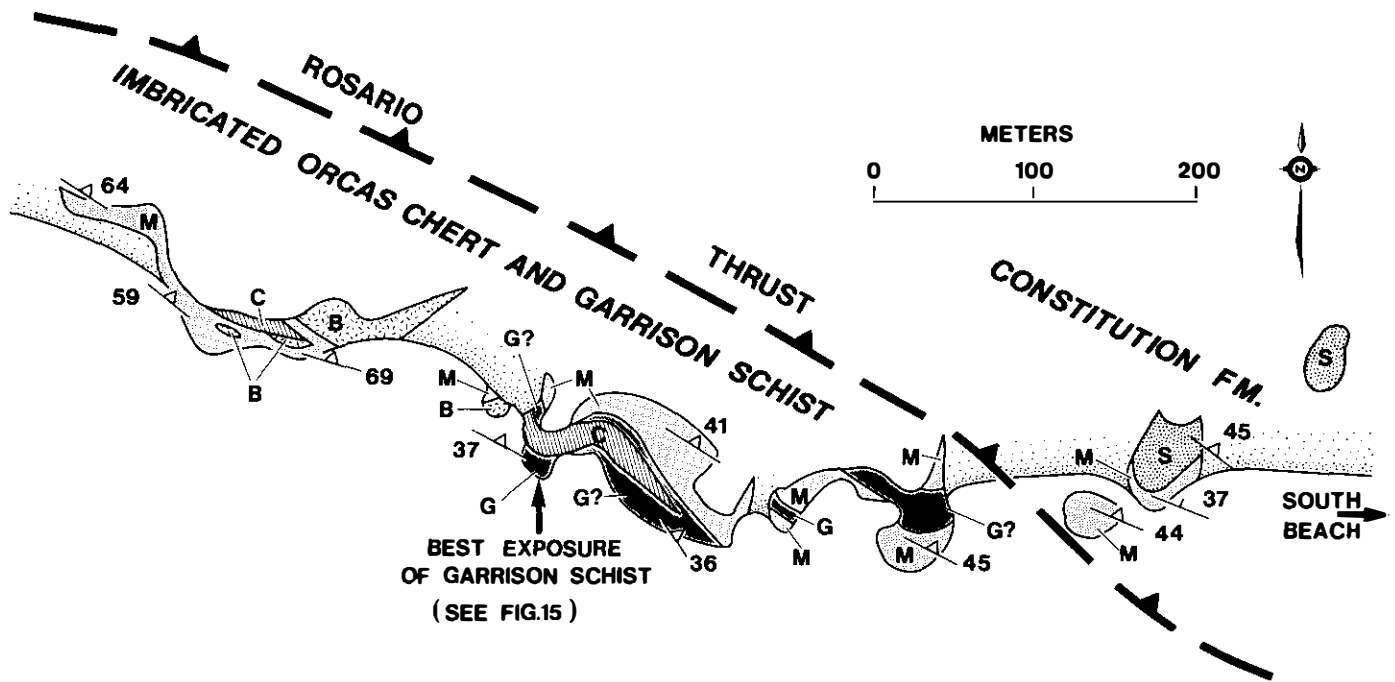


Figure 14. Outcrop map of the imbricate zone beneath the Rosario thrust at South Beach, southern San Juan Island (mapping from Brandon, 1980; see Fig. 2 for location). The legend for this map is shown in Figure 9. Massive sandstone (S) and mudstone (M) of the Constitution Formation lie above the Rosario thrust. The area below the thrust consists of an imbricated fault zone containing ribbon chert (C) and pillow basalt (B) of the Orcas Chert, and small fault slices of Garrison Schist (G). The mudstone-rich unit (M) beneath the Rosario thrust is of uncertain affinity, and may belong to the Constitution or to the Orcas (lowest unit in Fig. 17; see text for discussion). A photograph of one of the Garrison slices is shown in Figure 15.

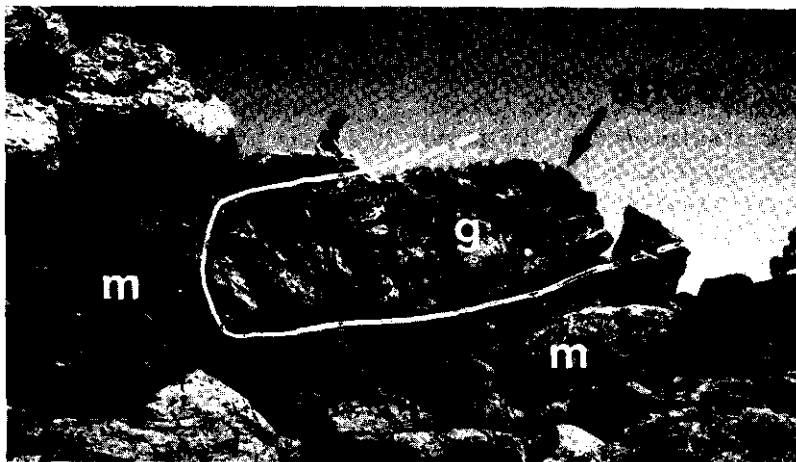


Figure 15. Fault slice of Garrison Schist (g) within the imbricate zone below the Rosario thrust on southern San Juan Island. The slice is about 2.3 m thick and is surrounded by mudstone and ribbon chert (m), probably belonging to the Orcas Chert. The mudstone and chert are highly faulted and imbricated at the contacts of the slice. The view is facing southeast. The geologic setting of this locality is shown in Figure 14.

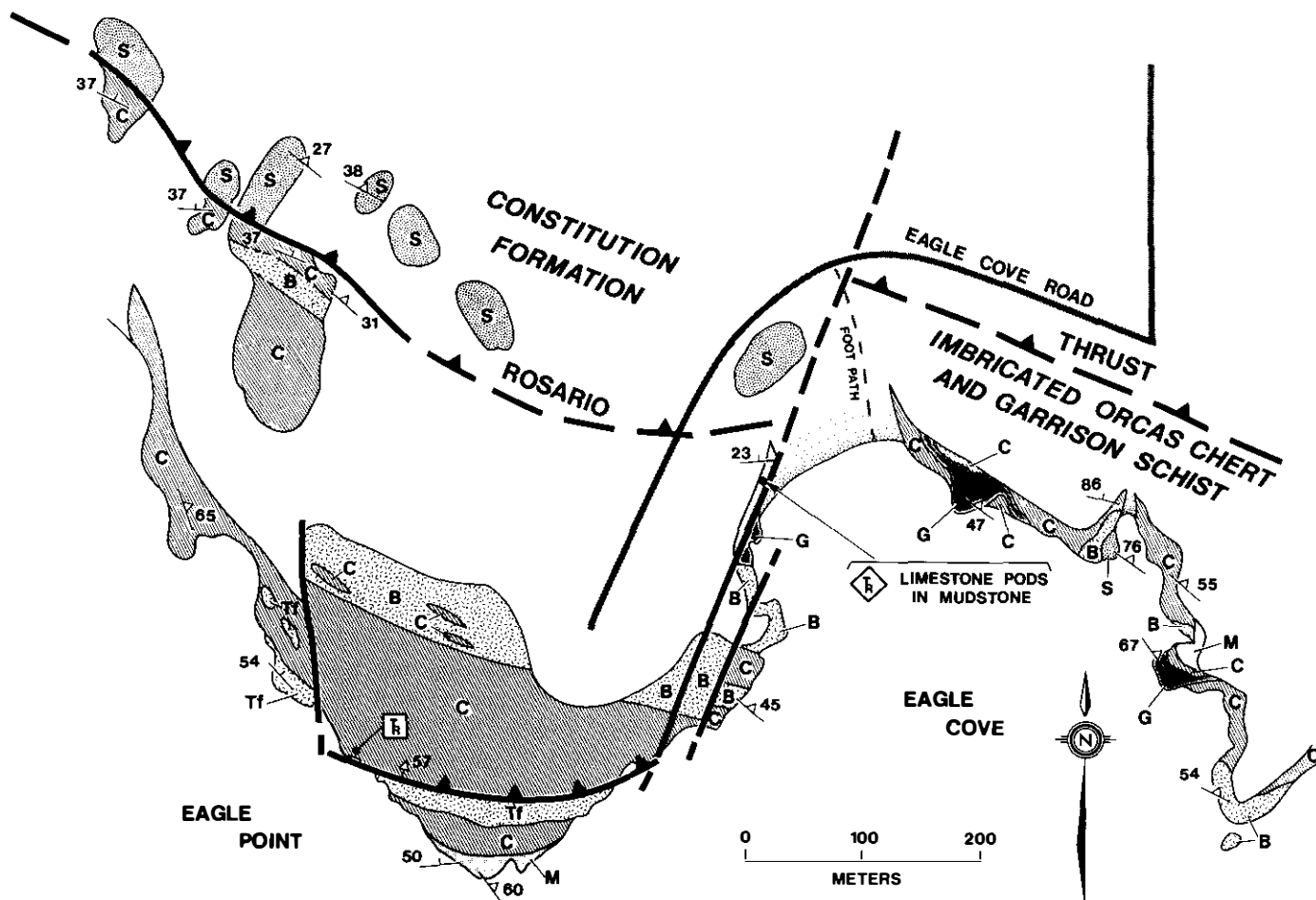


Figure 16. Outcrop map of the imbricate zone beneath the Rosario thrust as exposed at Eagle Cove on southern San Juan Island (mapping from Brandon, 1980; see Fig. 2 for location). The legend for this map is shown in Figure 9. Massive sandstone (S) of the Constitution Formation lies above the Rosario thrust. The area below the thrust consists of ribbon chert (C), pillow basalt (B) and basaltic tuff (Tf) of the Orcas Chert, and small fault slices of Garrison Schist (G). The mudstone-rich unit (M) beneath the Rosario thrust is of uncertain affinity and may belong to the Constitution or to the Orcas (lowest unit in Fig. 17; see text for discussion). At Eagle Cove, this mudstone unit contains a number of small limestone pods, probably slide blocks, which have yielded Late Triassic (Carnian) conodonts (C3 in Table A-5). Orcas ribbon chert at Eagle Point has yielded Triassic radiolaria (024 in Table A-4).

TABLE 5. K-AR DATES FOR THE GARRISON SCHIST

No.	Sample description and location	Dated material (size fraction)	K (wt.%)	<sup>40</sup> Ar(rad) (10 <sup>-10</sup> mol/gr)	<sup>40</sup> Ar(rad) (%)	Date (Ma)	Ref.
G1	amphibolite (S-161) Mt. Dallas, San Juan Is. 48° 31.0', 123° 07.9'	hornblende	0.523	2.3478	91.8	242 ± 14	1
G2	amphibolite (O-507) Rosario, Orcas Is. 48° 39.05', 122° 52.0'	hornblende (-100 + 200)	0.499	2.678	89.7	286 ± 20	2
G3	greenschist (7981J-1C) Parks Bay, Shaw Is. 48° 33.97', 122° 58.72'	amphibole (-80 + 140)	0.132	0.4002	62.6	167 ± 12	2

Note: See Figures 13 and B-1 for locations. All dates calculated using new decay constants (e.g., Harland and others, 1982). Errors for dates are estimated at the 95% confidence level ( $\pm 2$  sigma).

References: (1) R. B. Forbes (written communication, 1977), Vance (1977), p. 178; (2) R. L. Armstrong (written communication, 1981), J. Harakal, analyst (see Table 2 in Armstrong and others, 1983, for description of analytical procedure).

may have been part of the basement to the Constitution, and that during Late Cretaceous thrusting, slices of this basement were carried with the Constitution as it overrode the Orcas Chert along the Rosario thrust. This interpretation is consistent with the presence of Garrison clasts in the Constitution, indicating that these units were in close proximity prior to Late Cretaceous thrusting.

**Origin and tectonic setting.** The Garrison probably originated as a sequence of submarine basalts with minor chert and limestone. The submarine origin of the unit is based primarily on our interpretation that Garrison quartz-mica schist was originally ribbon chert, which is consistent with its quartz-rich composition and the presence of thinly laminated alternations of quartz- and mica-rich layers, reminiscent of ribbon chert bedding. Our conclusion is also supported by the immobile trace element composition of the mafic schists (Table 3; see Appendix B for descriptions of sample localities). Their high TiO<sub>2</sub>, Zr, and Cr content and their moderate Ti/V ratios (Figure 12c) suggests that they are ocean-floor basalts (Table 4), which in the modern oceans are only formed at divergent plate boundaries, such as mid-oceanic ridges and in back-arc basins (see Pearce and Cann, 1973).

Based on the evidence above, metamorphism and deformation of the Garrison probably occurred during accretion of oceanic crustal rocks at a Permo-Triassic subduction zone. At present, there is no sign of this original subduction-zone setting. Instead, the Garrison occurs only as fault-bounded slices in a Late Cretaceous fault zone.

**Regional correlation.** The Garrison Schist is probably equivalent to the Vedder Complex (Armstrong and others, 1983), which occurs as isolated fault slices along the Shuksan thrust in the North Cascades thrust system (Misch, 1966, 1977). Like the Garrison, the Vedder Complex consists of both mafic and quartz-

mica schist, although the Vedder apparently contains a greater proportion of coarse-grained albite-epidote amphibolite (Armstrong and others, 1983). Rb-Sr and K-Ar dating by Armstrong and others (1983) has demonstrated a Permian to Early Triassic metamorphic age (219 to 279 Ma), and a primary age probably no older than Mississippian. They estimate that metamorphism of the Vedder rocks occurred under high-pressure conditions of about 7 to 8 kb (700 to 800 Mpa). One difference between these two units is that the initial <sup>87</sup>Sr/<sup>86</sup>Sr ratio of the Vedder (0.7052 to 0.7072; Armstrong and others, 1983) is significantly higher than that for the Garrison (0.7042 to 0.7051; Table 6), which might mean that these units were derived from different basaltic protoliths. The initial Sr isotope ratios for both units, however, are higher than those of most modern oceanic basalts (0.7028 to 0.7040; Garcia, 1978), which suggests variable amounts of exchange with the more radiogenic Sr of seawater (0.709). Thus, we conclude that the evidence strongly favors the interpretation of the Garrison and Vedder as related metamorphic units.

It is important to note that Triassic, high-pressure, metamorphic rocks are present elsewhere in the western Cordillera. Hotz and others (1977) describe blocks and thrust slices of blueschist-facies mafic rocks, phyllite, and siliceous mica schist, located in the eastern Klamath Mountains, northern California, and in the Mitchell area, north-central Oregon. Four K-Ar dates on white mica indicate a Late Triassic metamorphic age (214 to 223 Ma; Hotz and others, 1977) for these two blueschist localities. Blueschist rocks from the Pinchi Lake area, central British Columbia, have yielded similar K-Ar muscovite dates, in the range 214 to 221 Ma (Paterson and Harakal, 1974). A notable distinction between the Klamath, Mitchell, and Pinchi Lake blueschists and the Garrison and Vedder rocks is that mafic rocks in

TABLE 6. Rb-Sr WHOLE-ROCK DATA FOR THE GARRISON SCHIST

No.	Sample description and location	Sr (ppm)	Rb (ppm)	$^{87}\text{Rb}/^{86}\text{Sr}$	$^{87}\text{Sr}/^{86}\text{Sr}$	Initial $^{87}\text{Sr}/^{86}\text{Sr}$
G2	amphibolite (O-507) Rosario, Orcas Is. 48° 39.0', 122° 52.0'	361	3.4	0.027	0.7052	0.7051
G3	greenschist (7981J-1C) Parks Bay, Shaw Is. 48° 33.97', 122° 58.72'	168	1.4	0.025	0.7043	0.7042
G4	amphibolite (8054J-1) Eagle Cove, San Juan Is. 48° 27.65', 123° 01.92'	114	1.5	0.037	0.7049	0.7047

Note: Analyses from R. L. Armstrong (written communication, 1981). Analytical procedures described in Table 1 of Armstrong and others (1983). Initial Sr ratios were calculated assuming a 240-290 Ma age. See Figures 13 and B-1 for sample locations.

the former group contain crossite and lawsonite, whereas the latter group contains barrositic amphibole and epidote. Despite differences in metamorphic grade, the similar age of these high-pressure rocks suggests that they may have had a common origin in a Permo-Triassic subduction complex.

### UPPER MESOZOIC ROCKS OF THE THRUST SYSTEM

Upper Mesozoic rocks of the thrust system are largely confined to the upper part of the system, above the Rosario thrust (Figs. 3-5), although slices of the Constitution Formation are locally present in structurally lower positions (Fig. 3). These rocks comprise three different tectonostratigraphic units, which are, from structurally lowest to highest: (1) the Constitution Formation, a thick clastic linking sequence; (2) the Lopez Structural Complex, an imbricated fault zone containing a mixed assemblage of Jura-Cretaceous clastic rocks, pillow basalt and chert, and rare slices of Turtleback tonalite; and (3) the Decatur terrane, composed of the Fidalgo Igneous Complex, a Jurassic ophiolite and arc, and the Lummi Formation, an Upper Jurassic and Lower Cretaceous clastic sequence that unconformably overlies the Fidalgo. These units are discussed below with special emphasis on their relationship to older terranes in the lower half of the thrust system.

#### *Constitution Formation: Upper Mesozoic clastic sequence*

The Constitution Formation (Vance, 1975) is a thick, upper Mesozoic clastic sequence composed of massive sandstone, black mudstone, ribbon chert, and minor pillow lava (Fig. 17). Late

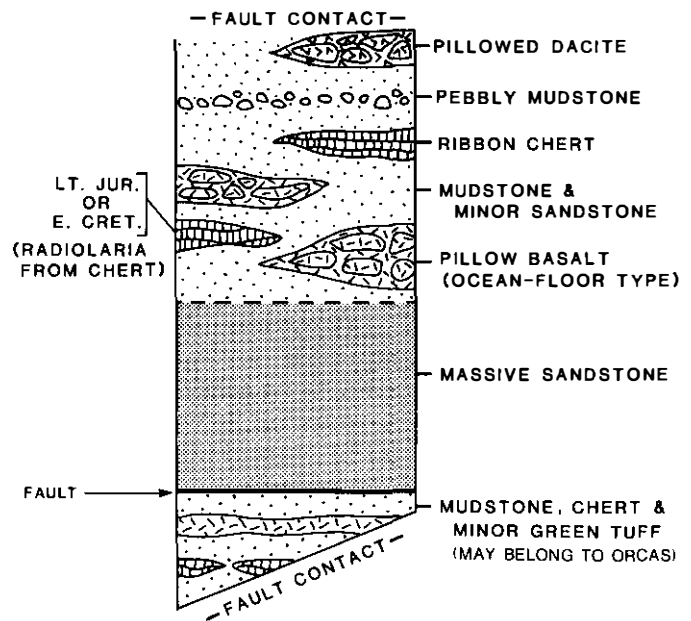


Figure 17. Generalized stratigraphy of the Constitution Formation as exposed on San Juan Island. Radiolaria from chert interbedded with mudstone and sandstone in the upper member are Late Jurassic or Early Cretaceous in age (C1 and C2 in Table A-5). The middle member, consisting of massive sandstone, is undated but probably is of similar age to the upper member. The lower member, which occurs primarily within the Rosario fault zone, is not continuous with the upper members. It is tentatively included with the Constitution because the other two members contain similar mudstone-rich rocks. Alternatively, this lower member may belong to the Orcas Chert.

Cretaceous metamorphic assemblages of prehnite, lawsonite, and aragonite are well developed in the Constitution, and a prehnite-isograd has been recognized on southern San Juan Island. We discuss these relationships in another section below on San Juan metamorphism. In this section, we focus on the stratigraphy and original depositional setting of the Constitution.

**Stratigraphy.** The thickest and perhaps most complete section through the Constitution occurs in a northeast-dipping, 4-km-thick sequence that is variably exposed across southern San Juan Island (Fig. 3). In this area, we recognize three informal units within the Constitution (Fig. 17; units D, A, and B of Brandon, 1980). (1) The lowest consists of black mudstone, green tuff, ribbon chert, and minor volcanoclastic sandstone. Pillowed and sheeted basalts and small pods of limestone are also locally present. (2) The middle unit is composed of massive volcanoclastic sandstone with minor clast-supported conglomerate. (3) The highest consists mainly of thinly interbedded black mudstone and cherty sandstone, with subordinate pebbly mudstone, massive sandstone, ribbon chert, and basalt and dacite pillow lavas.

The lowest unit on southern San Juan Island occurs within the imbricate fault zone at the base of the Constitution, where it is commonly interleaved with slices of Garrison Schist. Unfortunately, not enough is known about this unit to relate it confidently to either the Constitution or the underlying Orcas chert. At present, we tentatively include it with the Constitution because it contains interbedded volcanoclastic sandstone, which is atypical of the Orcas. Vance (1975), however, assigned the unit to the Orcas and considered it to mark a stratigraphic transition between the Orcas and Constitution. We agree that there may have been some stratigraphic tie between the Constitution and Orcas (discussed below) but suspect that any transitional relationship has been obliterated by imbricate faulting along the Rosario thrust.

In contrast, the middle and upper units of the Constitution on southern San Juan Island are relatively intact, with no evidence of exotic fault slices or structural repetition. Our discussion here focuses on this part of the section, which has been studied in more detail. These two units are interpreted to be deep-water deposits, mainly on the basis that the clastic rocks are interbedded with radiolarian ribbon chert (Brandon, 1980). The clastic rocks were probably deposited within a submarine fan system; turbidites, however, are notably absent. The predominance of mud-rich facies in the upper member, plus the presence of pebbly mudstone and soft-sediment deformational features, suggests a slope or base-of-slope depositional setting, whereas massive sandstone and conglomerate in the middle unit may represent large channelized bodies (Mutti and Ricci-Lucchi, 1978; for further discussion see Brandon, 1980).

The upper member contains about 30 percent pillow lava, which occurs as thin tabular bodies ranging from 10 to 45 m thick. Geochemical analyses show that they are mainly basalts, although dacites are also locally present (Table 7; see Appendix B for description of sample locations). Trace-element discriminant diagrams indicate an ocean-floor setting for the basalts and

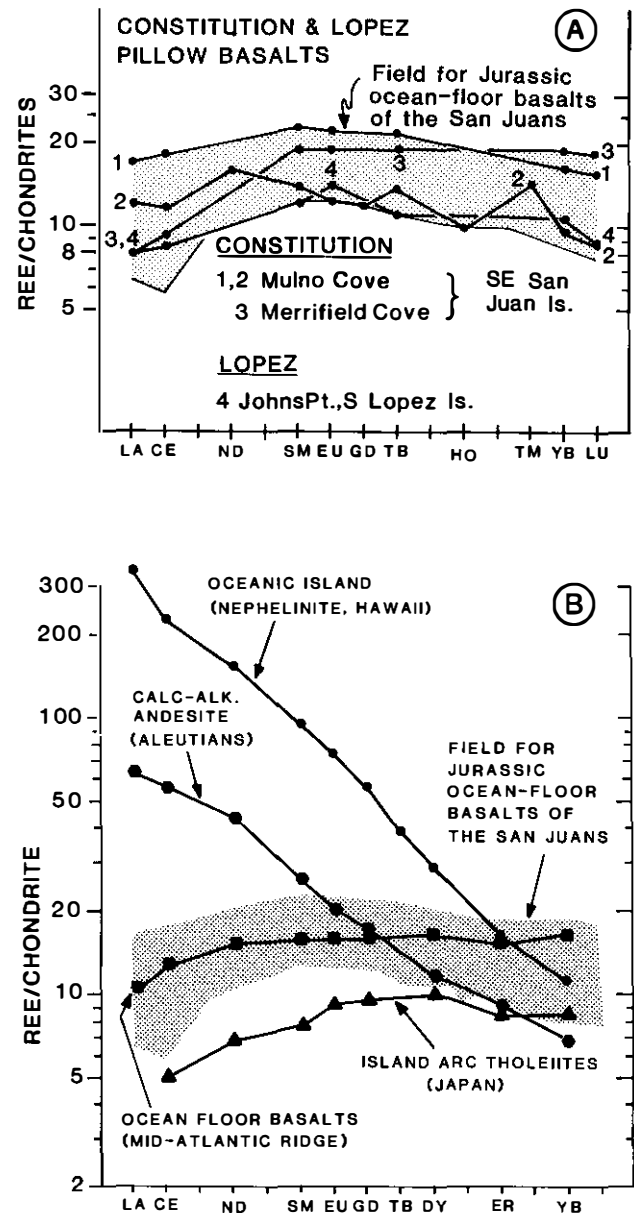


Figure 18. Normalized REE diagrams. (a) Jurassic(?) basalts of the Constitution Formation (GC6-8) and Lopez Structural Complex (GL1). (b) Some representative modern volcanic-tectonic settings (Garcia, 1978). The REE patterns for the Jurassic(?) basalts of the Constitution and Lopez are identical to modern ocean-floor basalts. The shaded region in both figures indicates the collective range for ocean-floor-type basalts in the Constitution, Lopez, and Fidalgo units (see Fig. 23 for Fidalgo data). Appendix B gives the analyses and their location; locality numbers of plotted analyses are shown above in parentheses. REE data are normalized to average chondrite values of Haskin and others (1968).

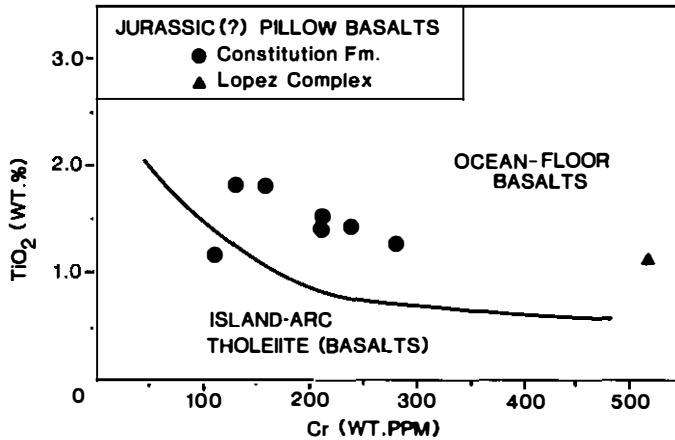


Figure 19.  $\text{TiO}_2$ -Cr discriminant diagram (Garcia, 1978) for Jurassic(?) basalts of the Constitution Formation (GCI-7) and Lopez Structural Complex (GL1). This diagram further supports the conclusion that these basalts were erupted in an ocean-floor setting, such as a mid-oceanic ridge or back-arc basin. These basalts are distinct from island-arc basalts in that they are not strongly depleted in the incompatible elements, such as Ti, Cr, and also REE (see Table 4). Appendix B gives the analyses and their location; locality numbers of plotted analyses are shown above in parentheses.

suggest a volcanic-arc setting for the dacites (Table 7; Figs. 18 and 19).

The origin of these pillow lavas is problematic. They are not exotic fault slices because, where exposed, the upper and lower contacts of the volcanic bodies are unfaulted and appear to be depositional. Thus, they may be interbedded flows within a clastic-rich sequence. For the pillow basalts, this relationship would imply that the Constitution was deposited at or near a spreading ridge since pillowed flows do not extend far from their vent area. Sedimentary sequences at modern sediment-dominated spreading centers, such as the Guaymas Basin in the Gulf of California (Einsele and others, 1980), are commonly intruded by numerous dikes and sills and also are extensively mineralized and metamorphosed since the sediments inhibit heat loss and thereby create a high geothermal gradient. There is no evidence in the Constitution for any of these features. Therefore, we suggest a third possibility: the Constitution pillow lavas represent submarine slide blocks derived from an older volcanic unit. The apparent depositional nature of the contacts around the bodies may be due to the slide blocks settling into the soft muddy sediment after emplacement. A situation similar to this one has been documented in the Pacific Rim Complex (Brandon, 1985; Fig. 1), a unit probably correlative to the Constitution (discussed below). In that case, a slide-block origin can be demonstrated because the pillow basalts are older (Late Jurassic) than the Lower Cretaceous clastic sequence that surrounds them. A possible source for the pillow lavas in the Constitution might have been the Fidalgo

Complex, which contains both ocean-floor basalts and arc-volcanic dacites (Table 7).

**Age.** The age of the Constitution Formation is not well defined. At two localities, radiolaria from ribbon cherts interbedded with clastic rocks of the upper member give an imprecise Late Jurassic or Early Cretaceous age (Fig. 17; C1 and C2 in Table A-5). Whetten and others (1978) reported several other radiolarian localities for the Constitution on Orcas Island; further work, however, suggests that these localities are probably part of the Decatur terrane (D22-24 in Table A-7). The age of the lower two members is not directly known, although conodonts from a limestone olistolith (C3 in Table A-5) indicate a Late Triassic maximum age for the lowest unit. We suspect that the Constitution is probably no older than Middle or Late Jurassic, based on the age range of other similar clastic units in the Pacific Northwest (Fig. 6).

**Provenance of clastic rocks.** The Constitution Formation is entirely fault-bounded and preserves no direct evidence of stratigraphic relationships with older or younger units. The provenance of clastic rocks, however, can help identify which terranes were adjacent to the Constitution during Jurassic and Early Cretaceous time. Our studies of sandstone and conglomerate clasts indicate that the source area of the Constitution was dominated by intermediate and silicic volcanic rocks with minor basalt (Brandon, 1980; Vance, 1975). Volcanic lithic clasts in the sandstone are angular and apparently represent first-cycle detritus eroded from an active(?) volcanic-arc terrane. A geochemical analysis indicates that Constitution ribbon chert also contains significant amounts of arc-volcanic detritus (Karl, 1982).

Both sandstone and conglomerate also contain minor but ubiquitous clasts of metamorphic minerals and rock fragments, which indicate that the source region included mafic schist that ranged in grade from greenschist to albite-epidote amphibolite to blueschist (Vance, 1975; Brandon, 1980). Metamorphic assemblages and textures are similar to those observed in nearby Permo-Triassic mafic schists, such as the Garrison Schist in the San Juan Islands and the Vedder Complex of the North Cascades (Misch, 1977; Armstrong and others, 1983).

Minor clasts of chert, locally containing radiolaria, indicate that a chert-rich sequence, such as the Deaman Bay terrane, was also present in the source area. This conclusion is further supported by Danner's discovery of a fusulinid-bearing limestone clast in a Constitution conglomerate located at Bell Point on San Juan Island (Danner, 1977, p. 484; Danner, written communication, 1979). Danner identified the fossils as Schwagerinids of "Tethyan aspect" and suggested that the clast was derived from limestones of the Deadman Bay Volcanics.

**Origin and tectonic setting.** The overall association of Constitution lithofacies suggests deposition at a continental margin. Volcanic-rich sandstones indicate the proximity of an extensive volcanic-arc terrane, although it is not known if this arc terrane was active during Constitution time. The Constitution also represents an important linking sequence since it was deposited in close proximity to a volcanic-arc terrane and an uplifted

**TABLE 7. SUMMARY OF GEOCHEMICAL DATA FOR THE CONSTITUTION FORMATION, LOPEZ COMPLEX, FIDALGO COMPLEX, AND HARO TERRANE**

Rock unit	Interpreted tectonic setting†	SiO <sub>2</sub> %	TiO <sub>2</sub> %	Ti/V	Y/Nb	Zr (ppm)	Cr (ppm)	REE pattern‡
<b>Constitution Formation</b>								
Jurassic(?) pillow basalts	ocean-floor basalt	51.4 [7] (47.1-53.9)	1.47 [7] (1.12-1.80)	32 [5] (25-39)	<3.2 [5]	90 [5] (73-120)	194 [8] (110-283)	flat pattern with depleted LREE [3]
Jurassic(?) pillowed dacite	volcanic arc(?)	61.7 [1]	0.56 [1]	n.d.	n.d.	n.d.	3 [1]	strong LREE enriched [1]
<b>Lopez Structural Complex</b>								
Jurassic pillow basalts of Johns Point	ocean-floor basalt(?)	54.4 [1]	1.14 [1]	n.d.	34 [1]	60 [1]	515 [1]	flat pattern with depleted LREE [1]
mid-Cretaceous pillow basalts of Richardson	oceanic island(?)	52.9 [1]	2.79 [1]	n.d.	1.9 [1]	185 [1]	74 [4] (10-110)	moderately LREE enriched [4]
<b>Fidalgo Igneous Complex</b>								
M. to U. Jurassic pillow basalts	ocean-floor basalt	50.1 [5] (47.3-52.5)	1.38 [5] (1.08-1.67)	n.d.	9 [1]	92 [1]	210 [6] (142-346)	flat pattern with depleted LREE [6]
M. to U. Jurassic volcanics, dikes and intrusives	volcanic arc built on ophiolite	60.3 [18] (49.3-75.6)	0.59 [18] (0.31-1.07)	n.d.	n.d.	47 [8] (38-55)	169 [11] (3-520)	slightly to moderately LREE enriched [5]
<b>Haro Terrane</b>								
Volcanic clasts from U. Triassic Haro Formation	derived from active low-K volcanic arc	72.9 [2] (67.6-78.3)	0.34 [2] (0.21-0.46)	n.d.	n.d.	n.d.	14 [2] (3-25)	flat pattern [2]
Volcanic clasts from Jura-Cret. Speiden Group	derived from a Lt. Jurassic moderate-K volcanic arc	67.3 [3] (63.8-73.6)	0.43 [3] (0.38-0.48)	n.d.	n.d.	n.d.	7 [3] (4-9)	moderately LREE enriched [3]

Note: The data format is: mean [number of analyses]; (min.-max.); n.d. = not determined. All elements and oxides are relative to a volatile-free basis.

See Appendix B for total analyses and description of sample locations.

†See Table 4.

‡REE (rare earth element) patterns normalized to chondritic abundances; number of analyses in brackets; Eu = Europium; LREE = light REE.

assemblage of older rock, which included a high-pressure metamorphic terrane and a Tethyan limestone-chert terrane. These older terranes are inferred to be the Garrison and Deadman Bay.

**Regional correlation.** The Constitution Formation is probably equivalent to other Jurassic–Lower Cretaceous units sporadically exposed around southern and western Vancouver Island, which include the Pandora Peak unit of Rusmore and Cowan (1985; part of LRS in Fig. 1) and the Pacific Rim Complex of western Vancouver Island (Brandon, 1985; PRC in Fig. 1). These units are characterized by a distinctive association of mudstone, chert, green tuff, massive sandstone, and minor ocean-floor basalt. Furthermore, all have been affected by Late Cretaceous lawsonite-prehnite metamorphism. Brandon (1985) considers the Pacific Rim Complex and Pandora Peak unit to be displaced pieces of the San Juan thrust system that were moved northwestward by transform faulting, probably during early Cenozoic time.

### ***Lopez Structural Complex: Late Cretaceous imbricate fault zone***

The Lopez Structural Complex (Cowan and Miller, 1981; Brandon, 1980) is exposed along the southern coast of Lopez Island and on the southeast tip of San Juan Island (Fig. 20). It represents a thick fault zone, about 2.5 km across, sandwiched between two more coherent units, the Constitution Formation and the Decatur terrane. At map-scale, the Lopez consists of an imbricated series of elongate, lenticular fault slices, that dip moderately northeast beneath the Decatur terrane (Fig. 20). Many of the fault slices are similar to, and were probably derived from, the Constitution Formation or Decatur terrane; others, however, contain exotic rock units that cannot be related to the upper or lower plates of the fault zone.

We consider the Lopez Complex to be a separate map unit, distinguished by its internal diversity of rock units and by its imbricate structural style. The base of the Lopez is not exposed. The top of the complex is the Lopez thrust, which marks the uppermost limit of significant structural interleaving among the various units within the Lopez Complex. This thrust is relatively easy to follow because it generally places igneous rocks of the Decatur terrane over sedimentary units of the Lopez Complex (Figs. 3 and 20). Note that in previous papers (e.g., Cowan and Whetten, 1977) the Lopez Complex was defined to include those rocks on southern Lopez Island with a pronounced flattening cleavage. We abandon this definition because further study has shown that this cleavage was developed after formation of the Lopez Complex, and that it is much more widespread in the San Juan Islands, occurring in the Decatur terrane on Lummi Island (Carroll, 1980) and in the Constitution Formation and Orcas Chert on southern San Juan Island (Brandon, 1980).

**Rock units and ages.** The most common rock unit in the Lopez Complex consists of well-bedded turbidite sandstone with interbedded mudstone and minor conglomerate. This unit is very similar to, and was probably derived from, the Lummi Forma-

tion, which makes up part of the overlying Decatur terrane. The distinctive feature that links these two units is the composition of the turbidite sandstone, which consists of either abundant shale chips or very coarse to granule-sized clasts of white and gray chert.

Other rock units derived from the Decatur terrane include Jurassic pillow basalt and minor brecciated gabbro. The part of the Decatur terrane that lies directly above the Lopez Complex contains similar pillow basalts, Middle to Late Jurassic in age, as well as brecciated mafic plutonic rocks (Lopez greenstone of Whetten, 1975). The age of the Jurassic pillow basalts in the Lopez Complex is based on radiolaria from interbedded ribbon chert at Johns Point (Fig. 20; L3 in Table A-6). A chemical analysis of the basalt at this locality suggests an ocean-floor setting, like the pillow basalts in the Decatur terrane (Table 7; Figs. 18 and 19; see Appendix B for a description of sample locality).

Rock units thought to be derived from the Constitution Formation include: (1) chaotic mudstone-rich sequences consisting mainly of olistostromal pebbly and bouldery mudstones, with clasts of sandstone, basalt, and chert dispersed in a black mudstone matrix; and (2) sandstone sequences with interbedded chert, green tuff, and basalt. The first of these two units has yielded Early Cretaceous (Valanginian) *Buchia*, and the second has yielded Jurassic or Cretaceous radiolaria from interbedded chert (L1 and L2 in Table A-6).

Exotic rock units in the Lopez Complex consist of two small slices of early Paleozoic tonalite and a large slice, about 2.5 km long, of middle Cretaceous pillow basalt and gabbro (Fig. 20). The slices of tonalite, both of which have been dated by the U/Pb zircon method (T5-6 in Table A-6), are identical in age, rock type, and geochemistry to tonalite of the Turtleback Complex (see Table B-2 for comparison of geochemistry). Even though we can identify a source for these tonalite slices, they are certainly unusual because they lie in such a structurally high position with respect to the main occurrence of the Turtleback Complex (Fig. 4).

The middle Cretaceous unit, however, is truly exotic in that it has only been found in the Lopez Complex. It occurs in the vicinity of the town of Richardson (Fig. 20) and consists mainly of vesicular pillow basalts, pillow breccia, and related diabase and gabbro. An interbed of red and black shale has yielded middle Cretaceous (latest Albian) foraminifera (L4 in Table A-6), which makes these the youngest dated rocks in the San Juan thrust system. In contrast to other Jura-Cretaceous units, sandstone is notably absent in this basaltic sequence. The shale interbed, however, contains minor amounts of sand-size volcanic quartz and feldspar, indicating that an intermediate or silicic volcanic terrane was located nearby. The basalts display a strongly enriched light REE pattern (Table 7; see Figure 5b in Vance and others, 1980; locality descriptions are in Appendix B), showing that they are not ocean-floor basalts. TiO<sub>2</sub>, Y, and Nb contents, which are available only for one sample, suggest that they may be oceanic-island basalts (Table 7).

As elsewhere in the San Juan thrust system, rocks of the

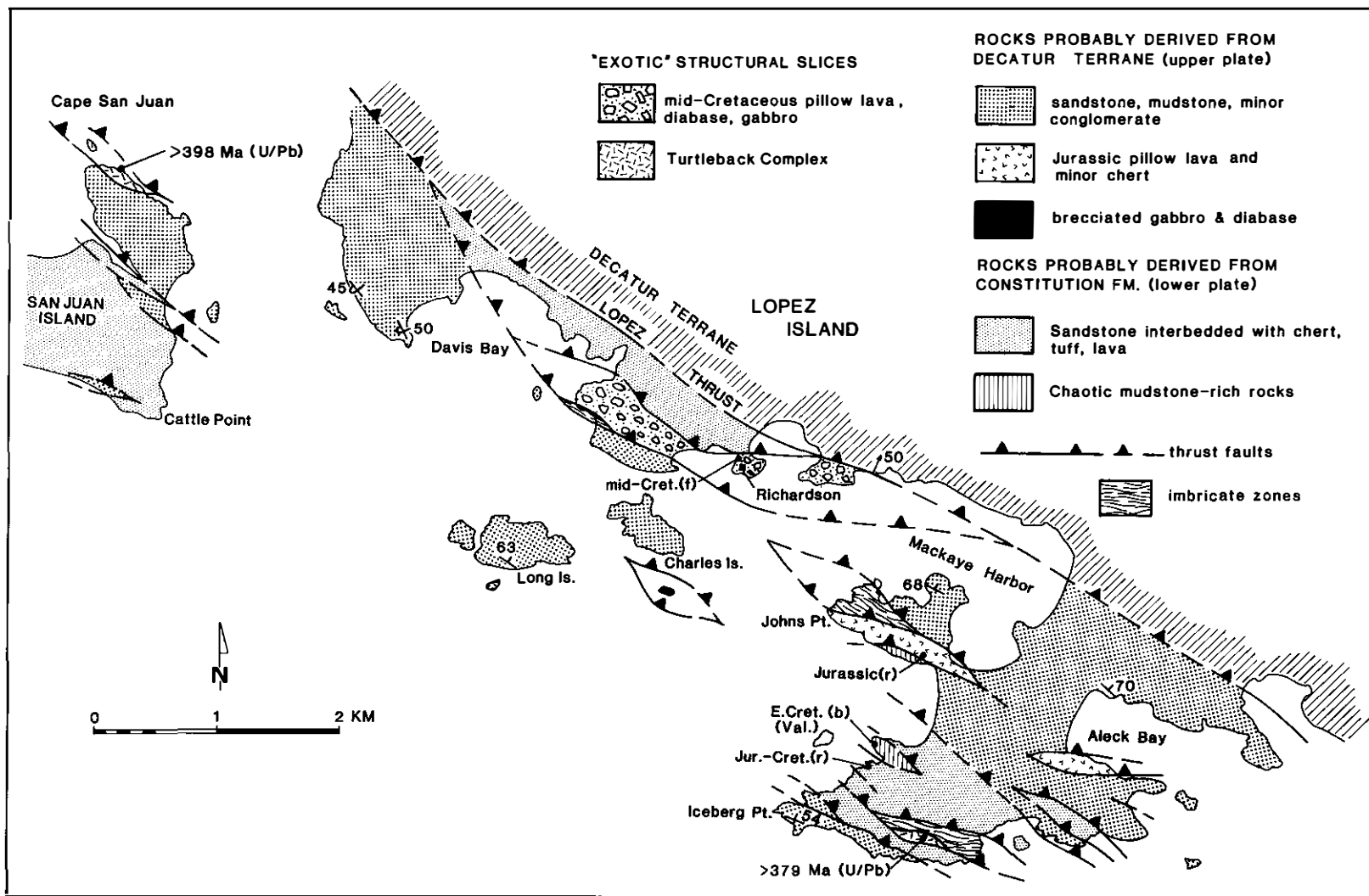


Figure 20. Geologic map of the Lopez Structural Complex, as exposed on southern Lopez and San Juan Islands. The Lopez represents an imbricate fault zone sandwiched between an upper plate of Decatur terrane and a lower plate of Constitution Formation. This map is compiled from Cowan (unpublished mapping) for southern Lopez Island and from Brandon (1980) for southern San Juan Island. The location of fossil ages and isotopic dates (Table A-6) are: f = foraminifera from mudstone at Richardson, r = radiolaria from chert, b = *Buchia pacifica* from sandstone, and U/Pb = U/Pb zircon dates from Turtleback tonalite.

Lopez Complex were affected by Late Cretaceous high-pressure metamorphism (Glassley and others, 1976; Brandon, 1980). Sandstones contain lawsonite and aragonite; the slices of Turtleback tonalite contain rare lawsonite. Basalts, including the Richardson basalts, contain aragonite, pumpellyite, and chlorite; gabbro associated with the Richardson basalts contains rare blue amphibole.

**Internal structural relations.** We consider the map-scale pattern of the Lopez Complex, which shows a diverse assemblage of lenticular rock units, to be the strongest evidence that the complex is an imbricate fault zone. Other supporting evidence includes the presence, in well-exposed outcrops, of brittle-style fault zones between these various rock units (Fig. 20), and the fact that the complex as a whole lies structurally beneath plutonic rocks of the Decatur terrane.

There are local indications, however, that some of the clastic units in the Lopez Complex were deformed prior to thrusting, perhaps by mass-movement processes. For instance, thick coherent sequences of turbidite sandstone are commonly upside-down (see west side of Davis Bay in Fig. 20), with no evidence of associated fold hinges or upright limbs. Outcrop-scale folds are not common, but where present they have variable orientations and unusual geometries; some are antiformal synclines and others are synformal anticlines (i.e., downward facing). These sequences apparently were overturned and folded prior to lithification because they lack a related axial-planar cleavage or evidence of pervasive cataclasis. A late-stage flattening cleavage is present, but is typically oriented at a high angle to the axial plane of these folds. The Pacific Rim Complex also contains thick upside-down turbidite sequences and randomly oriented folds (Brandon, 1985). In that case, a good argument can be made that these types of structures were formed by widespread submarine slumping during the Early Cretaceous.

**Decatur terrane: Upper Mesozoic ophiolite, arc, and clastic sequence**

The Decatur terrane (Whetten and others, 1978) lies above the Lopez thrust and represents the structurally highest unit in the San Juan thrust system. This terrane is widely exposed in the eastern part of the archipelago (Fig. 3) and appears to be a relatively coherent unit. An aeromagnetic map of the San Juan Islands demonstrates the regional continuity of this terrane between various island exposures (Whetten and others, 1980). The Decatur terrane is composed of two stratigraphically related units (Fig. 21): an ophiolite and arc-volcanic sequence called the Fidalgo Igneous Complex (Brown, 1977), and an overlying clastic sequence called the Lummi Formation (Vance, 1975).

**Composition and age of the Fidalgo Complex.** The Fidalgo Complex has been studied in detail on Fidalgo Island (Brown, 1977; Gusey, 1978; Brown and others, 1979). Our work elsewhere in the San Juan Islands indicates that the Fidalgo Island exposures are generally representative of the complex as a whole. A schematic section of the Fidalgo Complex is shown in Figure 21; age relationships are summarized in Figure 22.

The lower plutonic part of the complex consists of an older suite of mafic and ultramafic rocks (serpentinized harzburgite, clinopyroxenite, and gabbro), which are well exposed on Fidalgo, Blakely, and Cypress Islands, and a younger crosscutting suite consisting of irregular dikes and stocks of tonalite and subordinate diorite and quartz diorite (equivalent to the trondhjemite, albite granite, and diorite of Brown and others, 1979, and the plagiogranite of Whetten and others, 1978). Rocks of both plutonic suites are also present on Lopez Island (Lopez greenstone of Whetten, 1975; includes pyroxenite, gabbro, quartz diorite, and tonalite), although, in comparison with their Fidalgo Island counterparts, the Lopez Island rocks generally are more highly deformed and brecciated. On Lummi Island, only the younger suite is present (Carroll, 1980).

At three localities, the younger tonalitic intrusions have yielded nearly concordant U/Pb zircon dates, ranging from 170 to 160 Ma (DF1a, DF2a, and DF4a in Table A-7). Three K-Ar hornblende dates for diorite and layered gabbro on Fidalgo Island range from 162 to 152 Ma (DF1b and DF5-6 in Table A-7). These dates are slightly younger than the U/Pb dates, perhaps due to resetting during intrusion of the tonalitic suite. Brown and others (1979) concluded, based on field relations and chemical trends, that the younger intrusions were not comagmatic with the older mafic and ultramafic suite. Thus, these dates should only be considered as minimum ages for the older suite.

Zircons from tonalite at a fourth locality on Lopez Island have yielded a disparate group of discordant U/Pb dates, which lack a linear relationship on a concordia plot (DF3 in Table A-7; see Fig. 7 in Whetten and others, 1978). We consider dates from this locality to be spurious, perhaps a result of the laboratory contamination problems discussed in Whetten and others (1980). The  $167 \pm 5$  Ma date for the Fidalgo Complex reported by Whetten and others (1978) represents a composite intercept date using data from three localities (DF1-3), including this spurious Lopez Island locality.

The upper part of the Fidalgo Complex consists of a varied sequence of volcanic and sedimentary rocks. On Fidalgo Island, plutonic rocks of the complex are overlain by an interbedded sequence of mafic to silicic volcanic rocks, tuffaceous and pelagic argillite, and sedimentary breccia and conglomerate (Gusey, 1978; Brown and others, 1979). Radiolaria from the argillite give Late Jurassic ages (Fig. 22; DF15-18 and DF20 in Table A-7). The volcanic rocks do include minor basalts, but consist chiefly of altered andesite and dacite, locally with quartz phenocrysts. Brown and others (1979) concluded that these volcanic rocks are cogenetic with the tonalitic intrusions present lower in the complex. The breccia and conglomerate are composed of clasts derived entirely from plutonic and volcanic rocks of the complex and probably represent submarine talus and slide deposits, presumably formed along some type of fault scarp (Brown and others, 1979).

Parts of this Fidalgo Island volcanic-sedimentary sequence are also present on Lopez and Lummi Islands. For instance, Upper Jurassic (lower Tithonian) pelagic argillite is found on

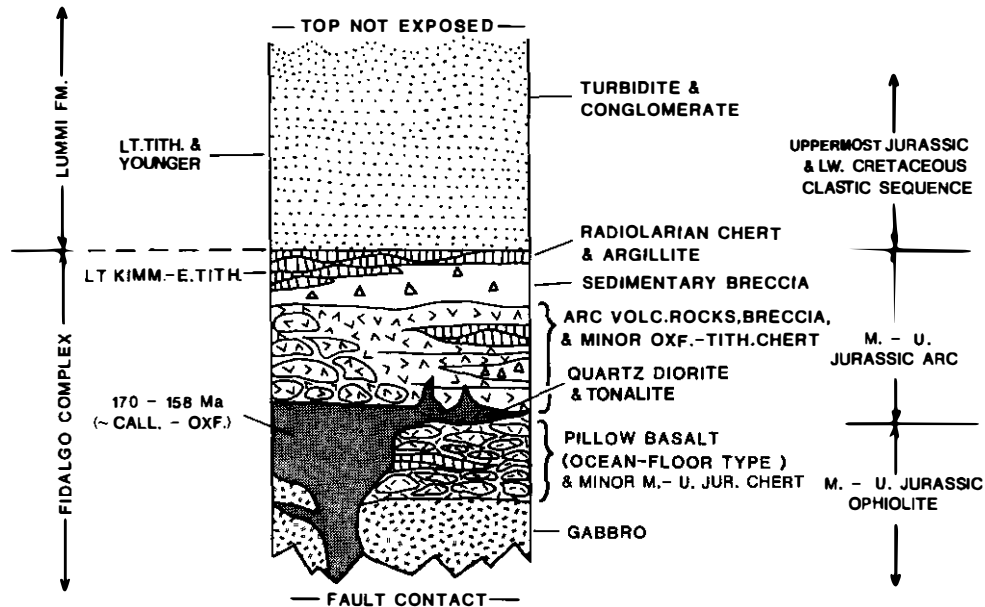
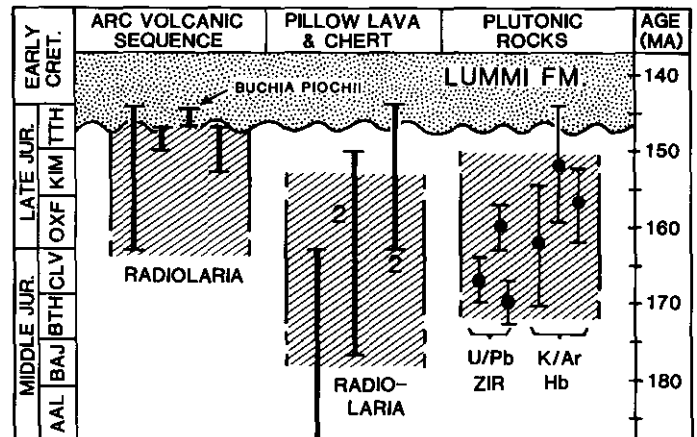


Figure 21. Generalized stratigraphy of the Decatur terrane, adapted from Brown and others (1979) and Gusey (1978). The lower part of the terrane consists of the Fidalgo Igneous Complex, a Middle to Upper Jurassic ophiolite and superimposed arc-volcanic sequence. The Fidalgo includes plutonic rocks and a stratigraphically higher sequence of volcanic flows and tuffs, argillite, and chert, and breccias cannibalized from volcanic and plutonic portions of the complex. The upper part of the terrane is the Lummi Formation, a Jura-Cretaceous clastic unit that depositionally overlies the Fidalgo Complex.

Figure 22. Age relations in the Fidalgo Igneous Complex. The columns show selected fossil ages and isotopic dates for different parts of the Fidalgo. The pillow basalt and chert unit, which has yielded both Middle and Late Jurassic ages, is considered to belong to the older, ophiolitic portion of the Fidalgo Complex because the basalts are ocean-floor type (Table 7). Tonalites and diorites, dated from the plutonic part of the Fidalgo Complex, are thought to represent the intrusive component of a younger superimposed volcanic arc. The Upper Jurassic arc-volcanic sequence, exposed on Fidalgo Island, represents the extrusive part of this proposed arc. The apparent mismatch in the age of the plutonic rocks and the arc-volcanic sequence may be due to large uncertainties ( $\pm 15$  m.y.) in the absolute age of the Middle to Late Jurassic boundary (Harland and others, 1982). Isotopic dates are shown with error brackets at the 95 percent confidence level. Brackets for fossil ages indicate their possible age range. A number is shown next to those brackets where there is more one locality with the same age range. The time scale is from Harland and others (1982). See Appendix A for further information on the dated localities shown here (arc-volcanic sequence: DF15-16, DF19-20; pillow basalt and chert: DF8-11, DF14; plutonic rocks: DF1a,b, DF2a, DF4-6; Lummi Formation: DLI).



Trump Island near Lopez Island (DF19 in Table A-7), and sedimentary breccia is common along the east coast of Lopez Island. Another volcanic unit, consisting of pillow basalt with interbedded radiolarian ribbon chert, is also present on Lopez and Lummi Islands and at Rosario Head, located at the southwest end of Fidalgo Island. Chert from this unit has yielded both Middle and Late Jurassic ages (Fig. 22; DF7-14), which suggests that it is older than the volcanic-sedimentary sequence on Fidalgo Island. This difference in age is important, especially in light of the geochemistry of these two volcanic units (discussed below).

**Geochemistry and tectonic setting of the Fidalgo Complex.** Stratigraphic and petrologic relationships indicate that the Fidalgo Complex is a fragment of oceanic lithosphere (Gusey, 1978; Brown and others, 1979; Vance and others, 1980). What remains controversial is the original tectonic setting in which this fragment formed. Vance and others (1980) suggested that the Fidalgo Complex and other coeval ophiolites in the Pacific Northwest formed in a small ocean basin that opened in a continental setting (also see Davis and others, 1978). Brown (1977) and Gusey (1978) proposed that the Fidalgo represents an island arc; in another publication, however, Brown and others (1979) concluded that the evidence was ambiguous.

Based on geochemical data from Brown and others (1979) and additional data of our own (Appendix B), we conclude that the Fidalgo Complex contains igneous rocks formed in two different volcanic-tectonic settings. The pillow basalt-chert unit, exposed on Lummi and Lopez Islands, was probably erupted in an ocean-floor setting, whereas the volcanic-sedimentary sequence of Fidalgo Island represents a younger arc-volcanic sequence.

The pillow basalt unit is characterized by flat REE patterns with slight light REE depletion (Fig. 23a) and by high TiO<sub>2</sub>, Cr, and Zr contents (Table 7), all features of modern ocean-floor basalts (Table 4). Analyses plotted on the TiO<sub>2</sub>-Cr discriminant diagram of Pearce (1975) clearly fall in the ocean-floor basalt field (Fig. 24); other discriminant diagrams from Pearce and Cann (1973) and Garcia (1978) give similar results.

Geochemical analyses of the volcanic, tonalitic and dioritic rocks of Fidalgo Island (Figs. 23b and 24) indicate that they are similar to island-arc tholeiites, a common magma suite in immature island arcs of the western Pacific (Jakeš and Gill, 1970; Gill, 1981). Gill (1981) has shown that for arc-volcanic rocks there is a complete gradation from low-K tholeiites to high-K calc-alkaline volcanics. Mafic rocks from the island-arc tholeiite suite are distinguished by low abundances of TiO<sub>2</sub>, Cr, Zr, and the REE (Table 4) and by flat REE patterns with minor amounts of light REE enrichment or depletion (Fig. 23b; Jakeš and Gill, 1970; Gill, 1981). Differentiation causes the more silicic varieties to be enriched in Zr, the light REE, and possibly TiO<sub>2</sub>. Analyses of mafic volcanics and diorite from Fidalgo Island cluster in the island-arc tholeiite field on a TiO<sub>2</sub>-Cr diagram (Fig. 24); the TiO<sub>2</sub>, Y, Zr diagram of Pearce and Cann (1973) gives the same result. REE patterns for basalts and a mafic dike also lie in the island-arc tholeiite field (Fig. 23b).

Another characteristic of the island-arc tholeiite suite is a

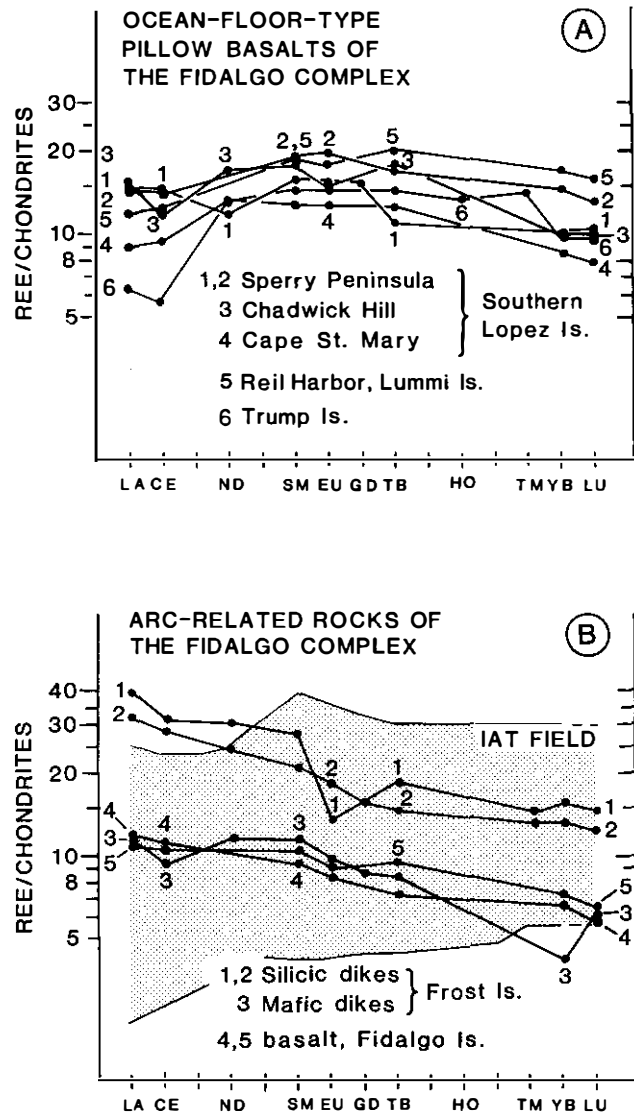


Figure 23. Normalized REE diagrams for volcanic rocks of the Fidalgo Complex. (a) Basalts (GF1-6) from the pillow basalt and chert unit (Fig. 22) have REE patterns identical to modern ocean-floor basalts (see Fig. 18b). They are considered to belong to the older ophiolitic portion of the Fidalgo Complex. (b) Volcanic rocks and dikes associated with the younger, arc-volcanic sequence of Fidalgo Island (Fig. 22) have REE patterns that, when taken together with other geochemical data, indicate that they are island-arc tholeiites (IAT). The more mafic samples (GDF14-15, GDF23; SiO<sub>2</sub> = 49 to 57 percent), labeled 3, 4, and 5 in the figure, show low REE abundances and minor light-REE enrichment, which is a typical pattern for mafic volcanics from modern IAT suites (Gill, 1981). The moderate light-REE enrichment of the more silicic samples (GDF24-25; SiO<sub>2</sub> = 67 percent and 75 percent), labeled 1 and 2 in this figure, is attributed to extensive differentiation. Appendix B gives the analyses and their location; locality numbers of plotted analyses are shown above in parentheses. REE data are normalized to average chondrite values of Haskin and others (1968).

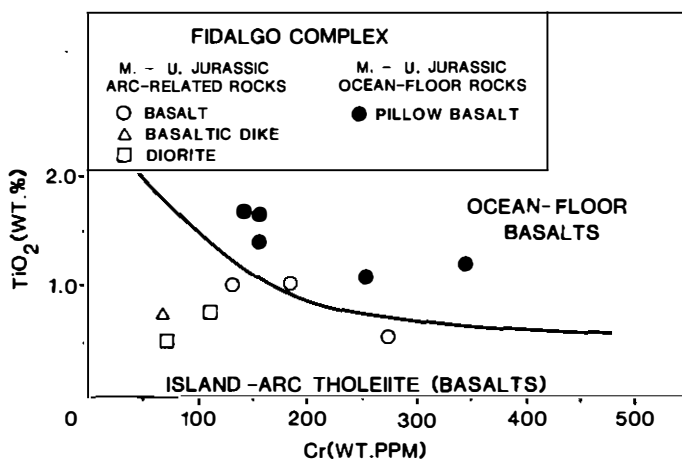


Figure 24. TiO<sub>2</sub>-Cr discriminant diagram (Garcia, 1978) for basaltic rocks of the Fidalgo Igneous Complex. Pillow basalts (GDF1-2, GDF4-6) from the pillow basalt and chert unit (Fig. 22) fall in the ocean-floor basalt field, consistent with their REE patterns (Fig. 23a). Basalts (GDF7-8, GDF14; SiO<sub>2</sub> = 50 to 57 percent) from the younger arc-volcanic sequence of Fidalgo Island plot in the island-arc tholeiite field, with one marginal exception. Mafic plutonic rocks (diorites) and a basaltic dike (GDF9-10, GDF23; SiO<sub>2</sub> = 49 to 58 percent), exposed on Fidalgo and Frost Islands, also fall in the island-arc tholeiite field and are considered to be related to the arc-volcanic sequence. Appendix B gives the analyses and their location; locality numbers of plotted analyses are shown above in parentheses. Only the more mafic samples from the Fidalgo Complex are plotted on this diagram, as specified by Pearce (1975) and Garcia (1978).

low K<sub>2</sub>O content over a wide range of silica contents (45 to 70 percent SiO<sub>2</sub>) (Jakeš and Gill, 1970), which is the case for volcanic rocks, diorite, and quartz diorite on Fidalgo Island (Fig. 25). Brown and others (1979) showed that the low K<sub>2</sub>O contents of the Fidalgo Island rocks was a primary feature and not a result of hydrothermal alteration.

The difference in the trace-element abundances of these two groups of igneous rocks indicates that they were produced from different mantle sources (Kay, 1984; Wilson and Davidson, 1984). In our interpretation, ocean-floor pillow basalts and ultramafic and mafic plutonic rocks of the Fidalgo Complex represent oceanic crust and mantle formed at a ridge or in a back-arc basin, probably during the latest Middle and earliest Late Jurassic. The arc-volcanic sequence of Fidalgo Island, and related diorite and quartz diorite, represent a younger island arc that was built on this older oceanic crust.

Sedimentary breccia interbedded with arc-volcanic rocks indicate that the basement of this proposed arc was uplifted and eroded as the arc developed. A similar situation exists in the Marianas arc (Bloomer, 1983) where submarine fault scarps have exposed the underlying arc basement, which consists of a variety of volcanic and plutonic rocks, including gabbros and ultramafic

rocks. The breccia deposits forming at the base of these fault scarps may represent a modern analogue for the distinctive breccias of the Fidalgo Complex.

An apparent problem with our ophiolite-arc interpretation is that, as illustrated in Figure 22, the U/Pb dates of the arc-related tonalites appear to be older than the Late Jurassic age of the arc-volcanic sequence. We note, however, that the absolute age of the Middle to Late Jurassic boundary is not well known and may be in error by as much as 15 m.y. (Harland and others, 1982).

**Stratigraphy and age of the Lummi Formation.** The Fidalgo Complex is overlain by a sequence of well-bedded turbidite sandstone, mudstone, and conglomerate, about 2 km thick (Garver, 1985). Vance (1975) introduced the name Lummi Formation for exposures of this unit on Lummi and Orcas Islands. We extend this name to include all Upper Jurassic and Lower Cretaceous clastic rocks that overlie the Fidalgo Complex. The basal contact of the Lummi is defined to lie directly above the stratigraphically highest occurrence of volcanic rocks and chert (Fig. 18). Representative sections of the unit are present on Decatur and Lopez Islands. Individual sections of the Lummi, as exposed on various islands, all appear to be broadly correlative. For more detailed stratigraphic information, refer to the recent work of Garver (1988), which provides a detailed sedimentological analysis of the Lummi.

The Lummi Formation is latest Jurassic and probably also Early Cretaceous in age. The age of the base of the unit is well constrained because it overlies Upper Jurassic (lower Tithonian or upper Kimmeridgian) argillite of the Fidalgo Complex (DF20 in Table A-7) and contains latest Jurassic (late Tithonian) *Buchia piochii* (DL1 in Table A-8). Additional fossil localities give only imprecise Late Jurassic-Early Cretaceous ages (DL2-4 in Table A-8). However, judging from the thickness of the unit, the Lummi probably ranges into the Lower Cretaceous.

Like the Constitution Formation, clastic rocks of the Lummi Formation were derived from a lithologically diverse source area. Two types of sandstones are present: one is dominated by volcanic detritus, the other by chert clasts. Minor amounts of detrital metamorphic fragments are also present, consisting of epidote, prehnite, and pumpellyite (Vance, 1975), and rare glaucophane-lawsonite blueschist. On James Island, conglomerates at the base of the Lummi contain clasts of pyroxenite and gabbro derived from the underlying Fidalgo Complex.

In comparison to other stratigraphic units in the San Juan Islands, the Lummi Formation is relatively undeformed. In several places, the Fidalgo Complex has been thrust over the Lummi (Fig. 3); fault slices from other San Juan terranes, however, are notably absent. Although there is little evidence for map-scale folds, parts of the Lummi are entirely upside-down, similar to the upside-down turbidite sequences in the Lopez Complex. This deformation may be due to syn-depositional slumping.

**Metamorphism of Decatur rocks.** The Decatur terrane clearly has been affected by Late Cretaceous high-pressure metamorphism, but the results of this metamorphism appear to be

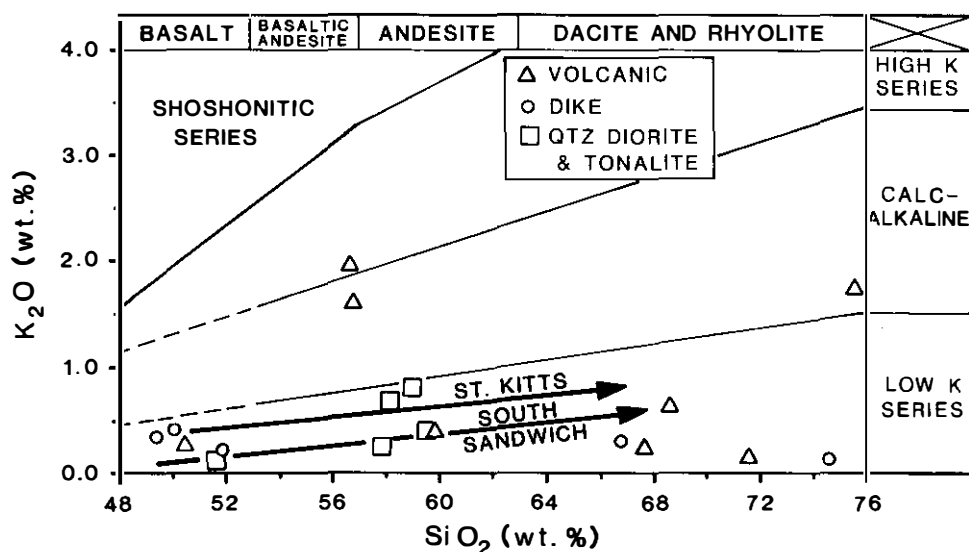


Figure 25.  $K_2O$ - $SiO_2$  diagram for arc-related volcanic and plutonic rocks of the Fidalgo Igneous Complex. This diagram illustrates the wide silica range and generally low  $K_2O$  content of this suite of rocks, which is another characteristic of low-K island-arc tholeiites. Representative trends for modern, low-K, island-arc tholeiites from St. Kitts and South Sandwich are shown for comparison. Diagram is from Wilson and Davidson (1984).

more variable than elsewhere in the San Juan Islands. Based on our reconnaissance study of Lummi sandstones on Decatur and northern Lopez Island, the characteristic assemblage appears to be prehnite + calcite, both in veins and in the matrix of the rocks; Mulcahey (1975) has reported the same assemblages for Lummi sandstones on Fidalgo and Guemes Islands. Lawsonite, aragonite, pumpellyite, and prehnite are widespread in sandstone and basalt on Lummi Island (Carroll, 1980). Lawsonite-bearing assemblages are also present in Decatur terrane rocks on southern Lopez Island. Aragonite is not common in the Decatur terrane except on Lummi Island. Rare aragonite veins are present in pillow basalts from Trump Island, near Lopez Island (Dailey, 1985). Interpillow limestones at Rosario Head on Fidalgo Island have been recrystallized to aragonite.

Plutonic rocks of the Fidalgo Complex have been variably recrystallized to static prehnite-pumpellyite and greenschist facies assemblages, probably related to hydrothermal sea-floor metamorphism. Carroll (1980) observed veins of prehnite, pumpellyite, quartz, and minor epidote in plutonic rocks of the Fidalgo Complex on Lummi Island. On Fidalgo Island, Brown and others (1979) reported alteration assemblages consisting of actinolite, chlorite, epidote, and albite. These same metamorphic assemblages are also found in plutonic clasts from Lummi conglomerates and sandstones, which indicates that this metamorphism predated deposition of the Lummi (Vance, 1977).

**Regional correlation.** When compared with other terranes in the San Juan Island, North Cascades, and Vancouver Island, the Decatur terrane is distinctive because it is the only terrane that

contains a Jurassic ophiolite and superimposed arc. The arc-volcanic sequence of the Fidalgo Complex does bear some resemblance to Jurassic arc-volcanic rocks in the North Cascades called the Wells Creek Volcanics (Misch, 1966) and the Harrison Lake Formation (Monger, 1970; Arthur, 1986). Two observations, however, preclude this correlation. First, the Harrison Lake and Wells Creek volcanic rocks are, at least in part, older than the Fidalgo Complex, including the ophiolite. This relationship is better demonstrated by the Harrison Lake, which ranges from uppermost Lower Jurassic (Toarcian) to Middle Jurassic (pre-Callovian, possibly as young as Bajocian or Bathonian) (Arthur, 1986). The more poorly fossiliferous Wells Creek is considered to be equivalent to the Harrison Lake but could range as high as lowermost Upper Jurassic (Oxfordian) (Misch, 1966). Even at this minimum age, the Wells Creek is still probably too old to be equivalent to the Fidalgo arc-volcanic sequence. The second observation is that the Harrison Lake, and presumably the Wells Creek, overlie an older stratigraphic sequence and not an ophiolite. Monger (1970) and Arthur (1986) describe a sequence of Lower Jurassic conglomerate (lower member of the Harrison Lake Formation) and Middle Triassic argillite and volcanic rock (Camp Cove Formation) that stratigraphically underlies the Harrison Lake Volcanics. Fossiliferous limestone cobbles in the conglomerate contain a distinctive fauna characteristic of the Upper Paleozoic Chilliwack Group and establish an Early Jurassic stratigraphic link between the Chilliwack and the Harrison Lake Volcanics (Monger, 1986) (see Chilliwack terrane in Fig. 6).

The Decatur terrane may be equivalent to the Ingalls Com-

plex (Miller, 1985), which occurs in a large thrust sheet to the southeast in the central Cascade Mountains, and to other coeval ophiolitic rocks that occur as fault slices in the North Cascades thrust system (Whetten and others, 1980). We note, however, that arc-volcanic rocks have not been recognized in these other ophiolitic units.

The Decatur terrane is strikingly similar to several Jurassic ophiolitic units located farther south, in the Klamath Mountains, western Sierra Nevada, and Coast Ranges of California. These units include Middle to Late Jurassic arc-related plutonic and volcanic rocks, and associated ophiolite complexes (e.g., Josephine, Smartville, Coast Range ophiolites) that probably formed in an arc and back-arc basin setting (Harper, 1984; Shervais and Kimbrough, 1985) at about 155 to 160 Ma (Hopson and others, 1981). The Coast Range ophiolite is overlain by the Great Valley Group, an Upper Jurassic and Lower Cretaceous clastic sequence, which is petrologically similar to the Lummi Formation (Garver, 1985).

When one compares the Lummi Formation with other broadly similar Jura-Cretaceous clastic units in the San Juan Islands, North Cascades, and Vancouver Island (stippled units in Fig. 6), it is tempting to consider that they might have originated as coextensive units. The fact remains, however, that clastic units of similar age and composition are present along the entire length of the western Cordillera (Dickinson, 1976). Terranes other than the Decatur must have been adjacent to the Lummi during the Jura-Cretaceous because the Lummi contains clastic material, such as blueschist, that could not have been derived from the Decatur terrane. Thus, the Lummi is considered to be a clastic linking sequence; unfortunately, we have not been able to establish links to specific terranes in the San Juan Islands or elsewhere. We envision that the Lummi, like the Great Valley Group of California, was deposited at a volcanically active continental margin that contained an older uplifted assemblage of terranes. Two important questions remain unanswered: (1) Where along the American continental margin was the Lummi deposited?, and (2) Did it form coextensively with or separately from other Jura-Cretaceous clastic units in the Pacific Northwest? These questions highlight a general problem concerning the interrelationship of Jura-Cretaceous clastic units in the Pacific Northwest. We discuss this problem in more detail at the end of the paper and consider its broader implications for tectonostratigraphic interpretation.

#### **EXTERNAL UNITS: MESOZOIC UNITS FORWARD OF, AND BELOW, THE SAN JUAN THRUST SYSTEM**

The external units consist of two fault-bounded Mesozoic units and Upper Cretaceous syn-orogenic clastic strata of the Nanaimo Group. These units are considered to be external to the San Juan thrust system because they lack high-pressure metamorphic assemblages. Unlike units in the thrust system, the external units have never been in a deeply-seated structural setting.

The two older external units are the Upper Triassic Haro Formation and the Jura-Cretaceous Spieden Group, both of which are clastic sequences composed dominantly of arc-volcanic material. The Haro does not correlate with any other nearby Upper Triassic unit (Fig. 6); we consider it to be a separate terrane called the Haro terrane. We tentatively include the Spieden in the Haro terrane because of its close proximity to the Haro Formation and its similar structural setting. We note, however, that no direct connection has been established between the Spieden and Haro.

The youngest external unit is the Upper Cretaceous Nanaimo Group, which we consider to be a syn-orogenic clastic unit. This unit is important because it records the uplift and erosion of the San Juan and Cascades thrust system, and therefore provides a link between terranes of the San Juan Islands, North Cascades, and Vancouver Island (Fig. 6).

The external units were probably juxtaposed with each other and with the leading edge of the San Juan thrust system during the last stages of San Juan thrusting. Although contacts are not exposed, Johnson (1978) argued that the external units are bounded by a series of south-dipping thrusts (Fig. 4), based on the overall dip and direction of younging of the units. Vance (1977) also has argued for a thrust contact between the Nanaimo Group and San Juan thrust system on Orcas Island, but he interprets this thrust to be north-dipping. A south-dipping thrust seems to be required between the San Juan nappes and the external units to explain the sharp contrast in metamorphic grade and the uplift of the nappes relative to the Nanaimo Group. The age of these inferred thrusts is latest Cretaceous or possibly Paleocene, because the post-orogenic Chuckanut Formation, of Eocene age, rests with angular unconformity on nappes of the San Juan and North Cascades thrust systems and disconformably on the Nanaimo Group on Sucia Island (Fig. 3). This evidence suggests that these thrust faults were active during the last stages of San Juan thrusting, and therefore may have represented the youngest and most forward part of the thrust system. As a consequence, we suspect that the external units, including the Nanaimo Group, at least partially underlie the San Juan thrust system (Fig. 4). A minor amount of mid-Tertiary deformation is responsible for the broad northwest-trending folds affecting the Nanaimo Group, Chuckanut Formation, and thrusts of the San Juan system (Fig. 3).

#### ***Haro terrane: Upper Triassic and Jura-Cretaceous volcaniclastic units***

***Haro Formation (Upper Triassic).*** A 700-m-thick section of steeply dipping, Upper Triassic strata crops out in a small area surrounding Davison Head at the north end of San Juan Island (Figs. 2 and 3). The Haro Formation (McLellan, 1927) consists of well-bedded siltstone, sandstone, tuff, conglomerate, and breccia, all of which contain abundant andesitic and dacitic volcanic detritus (Tables 7 and B-8) (Vance, 1975; Johnson, 1978). The local presence of crystal tuff indicates volcanism was

contemporaneous with deposition (Johnson, 1978). South of Davison Head, thin coquina beds contain the fossil *Halobia*, indicating a Carnian or Norian age for the Haro (H1-2 in Table A-9). Igo and others (1984) have recently found minor interbeds of radiolarian siliceous shale in the Haro. Radiolaria from two localities indicate ages similar to the *Halobia* localities: (1) Late Triassic (Carnian or Norian) and (2) Late Triassic or earliest Jurassic (Norian to Pleinsbachian; H3-4 in Table A-9). Metamorphism of the Haro is restricted to the zeolite facies (Johnson, 1978).

Johnson (1978) suggests that quartz porphyry found on Barren Island, a small island to the west of the Haro Formation, may be an intrusion related to Haro volcanism since the Haro contains clasts of similar lithology and chemistry (compare analyses in Table B-8). K-Ar whole-rock date, however, suggests an Early Cretaceous age for the Barren Island porphyry (H5 in Table A-8), although the date may be reset. We note that if the Barren Island porphyry is Early Cretaceous in age, then it may be related to Spieden volcanism; the Spieden Group contains similar-age dacite porphyry clasts (S6a and S6b in Table A-9). In any case, the zeolite-facies metamorphic grade of the Barren Island porphyry (Johnson, 1978) indicates that the porphyry, like the Spieden Group and Haro Formation, is external to the San Juan thrust system.

The Haro Formation does not appear to be correlative with other nearby Upper Triassic units (Fig. 6). It is clearly different from the chert-rich Deadman Bay terrane. Coeval units in the Wrangellia terrane of Vancouver Island consist of a thick sequence of tholeiitic basalt overlain by limestone and shale (Karmutsen, Quatsino, and Parsons Bay Formations; Muller, 1977), with no evidence of intermediate or silicic volcanic rocks. One unit that may be related to the Haro is the Upper Triassic and Jurassic Cultus Formation of the Cascade Mountains. In its type area in southernmost British Columbia, the Cultus consists of volcanoclastic siltstone and sandstone (Monger, 1970), but lacks the coarse-grained pyroclastic sediments that characterize the Haro. About 35 km to the north in the Harrison Lake area, the Camp Cove Formation, which Monger (1970) tentatively included with the Cultus, consists of a 700-m-thick sequence of tuff, plagioclase-porphyry flows, sandstone, and siliceous argillite (Monger, 1970; Arthur, 1986). Radiolaria and conodonts from a siliceous argillite bed in the middle of the Camp Cove are Middle Triassic. These preliminary data indicate that the Haro and Camp Cove are lithologically similar but may be slightly different in age; further study and comparison are definitely warranted.

**Spieden Group (Upper Jurassic and Lower Cretaceous).** The Spieden Group (Johnson, 1981), exposed only on Spieden Island and a smaller island to the south (Figs. 2 and 3), consists of a well-bedded sequence, about 840 m thick, of mudstone, volcanoclastic sandstone, and conglomerate. The Upper Jurassic Spieden Bluff Formation (Johnson, 1981) contains volcanic breccia and conglomerate that were deposited near an active volcanic source. *Buchia* from this unit (S1 in Table A-9) indicate an Oxfordian or Kimmeridgian age (approximately 163 to 150 Ma; Harland and others, 1982). A volcanic cobble has

yielded a  $152 \pm 4$  Ma K-Ar hornblende date (S2 in Table A-9), which attests to the contemporaneity of volcanism. The Lower Cretaceous Sentinel Island Formation (Johnson, 1981) includes shallow marine and alluvial sediments, also rich in volcanic detritus. Fossils from this unit (S3-5 in Table A-9) are Valanginian and Hauterivian (approximately 138 to 125 Ma; Harland and others, 1982). A volcanic clast from a conglomerate above the Hauterivian fossil locality has yielded a  $145 \pm 3$  Ma K-Ar hornblende date (S6 in Table A-9), which suggests that this unit was derived, at least in part, from an older volcanic source. Geochemical analyses of several volcanic clasts from the Spieden Bluff and Sentinel Island Formations indicate that the source area for the Spieden was probably a mature(?) volcanic-arc terrane, characterized by high  $\text{SiO}_2$  content, moderate  $\text{K}_2\text{O}$  content, and moderate LREE enrichment (Tables 7 and B-8).

Metamorphism of the Spieden Group is restricted to the zeolite facies (Johnson, 1978). Apatite and zircon from igneous cobbles give unreset Late Jurassic fission-track dates (S6 in Table A-9), indicating that the Spieden beds have never been above about 100°C (Gleadow and Brooks, 1979).

Although the Spieden Group is time-correlative with other nearby units in the San Juan Islands (Lummi and Constitution Formations), Vance (1975) and Johnson (1981) conclude that these units have significant differences in their sedimentology, petrology, and metamorphism. Furthermore, the high  $\text{K}_2\text{O}$  content and moderate LREE enrichment typical of the Spieden volcanic clasts precludes the Fidalgo Complex as a source for the Spieden. Johnson (1981) has suggested that the Spieden might be equivalent to the Kyugot Group of the Wrangellia terrane (Fig. 6); he noted, however, that Wrangellia contains no Upper Jurassic arc-volcanic rocks (Muller, 1977). Another possibility is that the volcanic clasts came from the Harrison Lake and Wells Creek Volcanics, which would imply that the Spieden was closely linked or equivalent to the Nooksack Group (Fig. 6). As described by Arthur (1986), units equivalent to the Nooksack Group at Harrison Lake (Mysterious Creek, Billhook Creek, Peninsula, and Brokenback Formations) do bear a close resemblance to the Spieden; the Harrison Lake Volcanics, however, are too old (Early and Middle Jurassic: Arthur, 1986) to be the source for the Spieden clasts.

**Nanaimo Group: Upper Cretaceous syn-orogenic clastic sequence.** The Nanaimo Group consists of a sequence, about 2.5 km thick, of marine and nonmarine strata (Muller and Jletzky, 1970; Ward and Stanley, 1982; Pacht, 1984). It is widely exposed on Vancouver Island, in the Gulf Islands of Canada, and in the northern San Juan Islands (Figs. 1 and 3). Fossils are common and indicate that the unit is mostly restricted to the Upper Santonian, Campanian, and Maastrichtian (Ward, 1978). Recently discovered fossils indicate that the Nanaimo locally ranges down into the Coniacian or Turonian (P. Ward, oral communication, 1985). Stewart and Page (1974) show that zeolite metamorphic assemblages are widespread in the Nanaimo Group.

In the San Juan Islands, the Nanaimo consists of gently

folded sandstone, conglomerate, and mudstone (Johnson, 1978; Ward and Stanley, 1982). In this area, the base of the unit is not exposed, but conglomerates contain clasts that clearly were derived from the San Juan and Cascades thrust systems (Vance, 1975; Johnson, 1978; Ward and Stanley, 1982; Pacht, 1984), indicating that they were exposed near the Nanaimo basin (discussed in next section). On Vancouver Island, the Nanaimo unconformably overlies older rocks of the Wrangellia terrane (Muller and Jeletzky, 1970). Thus, major displacements between Wrangellia and the thrust-bounded terranes of the San Juan Islands occurred prior to Nanaimo time.

### POST-OROGENIC UNIT: THE EOCENE CHUCKANUT FORMATION

Eocene strata of the Chuckanut Formation occur on Sucia and Lummi Islands in the northern San Juan Islands (Vance, 1975; Carroll, 1980; Johnson, 1984a, b). The Chuckanut is best exposed in the northwestern Cascade Mountains where it consists of a fluvial sequence, about 6 km thick, composed dominantly of arkosic sandstone (Johnson, 1984a, b). Johnson (1984b) has established an Eocene age (Middle Eocene, and possibly Early and Late Eocene as well) for Chuckanut strata in the Cascades and also on Sucia Island. The Chuckanut unconformably cuts out the Nanaimo Group in an eastward direction. On Sucia Island, the Chuckanut overlies the Cedar District Formation of the Nanaimo Group (depositional contact exposed at low tide), whereas, farther east on Lummi Island and in the Cascades, the Chuckanut directly overlies pre-Upper Cretaceous rocks. The Chuckanut may extend farther west to the Canadian Gulf Islands where it would be equivalent to the Gabriola Formation (Vance, 1975; Johnson, 1984b), a poorly dated unit that is presently mapped as the highest unit of the Nanaimo Group (Muller and Jeletzky, 1970).

### HIGH-PRESSURE METAMORPHISM AND ITS RELATION TO THRUSTING

As outlined above, the San Juan thrust system has been affected by a very low grade, high-pressure, metamorphic event that resulted in the widespread formation of lawsonite, prehnite, and aragonite (Vance, 1968; Glassley and others, 1976; Brandon, 1980, 1982). This metamorphic event was caused by rapid structural burial during Late Cretaceous thrusting. We review the evidence for this structural burial here because it provides important information on the timing and tectonic setting of San Juan thrusting.

Prehnite- and lawsonite-bearing assemblages are found in all rock units of the San Juan thrust system, although they are generally best developed in volcanoclastic sandstones of the Jura-Cretaceous units. Metamorphic aragonite is also widely present within the thrust system (Vance, 1968). Limestones commonly have been recrystallized to a coarse-grained aragonite marble, whereas other rock types contain numerous cross-cutting veins of

aragonite. There is no indication that aragonite has formed metastably from highly strained calcite, as suggested by Newton and others (1969). In fact, the presence of undeformed veins of coarse-grained aragonite indicates that it crystallized from a fluid phase, and therefore in the local absence of deviatoric stress.

There are three lines of evidence that indicate that high-pressure metamorphism was related to structural burial during thrusting.

(1) The first is based on textural evidence. Lawsonite, prehnite, and aragonite occur exclusively in crosscutting veins or as small, randomly oriented aggregates, indicating that metamorphism was under static conditions. Further evidence of this relationship is found in the exotic fault slices of Garrison Schist and Turtleback Complex. Cataclastic fabrics in these slices, which were developed during their emplacement along the San Juan thrusts, are overprinted by undeformed aggregates and veins of lawsonite, prehnite, and aragonite, demonstrating that high-pressure metamorphism postdated the thrust emplacement of these slices (Brandon, 1980). Broken and folded veins of prehnite and lawsonite are present locally in Constitution sandstones (Vance, 1975; Brandon, 1980), indicating that some deformation postdated metamorphism.

(2) A second line of evidence is the presence of a systematic distribution of metamorphic assemblages that does not appear to be disrupted by thrusts of the San Juan system. On southern San Juan Island, this distribution was at least locally controlled by temperature conditions that increased with increasing structural depth. This conclusion is based on the recognition of a prehnite-in isograd in volcanoclastic sandstones (Fig. 26), which records the reaction: lawsonite + quartz + aragonite = prehnite + CO<sub>2</sub> + H<sub>2</sub>O (Brandon, 1980). There is thin-section evidence for this reaction, such as a significant decrease in the modal amount of lawsonite at the isograd, and reaction textures showing prehnite replacing aragonite. Thermodynamic calculations indicate that this reaction has a steep P-T slope (about 30° C/kb), and that prehnite lies on the high-temperature side, which is compatible with the fact that prehnite-bearing assemblages occur to the west of the isograd in the direction of increasing structural depth (Fig. 26).

Our general knowledge of the regional distribution of prehnite- and lawsonite-bearing assemblages indicates that the higher-temperature prehnite-bearing assemblages, with little to no lawsonite, are widespread throughout the San Juan thrust system, whereas the lower-temperature lawsonite-only assemblages are confined to southern San Juan Island, southern Lopez Island, and southern Lummi Island. There is no simple explanation for this pattern; some possibilities are considered below in a discussion on fission-track dates from rocks of the thrust system.

It is important to note that in our review of the distribution of metamorphic assemblages in the San Juan system, we have purposely focused on lawsonite-prehnite assemblages in volcanoclastic sandstones of the Jura-Cretaceous units. This strategy avoids two problems. The first is that sandstones without lawsonite or prehnite commonly contain the assemblage: calcium carbonate + white mica, which indicates the breakdown of lawsonite

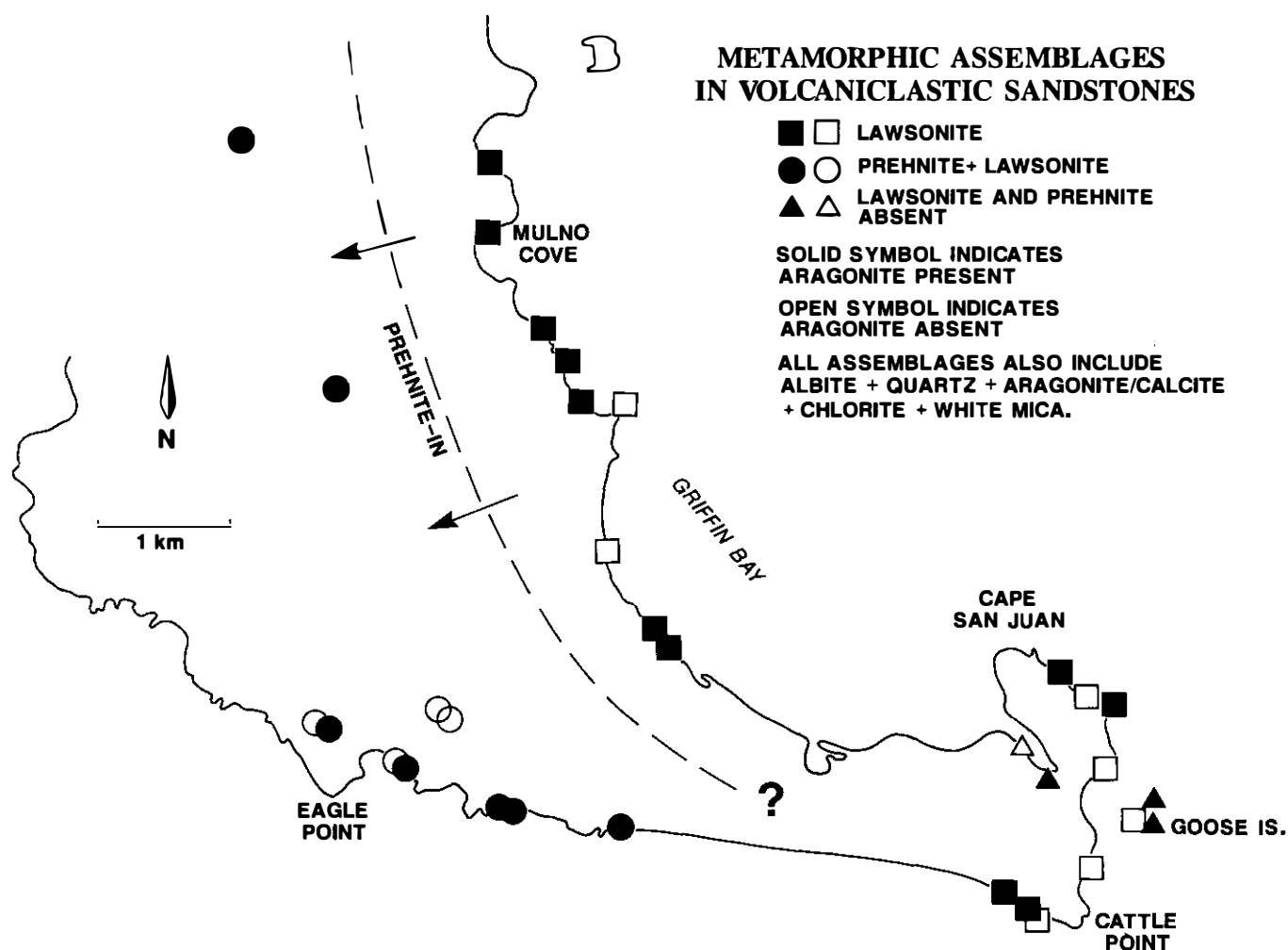


Figure 26. Distribution of prehnite- and lawsonite-bearing assemblages in volcaniclastic sandstones on southern San Juan Island (from Brandon, 1980). A prehnite-in isograd marks an increase in metamorphic grade from east to west, coincident with increasing structural depth (thrusts and nappes dip to the east and northeast in this area; see Fig. 3). Those samples with prehnite and lawsonite absent show a greater amount of calcite, suggesting that the calcium aluminium silicate phases have reacted out due to locally high  $\text{CO}_2$  in the fluid phase.

and/or prehnite in the presence of  $\text{CO}_2$  in the fluid phase. The second problem is that the older plutonic and volcanic rocks of the San Juan system commonly contain a more complex poly-phase assortment of metamorphic assemblages because they have been subjected to older metamorphic events: for example, the Permian metamorphism of the Turtleback Complex and Jurassic sea-floor metamorphism of the Fidalgo Complex.

(3) A third and final line of evidence is based on stratigraphic constraints (Fig. 27), which indicate that thrusting and metamorphism occurred during a very short interval of time, about 16 m.y. The youngest rocks involved are the middle Cretaceous basalts at Richardson. Foraminifera from this unit belong to the lower half of the *Planomina buxtorfi* (= *Rotalipora appennica*)

biozone of latest Albian age (L4 in Table A-6), which corresponds to about 100 Ma (Sliter, 1984; Sliter, personal communication, 1986; note that the absolute age of the Albian-Cenomanian boundary is quite accurately known to be  $97.5 \pm 1.0$  Ma; see Harland and others, 1982). The upper limit of thrusting and metamorphism is based on the age of conglomerates in the Extension Formation of the Nanaimo Group (Ward, 1978), which on Orcas and Stuart Islands contain minor clasts of lawsonite- and prehnite-bearing volcaniclastic sandstone (Brandon, 1982). Although these sandstone clasts do not contain aragonite, they are identical in every other way to metamorphosed Constitution sandstone, and therefore indicate uplift and exposure of the San Juan thrust system during the latest Cretaceous. These

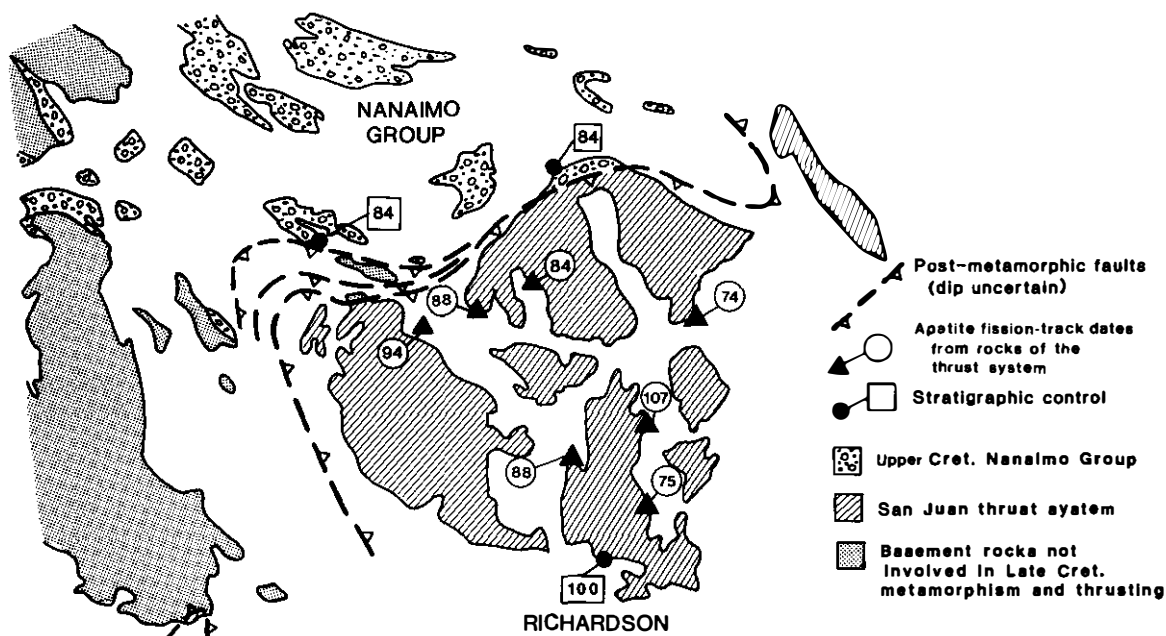


Figure 27. Summary map of age constraints for San Juan thrusting and high-pressure metamorphism. The youngest rocks involved in thrusting and metamorphism are the basalts at Richardson on southern Lopez Island, which are latest Albian or about 100 Ma (L4 in Table A-6). Cobbles of Constitution sandstone with lawsonite-prehnite assemblages occur on northern Orcas and Stuart Islands in conglomerate of the Extension Formation (Nanaimo Group). This conglomerate is latest Santonian-earliest Campanian, which is 84 Ma. Thrusting, metamorphism, and subsequent uplift are therefore constrained to the interval 100 to 84 Ma. Also shown are apatite fission-track dates from rocks of the thrust system (Johnson and others, 1986), which support the stratigraphic evidence for rapid uplift of the San Juan nappes.

conglomerates lie at or slightly below the boundary between the Chicoensis and Schmidt biozones (see Ward, 1978, p. 418). Based on magnetic polarity stratigraphy, Ward and others (1983) have shown that the boundary between these two biozones, and therefore the conglomerates themselves, corresponds to the Campanian-Santonian boundary, which has an absolute age of  $84 \pm 2.3$  (Kent and Gradstein, 1985; Harland and others, 1982, p. 52).

Further evidence of latest Cretaceous uplift and erosion of the San Juan and North Cascades thrust systems is preserved in Upper Campanian Nanaimo conglomerates on Sucia Island (Cedar District Formation; Ward, 1978), which contain clasts of Upper Triassic radiolarian chert (Johnson, 1978) presumably derived from the Deadman Bay terrane, and blueschist, greenschist, and phyllite (Vance, 1975) derived from high-pressure metamorphic rocks of the Shuksan nappe (Misch, 1966, 1977) in the Cascades thrust system.

These timing constraints indicate that thrusting, metamorphism, and subsequent uplift of at least part of the San Juan system occurred very rapidly during a 16-m.y. interval between

100 and 84 Ma. Apatite and zircon fission-track dates, recently published by Johnson and others (1986), provide independent support for our interpretation. (Fission-track dates judged unreliable by Johnson and others are not included in this discussion.) Figure 27 shows apatite dates for rocks from the San Juan thrust system. These dates were reset during Late Cretaceous thrusting and metamorphism because they are all clearly younger than the formational age of the units that they come from (Turtleback Complex, Fidalgo Complex, and Lummi Formation) and because all but one are younger than the beginning of San Juan thrusting, estimated at about 100 Ma. The average of these dates is 87.2 Ma, which agrees well with the stratigraphic evidence for uplift at 84 Ma. The large variance among the dates, from 107 to 74 Ma, is due in part to the imprecise nature of the dates; Johnson and others (1986) report error limits of  $\pm 9.5$  to  $\pm 19.5$  (two sigma). Thus, the stratigraphic evidence from the Nanaimo provides a more precise record of uplift of the San Juan system.

The fission-track dates also provide information about maximum temperatures during San Juan thrusting and metamor-

phism. The reset apatite dates from the thrust system indicate temperatures higher than  $100 \pm 20^\circ\text{C}$ , the blocking temperature for apatite (Gleadow and Brooks, 1979). Zircon fission-track dates, however, show that temperatures rarely exceeded  $200 \pm 50^\circ\text{C}$ , the blocking temperature of zircon (Gleadow and Brooks, 1979). Out of the 17 zircon dates from the thrust system, only one could have been reset during Late Cretaceous thrusting (79 Ma date from the Lummi Formation). Johnson and others (1986) suggest that several other zircon dates from the Decatur terrane were partially reset during thrusting (113 Ma date from the Fidalgo Complex; 105 and 107 Ma dates from the Lummi Formation); there is no clear evidence, however, that this is the case.

Based on these four zircon date, Johnson and others (1986) propose that high temperatures were developed locally within the Decatur terrane due to frictional heating along a higher thrust fault or to emplacement of a higher and warmer thrust sheet. This proposed thrust or thrust sheet was subsequently removed by erosion during uplift. The problem that Johnson and others (1986) are trying to address is why the Decatur terrane, which lies in the upper part of the San Juan thrust system, was subjected to relatively high metamorphic temperatures. Our main criticism of their interpretation is that none of the other major thrust faults in the San Juan Islands show local metamorphic or thermal effects. Thus, we propose an alternative: that the southeastern part of the San Juan system was unroofed more slowly, permitting a greater degree of thermal relaxation and the development of steeper geothermal gradients (see Draper and Bone, 1981). Evidence for this interpretation is based on the fact that the youngest apatite fission-track dates (73 and 75 Ma) are located in the southeastern part of the system (Fig. 27). These dates suggest a lag of about 10 m.y. between initial unroofing of lawsonite-prehnite rocks in the thrust system, as indicated by the 84-Ma Nanaimo conglomerate, and uplift and cooling of the southeastern part of the thrust system at about 74 Ma.

Based on the evidence above, we conclude that the San Juan thrust system preserves a relative coherent metamorphic sequence that was formed at the same time as Late Cretaceous thrusting. Experimental data, summarized in Figure 28, broadly outline the pressure and temperature conditions during metamorphism. The presence of lawsonite + quartz indicates pressures greater than 3 kb (300 Mpa), which corresponds to depths greater than 11 km. The presence of aragonite and its coexistence with lawsonite-bearing assemblages indicates much higher pressures, probably about 5 kb (500 Mpa), which is equivalent to a depth of about 18 km. Relatively low temperatures during metamorphism (estimated at 150 to  $200^\circ\text{C}$ ) and subsequent rapid uplift explain why aragonite, which typically inverts to calcite during uplift (Carlson and Rosenfeld, 1981), was preserved in these rocks.

Given these depth estimates and the short time interval, we can only conclude that metamorphism and subsequent uplift were due to structural burial and crustal thickening during thrusting. The round trip to 18 km depth and back to the surface during 16 m.y. indicates an average vertical displacement rate of about

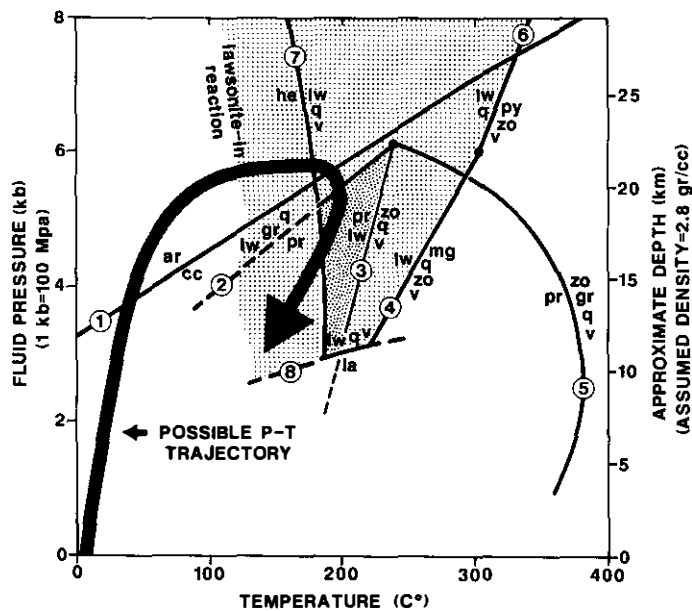


Figure 28. Petrogenetic grid showing pertinent reactions for the prehnite, lawsonite, and aragonite assemblages in the San Juan Islands, assuming fluid pressure equal to total pressure and pure  $\text{H}_2\text{O}$  fluid phase (the presence of lawsonite and prehnite indicate the near absence of  $\text{CO}_2$  in the fluid phase). The light pattern shows the approximate stability range for lawsonite + quartz. The heavier stippled pattern shows the range for prehnite + lawsonite + quartz. The aragonite stability field lies above reaction 1. Based on these reaction boundaries, maximum metamorphic conditions are estimated at about 5 kb (500 Mpa) and 150 to  $200^\circ\text{C}$ . The proposed P-T trajectory illustrates the metamorphic succession found in the San Juan nappes: early formation of lawsonite and aragonite, followed by the formation of prehnite. Mineral abbreviations are: ar = aragonite; cc = calcite; lw = lawsonite; gr = grossular; q = quartz; he = heulandite; pr = prehnite; zo = zoisite; la = laumontite; mg = margarite; py = pyrophyllite; v = vapor ( $\text{H}_2\text{O}$ ). Reaction boundaries are from the following sources: (1) determined experimentally by Boettcher and Wyllie (1968) and Crawford and Hoersch (1972); (2–6) calculated from thermodynamic data by Perkins and others (1980); (7) determined experimentally by Nitsch (1968); (8) determined experimentally by Liou (1971). The lawsonite-in reaction for rocks of the San Juan Islands is not known, but must lie at temperatures less than reaction (7) and may be related to the breakdown of plagioclase or carbonate and clay (Ernst, 1971). Based on the fact that prehnite and aragonite appear to coexist stably in rocks of the San Juan Islands, we suspect that the upper limit of the prehnite stability field (reactions 2 and 5) actually overlaps with the aragonite stability field; this possibility is probably within the error limits of the thermodynamic calculations of Perkins and others (1980).

2 km/m.y. While this rate may seem high, it is only a fraction of typical rates of plate motion (20 to 100 km/m.y.). We envision that, like other onland thrust belts, the San Juan thrust system was formed by successive accretion of thrust slices between an overriding thrust wedge (e.g., Boyer and Elliott, 1982; Davis and others, 1983). Figure 29 illustrates how this process results in a

cycle of structural burial and subsequent uplift. The peak of metamorphism for an individual thrust slice would occur during and shortly after the slice was accreted to the base of the thrust wedge. Subsequent accretion of new thrust slices would cause older slices to move upward from the active basal thrust. Upward movement of these slices from the basal thrust, plus erosion of the top of the thrust wedge as recorded by the Nanaimo Group, would eventually expose the metamorphosed thrust slices at the surface. This process requires high erosion rates, but rates of this magnitude have been measured in modern active thrust belt (e.g., about 5 km/m.y. in Taiwan: Li, 1976; Suppe, 1981; regional average of 0.7 km/m.y. for the Himalayas: Curran and Moore, 1971). In Figure 28, we show a possible P-T trajectory that is comparable with this type of structural burial and uplift history and also with the metamorphic assemblages present in the thrust system.

There are several implications of our interpretation of thrusting and metamorphism. One is that the San Juan system must have included structurally higher thrust sheets, which were subsequently eroded away, in order to account for the metamorphism of the nappes. We suggest, as one possibility, that part of the Cascade thrust system, in particular the thick Shuksan thrust sheet (Misch, 1966, 1977), may have extended westward over the San Juan Islands, which is consistent with other evidence indicating that thrusts and nappes of the San Juan Islands and North Cascades are part of a related Late Cretaceous thrust system (Brandon and Cowan, 1985). Another implication is that there must be a relatively large amount of displacement on the thrust that separates the external units from the San Juan system because the external units were unaffected by high-pressure metamorphism and because the Nanaimo Group contains cobbles derived from metamorphosed rocks of the thrust system. This relationship suggests that the external units extend a considerable distance beneath the nappes of the San Juan system.

#### TERRANE ACCRETION AND LATE CRETACEOUS THRUSTING

In this section, we consider the tectonic setting of Late Cretaceous thrusting, and how it might have related to the accretionary history of terranes in the Pacific Northwest. In many tectonic syntheses (e.g., Hamilton, 1978; Whetten and others, 1980), thrusts and nappes in the San Juan Islands and North Cascades have been considered to represent a late Mesozoic subduction complex, an interpretation broadly consistent with the fact that the nappes are an assemblage of largely oceanic rocks. We, however, have emphasized the similarity of the San Juan-Cascades orogen to onland thrust belts. From a structural point of view, there may not be much difference between a subduction complex and an onland thrust belt since both consist of a wedge of thrust-imblicated slices (e.g., Davis and others, 1983; von Huene, 1984; Cowan, 1985). Even so, one important distinction is that a subduction complex or accretionary wedge is composed almost entirely of imbricated sediments and mafic crustal rocks accreted from a subducting oceanic plate (e.g., von Huene, 1984). The

diversity of terranes in the San Juan-Cascade thrust system, plus the relatively short duration of this thrusting event, seems to preclude its origin as a simple subduction complex. In fact, these features suggest that the San Juan-Cascade system represents a collision-like orogen.

This interpretation raises two important questions: (1) What was the paleogeographic relationship of Wrangellia and the San Juan-Cascade terranes to continental America?, and (2) What actually drove the collision, or stated another way, what collided with what?

With regard to the first question, we agree that at least some terranes are far traveled with respect to North America: examples are the Deadman Bay terrane with its exotic Tethyan fusulinid fauna and the Wrangellia terrane with its paleomagnetic record of low latitudes during the Mesozoic (Yole and Irving, 1980). Moreover, geologic evidence indicates that most, if not all of these terranes were originally widely separated from each other (Fig. 6). For instance, the Decatur terrane is underlain by Middle or Upper Jurassic oceanic crust, and therefore is unrelated to older San Juan terranes. The Garrison terrane is the only Paleozoic-lower Mesozoic terrane affected by Permo-Triassic high-pressure metamorphism. The Turtleback and Chilliwack terranes, which may be equivalent to each other, are differentiated from the Deadman Bay and Wrangellia terranes by fundamental differences in Paleozoic stratigraphy and fusulinid fauna. Furthermore, Wrangellia has a unique record of Early and Middle Jurassic arc-related volcanism and plutonism (Fig. 6; Muller, 1977). Finally, the Haro terrane may be related to the Turtleback/Chilliwack terranes but is clearly distinguished from other nearby terranes by its record of Late Triassic arc volcanism.

The differences among these terranes become less apparent during the Late Jurassic and Early Cretaceous since units of this age are thick, monotonous, clastic sequences (stippled units in Fig. 6). Some of these clastic units directly overlie or are closely linked to older terranes, such as the Kyuquot and Queen Charlotte Groups of Wrangellia, the Lummi Formation of the Decatur terrane, and the Nooksack Group of the Chilliwack terrane. Others, such as the Spieden Group and the Constitution Formation, are entirely fault-bounded. Even so, clasts in the Constitution suggest that older terranes, such as Deadman Bay and Garrison, were close by.

Based on two lines of indirect evidence, we consider this record of widespread sedimentation to indicate that most, if not all of these Mesozoic and Paleozoic terranes were close to or part of continental America by the Late Jurassic. First, where studied, the petrology of these clastic units indicates that they were eroded from a diverse source region that included intermediate to silicic arc volcanics, metamorphic rocks, and chert. This type of source region suggests a large, continent-like land mass (Dickinson and Suzcek, 1979). At present, this argument cannot be applied to Wrangellia because provenance studies of the Jura-Cretaceous clastic units overlying that terrane are not available. However, we infer that the Wrangellian clastic units were also derived from a continent-like mass since the areal dimensions and accumulation

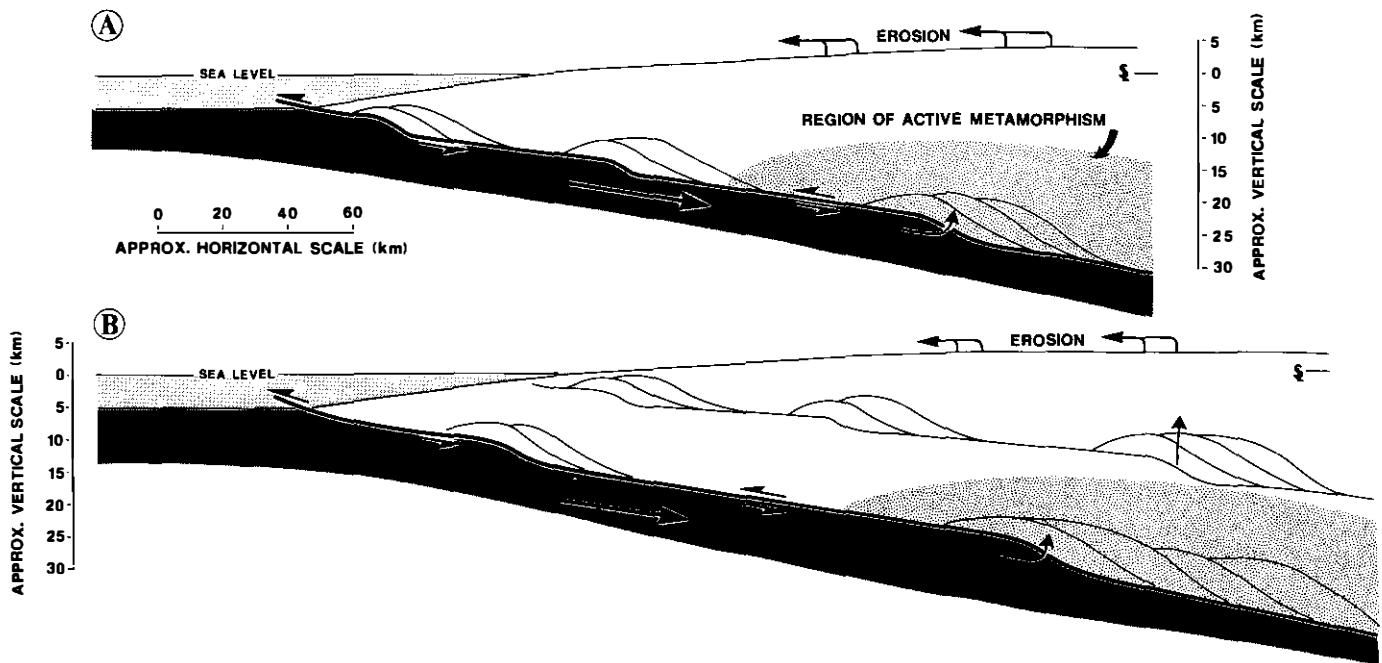


Figure 29. A model showing the proposed relationship between thrusting and high-pressure metamorphism. Thrust slices are progressively added to the front and base of an overriding thrust wedge. Rocks of the San Juan system are first overridden by the wedge and then accreted to the base of the wedge at a depth of about 20 km, which corresponds to the maximum pressure during metamorphism. Subsequent accretion of new thrust slices causes the older slices to move upward from the active basal thrust. Erosion at the top of the wedge, which would be accelerated by rapid rates of thrust-related thickening and uplift, eventually exposes the metamorphosed thrust slices at the surface. In this model, the peak of metamorphism occurs during, and shortly after, the accretion of each thrust slice.

rates for these units require close proximity to a large, subaerially exposed drainage area. For comparison, consider the Paleogene Zodiac Fan, an abyssal-plain turbidite sequence in the North Pacific that covers a circular region some 1000 km across. Stevenson and others (1983) estimate that this fan sequence had a source area equal to about one-half the size of the state of Alaska and was deposited less than 500 km from the continental margin. The fan has an average thickness of 250 m and was deposited in 8 to 16 m.y., with an average accumulation rate of 16 to 31 m/m.y. The oldest of the Jura-Cretaceous marine clastic units on Wrangellia, the Kyuquot Group (Muller and others, 1981), represents a marine basin that was at least 500 km across, judging from its present exposed length from Vancouver Island to Queen Charlotte Islands (Sutherland Brown, 1968; Muller and others, 1974, 1981). The presence of coeval marine strata on the Alaska portion of Wrangellia (Jones and others, 1981) is further evidence of the large areal dimension of this basal sequence. Accumulation rate for these Wrangellian clastic units appear to be similar to those for the Zodiac Fan. For instance, the Kyuquot Group has a thickness of about 800 to 1200 m and was deposited over a 55-m.y. interval (Callovian to Barremian), indicating an average

accumulation rate of 15 to 22 m/m.y.; correction for compaction would increase this estimate.

Thus, we conclude that the Kyuquot Group, together with other Jura-Cretaceous clastic units of Wrangellia, had a subaerial drainage area probably similar in size to that estimated for the Zodiac Fan. This drainage area must have extended well beyond the present boundaries of Wrangellia because, during the Late Jurassic and Early Cretaceous, the terrane was volcanically quiescent and the site of widespread marine sedimentation. We infer that this large drainage area was the American continental landmass simply because none of the accreted terranes in the western Cordillera appear to be large enough to supply the necessary volume of sediment.

Our second argument is that terranes similar and probably equivalent to the pre-Late Jurassic terranes of the San Juan Islands and North Cascades are also present in the Sierra Nevada, Klamath Mountains, and Coast Ranges of California where there is clear evidence that they had been accreted to or were part of North America by Late Jurassic time (see papers in Ernst, 1981). Specific correlations include: (1) Turtleback and Chilliwack terranes with the Eastern Klamath belt (Irwin, 1981) and arc-

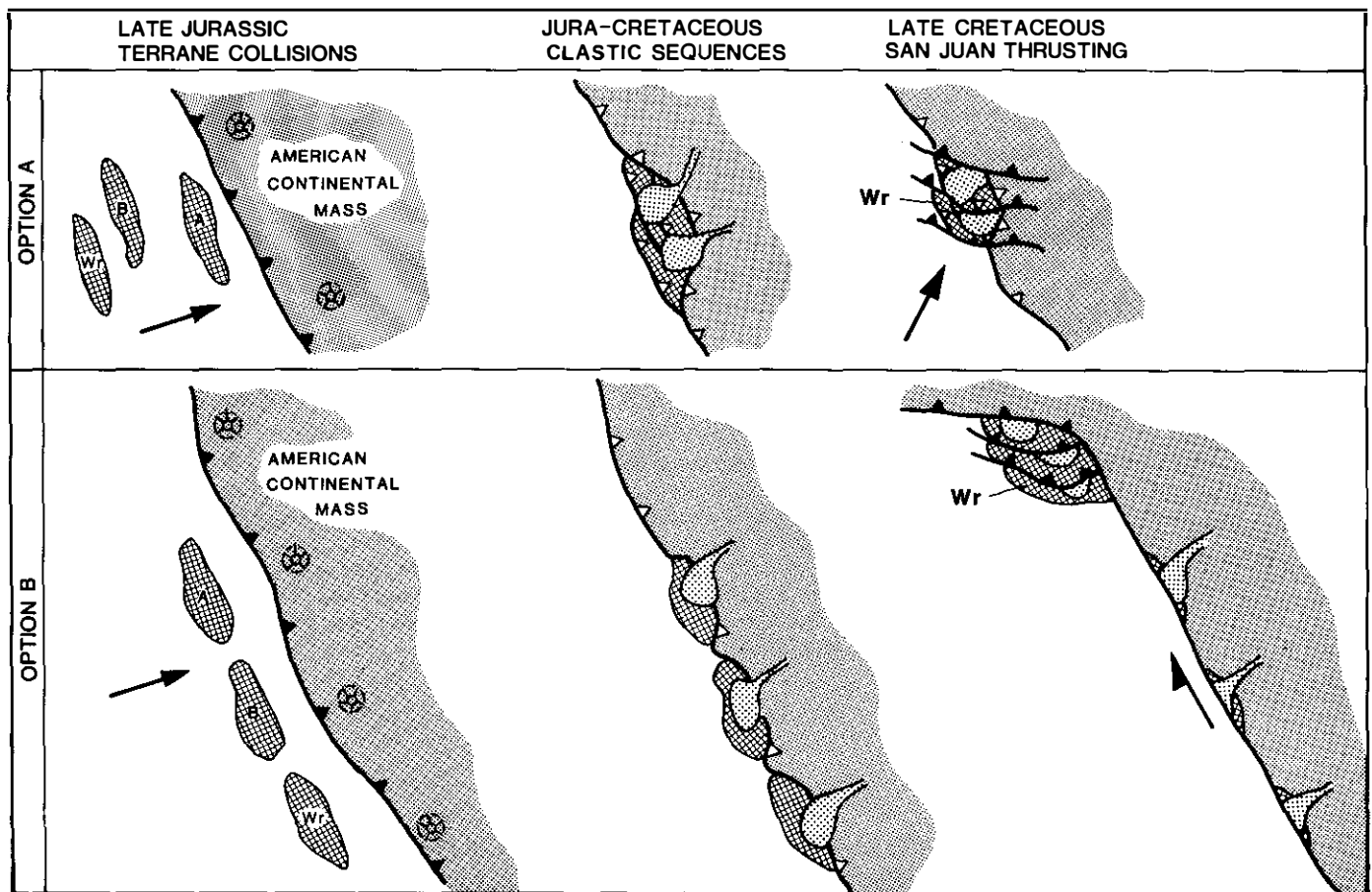


Figure 30. Two models for the accretionary history of terranes in the vicinity of the San Juan Islands. Both models are based on the conclusion that terranes in this area, including Wrangellia (Wr), were accreted to the American continental mass by latest Jurassic, as indicated by the widespread development of thick, Jura-Cretaceous, clastic sequences. In option A orogenic deformation is attributed to greater coupling across a subduction boundary, which results in extensive shortening within the overriding continental plate. In this case, Late Cretaceous thrusting simply telescoped an older assemblage of terranes and associated clastic overlap sequences. Option B invokes an irregular transform margin where terranes and Jura-Cretaceous clastic sequences are transported northward within a system of coast-parallel faults. Orogenic shortening occurs when these fault slices collide with a reentrant in the margin. It is important to note that neither of these options consider the large northward translation indicated by the paleomagnetic data of Beck and others (1981) and Irving and others (1985a). The reason is that this proposed translation occurred after Late Cretaceous thrusting. In fact, the paleomagnetic data indicate that the San Juan-Cascade thrust system formed at the latitudinal position of Baja California.

volcanic rocks of the eastern Sierra Nevada (Schweickert, 1981), based on their similar fusulinid faunal and arc-volcanic composition (Davis and others, 1978); (2) the Deadman Bay terrane with the Western Paleozoic and Triassic belt of the Klamaths (Irwin, 1981; Wright, 1982; Ando and others, 1983), both of which contain Permian to Middle(?) Jurassic sequences of chert, argillite, basalt, and limestones with Tethyan fauna, including Tethyan fusulinids, (3) the Garrison terrane possibly with Triassic blueschists of the Klamath Mountains (Davis and others, 1978; Irwin, 1981), although the metamorphic age of the Garrison is somewhat older than that of the Klamath blueschists; and (4) the Decatur terrane with the Coast Range ophiolite and basal Great Valley Group (Hopson and others, 1981; Shervais and Kimbrough, 1985; Garver, 1986).

If our interpretation is correct, then Late Cretaceous thrusting apparently involved the tectonic reworking of an older assemblage of accreted terranes, located somewhere along the American continental margin. We hesitate to say the *North* American continent margin because of increasing evidence that most of British Columbia and western Washington, including Wrangellia, the Coast Plutonic Complex, and the San Juan–Cascades thrust system, were at the latitude of Baja California ( $37 \pm 5^\circ\text{N}$ ) during the Late Cretaceous (about 85 Ma; Beck and others, 1981; Irving and others, 1985a). According to Irving and others (1985a, b), this collage of terranes was displaced northward en masse about 2500 km and rotated about  $65^\circ$  clockwise during the latest Cretaceous and earliest Tertiary. If these paleomagnetic data are correct, then terranes in the San Juan Islands and North Cascades are not simply northward continuations of California geology, but instead originated somewhere to the south of California. While this possibility may seem like a major problem, we note that equivalent terranes in California were accreted in long belts that extended at least the length of California and probably farther. Therefore, rocks of the San Juan Islands, North Cascades, and southern British Columbia may have been removed from the southern end of these accreted belts and transported northward during the latest Cretaceous and early Tertiary. A similar history of latest Cretaceous and early Tertiary northward displacement of about 2500 km has been documented for the Salinian block of California (Page, 1982; Champion and others, 1984).

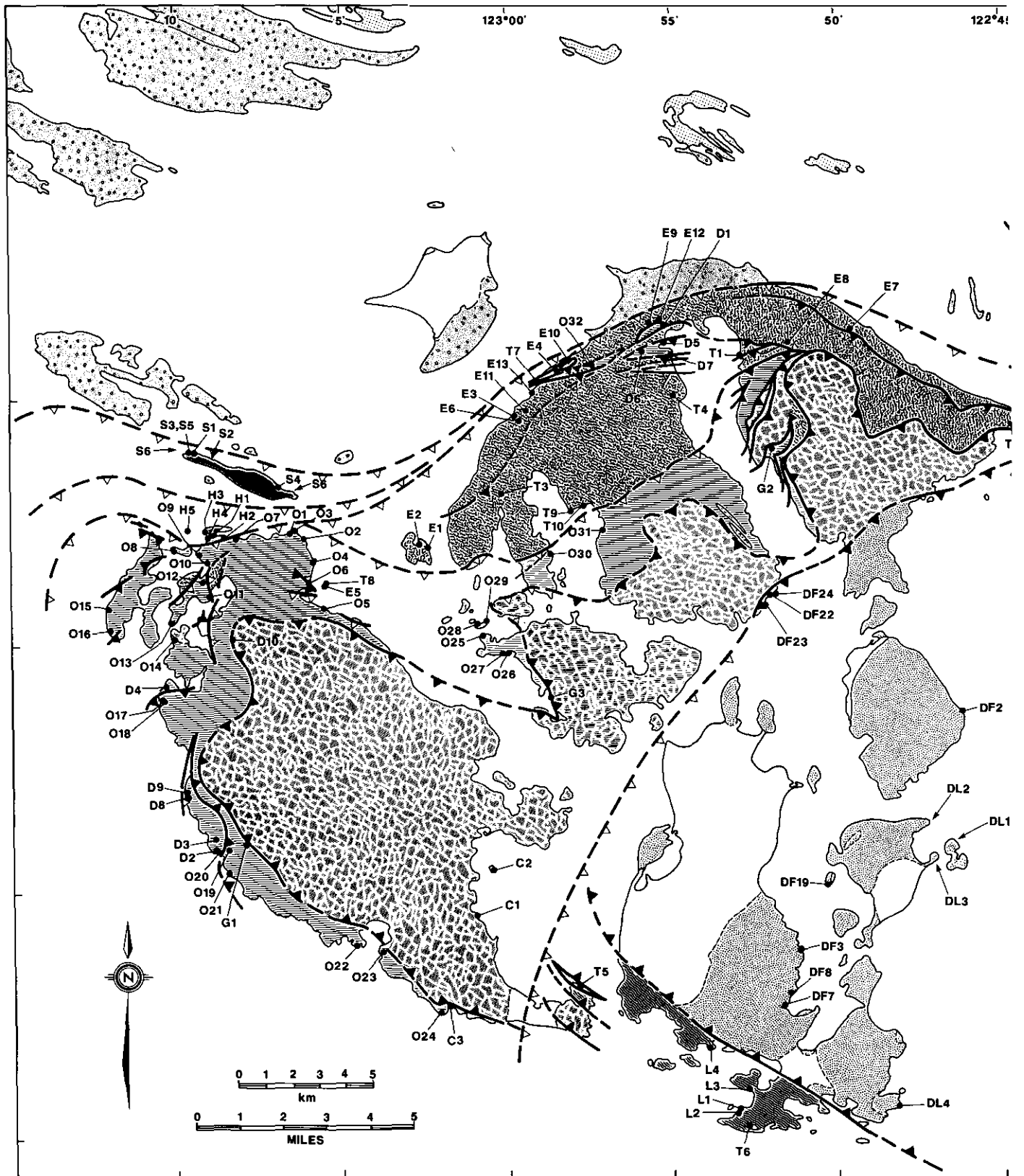
We now consider the second question: what collided with what? The clastic-rich Jura-Cretaceous units imply that Wrangellia and the San Juan–North Cascade terranes were adjacent to or part of the America continent by the latest Jurassic. Moreover, there is no evidence for arrival and collision of an exotic terrane during the Cretaceous. Even so, we consider the San Juan–Cascade orogen to be collisional in nature because it involved widespread thrusting and rapid contractional deformation within an active continental margin. This situation is in contrast to normal subduction at a convergent margin, where deformation is typically concentrated at the front and base of the overriding accretionary wedge (Karig, 1983).

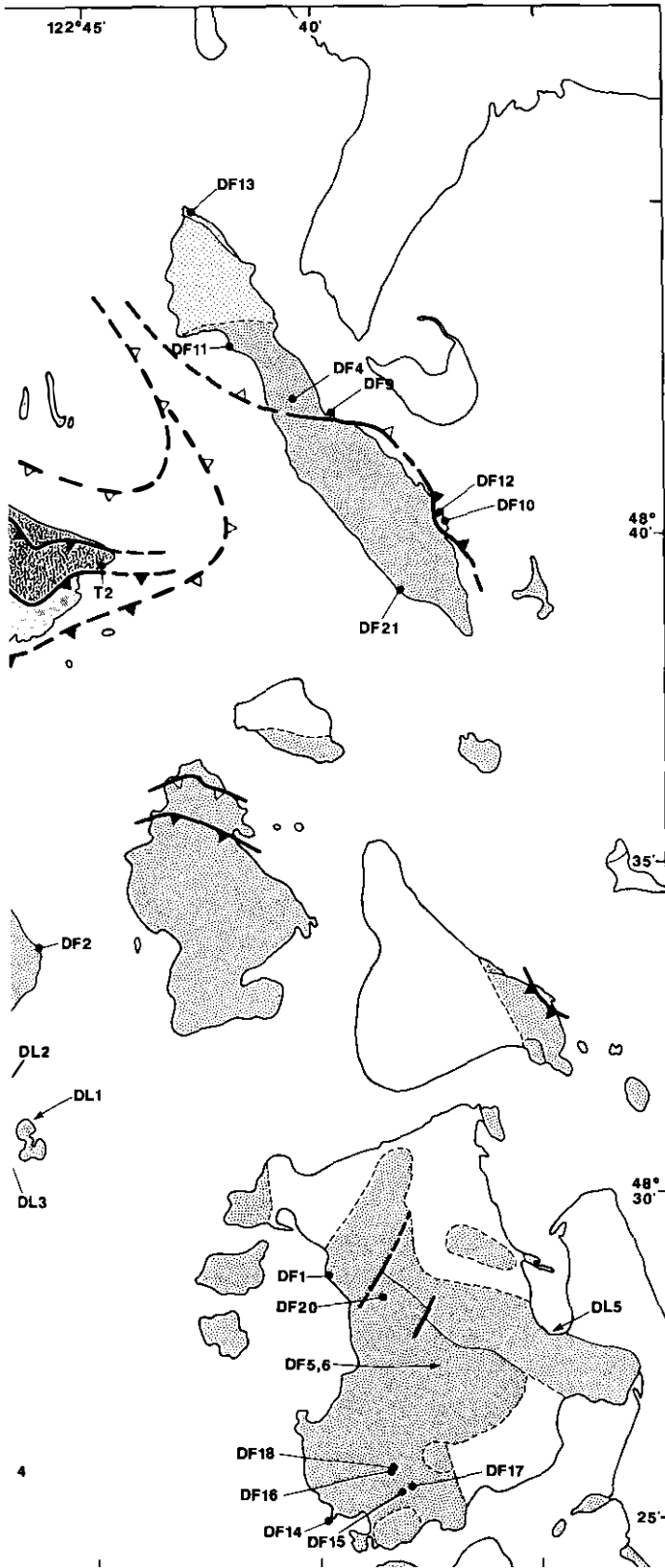
Figure 30 illustrates two simple models for the Late Cretaceous event, both of which are compatible with our conclusion that Pacific Northwest terranes were in continental-margin settings prior to thrusting. The first model (option A in Fig. 30) attributes orogenic deformation to greater coupling across a subduction boundary, which causes extensive shortening within the overriding continental plate. In this case, the Jura-Cretaceous clastic units are interpreted to be an originally coextensive overlap sequence that rested on an older sutured assemblage of terranes. Late Cretaceous thrusting, therefore, simply telescoped this assemblage and imbricated the Jura-Cretaceous sequence. In this model, major displacements, greater than about 100 to 200 km, between various terranes would be restricted to pre-Late Jurassic, before the development of the clastic overlap sequence.

The second model (option B in Fig. 30) invokes an irregular transform margin where terranes and Jura-Cretaceous clastic sequences are transported northward within a system of coast-parallel faults. Orogenic shortening occurs when these fault slices collide with a reentrant in the margin, perhaps similar to the present collision of the Yakutat block in the Gulf of Alaska (Bruns, 1983). An important implication of this model is that the Jura-Cretaceous sequences might have formed at widely separate locations along the margin. Option B shows an east-west strike for the Pacific Northwest margin and the resulting collision zone. This is based on the paleomagnetic data cited above, which indicates  $65^\circ$  of clockwise rotation after Late Cretaceous thrusting. Within this proposed collision, Wrangellia (labelled “Wr” in Fig. 30) would represent the colliding block, and the San Juan–Cascade thrust system the collision zone. Jura-Cretaceous marine strata of the Methow-Tyughton area, located east of the Cascade Range, would represent the more inboard continental margin.

## CONCLUDING REMARKS

In this synthesis of the geology of the San Juan Islands, we show how terrane analysis is built on a foundation of individual rock units, which are the primary record of depositional setting, provenance, metamorphism, and deformation. In the case of the San Juan thrust system, we have utilized detailed mapping in combination with petrologic, isotopic, and paleontologic analyses to identify terranes, compare them, and assess their original paleogeographic relationships. Our work supports the hypothesis that, at the time of their emplacement during the Late Cretaceous, terranes in the San Juan Islands were not exotic but instead were already adjacent to a continent, probably North or Central America. Moreover, we suggest that thrust faults bounding these terranes record collisional telescoping rather than long-lived subduction. We believe that our methods and tectonic models are more generally applicable to the study of the process of terrane accretion elsewhere in the western Cordillera.





**APPENDIX A  
SUMMARY OF FOSSIL AGES AND ISOTOPIC DATES**

Tables A-1 to A-9 in this appendix contain a complete list of available fossil ages and isotopic dates for the San Juan Islands, except for isotopic dates for the Garrison Schist, which are presented in Table 5 of the text, and some fission-track dates recently published by Johnson and others (1986). Altogether there is a total of 115 localities with 146 fossil ages and isotopic dates, 56 of which are new or have been revised since the summary of Whetten and others (1978). All isotopic dates are calculated using new decay constants, and estimated errors are consistently cited at the 95 percent confidence level ( $\pm 2$  sigma). Fossil ages cite information at the stage level where available. Table A-10 lists unpublished paleontologic data and analytical data for some of these localities.

Johnson and others (1986) provide a compilation of all fission-track dates from the San Juan Islands. Some of these dates are tabulated here from the original published sources or, in the case of unpublished dates, from written communications with C. W. Naeser and R. A. Zimmerman.

Locations are shown in Figure A-1, and latitudes and longitudes are given where the exact locations are known. This compilation also includes a description of the geologic setting at each locality. Volcanic and plutonic rocks were collected at a number of these localities for geochemical analysis. The analyses and their relation to the dated localities listed here are given in Table B-1 of Appendix B.

Figure A-1. Location map for fossil ages and isotopic dates listed in Appendix A. Lines with an arrowhead indicate localities where the exact location is only approximately known.

TABLE A-1. ISOTOPIC DATES FOR THE TURTLEBACK COMPLEX

No.	Rock type and location	Dating method	Date (Ma)	References (sample no.)
<b>Older, Gabbroic Phase</b>				
T1	gabbro pegmatite. East Sound, Orcas Is. 48° 40.90', 122° 52.90'	K-Ar hornblende	554 ± 16	1 (#SJ-13A)
T2†	gabbro. Lawrence Pt., E. Orcas Is. 48° 39.49', 122° 44.69'	K-Ar hornblende	332 ± 16	2 (#O-511)
<b>Younger, Tonalitic Phase</b>				
T3	tonalite. Deer Harbor, W. Orcas Is. 48° 38.10', 123° 0.13'	<sup>207</sup> Pb/ <sup>206</sup> Pb zircon‡	409 ± 25	3,1 (#68-20)
T4	tonalite. East Sound, Orcas Is. 48° 40.09', 122° 54.89'	a) <sup>207</sup> Pb/ <sup>206</sup> Pb zircon † b) fission-track zircon	437 ± 10 246 ± 45	3,1 (#68-21) 1 (#68-21)
T5	tonalite, occurs as a fault slice in the Lopex Complex. Cape San Juan, S. San Juan Is. 48° 28.10', 122° 57.95'	a) <sup>207</sup> Pb/ <sup>206</sup> Pb zircon‡ b) fission-track zircon	398 ± 10 265 ± 32 294 ± 42	1 (#75-92) 1 (#75-92) 4
T6†	tonalite, occurs as a fault slice in the Lopez Complex. Iceberg Pt., S. Lopez Is. 48° 25.22', 122° 52.75'	<sup>207</sup> Pb/ <sup>206</sup> Pb zircon‡	379 ± 10	5 (#75-91)
T7	gneissic diorite. NW Orcas Island 48° 40.36', 122° 58.98'	K-Ar whole rock	259 ± 16	6; 1 (#D-18)
T8	tonalite. O'Neal Island 48° 36.25', 123° 5.45'	fission-track zircon	260 ± 24	4
T9	tonalite. West Sound, Orcas Is. 48° 37.74', 122° 58.03'	fission-track zircon	275 ± 31	4
<b>Cross-cutting Dike (related to East Sound Volcanism?)</b>				
T10†	dacite dike. West Sound, Orcas Is. 48° 37.84', 122° 57.65'	fission-track zircon	246 ± 41	7 (#JV-270)

Note: Dates have been recalculated using new decay constants (e.g., Harland and others, 1982).

Errors for dates are estimated at the 95% confidence level (± two sigma).

†See Table A-10 for original analytical data.

‡Discordant U/Pb zircon analyses; <sup>207</sup>Pb/<sup>206</sup>Pb date represents a minimum age (see Fig. 8).

References: (1) Whetten and others, 1978; (2) R. B. Forbes, written communication, 1980; (3) Mattinson, 1972; (4) C.W. Naeser and R. Zimmerman, written communication, 1983; (5) R. E. Zartman, written communication, 1983; (6) Danner, 1977, p. 484; (7) determined by J. A. Vance.

TABLE A-2. FOSSIL AGES FROM THE EAST SOUND GROUP

No.	Geologic setting and location	Age-diagnostic fossils	Age	References (sample no.)
<b>Devonian Localities</b>				
E1	isolated limestone body surrounded by volcanic rocks. Deposit #3, Jones Island 48° 36.97', 123° 2.33'	conodonts	Early Devonian (prob. Lochkovian)	1; 2, p. 131-134; 4 (#D7)
E2	Coastal outcrop of limestone interbedded in volcanic sequence. Deposit #1, Jones Island 48° 37.05', 123° 2.62'	conodonts	Middle or Late Devonian (lt. Givetian-e. Frasnian)	1; 2, p. 131-134; 4 (#D7)
E3	poorly exposed limestone bodies, interbedded in volcanic sequence. Orcas Lime Co., NW Orcas Island 48° 39.69', 122° 59.72'	brachiopods	Middle or Late Devonian (Givetian-Frasnian)	3, p. 494; 2, p. 177-179; 4 (#D13)
E4	poorly exposed limestone bodies interbedded in volcanic sequence. Red Cross Quarry, NW Orcas Island 48° 40.58', 122° 58.38'	corals, algae, brachiopods, protozoa	late Middle Devonian	2, p. 142-144; 4 (#D8)
E5	limestone interbedded in tuffaceous argillite; may unconformably overlie Turtleback rocks. O'Neal Island 48° 36.19', 123° 5.48'	corals	probably Devonian	2, p. 123-124; 4 (#D6)
E6	poorly exposed limestone body, interbedded in volcanic sequence. Soderberg Quarry, NW Orcas Island 48° 39.61', 122° 59.57'	stromatoporoids	probably Devonian	2, p. 183-184
<b>Pennsylvanian Localities</b>				
E7	isolated limestone body, probably associated with nearby argillite sequence. Mt. Constitution, E. Orcas Island 48° 41.40', 122° 49.51'	fusulinids	Middle or possibly Early Pennsylvanian	2, p. 198; 3, p. 495; 4 (#D15)
E8	limestone interbedded in siliceous argillite sequence. Mt. Constitution, E. Orcas Island 48° 41.14', 122° 51.38'	fusulinids	Early Pennsylvanian	2, p. 203; 4 (#D16)
E9	isolated limestone body. Double Hill deposit #3, East Sound, Orcas Island 48° 41.58', 122° 55.57'	fusulinids	Early Pennsylvanian	2, p. 154; 4 (#D10)
E10	isolated limestone body, surrounded by volcanic sequence. Englehartson deposit, NW Orcas Is. 48° 40.82', 122° 58.01'	fusulinids	Early Pennsylvanian or possibly Late Mississippian	2, p. 161-162; 4 (#D11)

TABLE A-2. FOSSIL AGES FROM THE EAST SOUND GROUP (continued)

No.	Geologic setting and location	Age-diagnostic fossils	Age	References (sample no.)
E11	fragments of fossiliferous limestone in volcanic breccia. Locally limestone is interbedded in the breccia. Orcas Knob, NW Orcas Island 48° 39.80', 122° 59.37'	(a) fusulinids (b) brachiopods (c) coral	E. or M. Pennsylvanian (Desmoinesian-Atokan) probably Lt. Mississippian probably Pennsylvanian	2, p. 66; 3, p. 494-495 and Fig. 28; 5, p. 105-112
<b>Permian Localities</b>				
E12	poorly exposed limestone body, volcanic rocks exposed nearby. Double Hill deposit #1, East Sound, Orcas Island 48° 41.60', 122° 55.27'	fusulinids	Early Permian (Wolfcampian)	2, p. 151-153, 73; 4 (#D9a)
E13	coastal outcrop of limestone interbedded in volcanic sequence; may belong to Deadman Bay Volcanics. Soderberg Beach, NW Orcas Island 48° 40.18', 122° 59.15'	fusulinids, algae	Permian	2, p. 188; 4 (#D14)
References: (1) Savage, 1984; (2) Danner, 1966; (3) Danner, 1977; (4) Whetten and others, 1978; (5) Danner, 1957.				

*The Late Cretaceous San Juan thrust system*

**TABLE A-3. FOSSIL AGES FROM THE DEADMAN BAY VOLCANICS**

No.	Geologic setting and location	Age-diagnostic† fossils	Age	References (sample no.)
D1	isolated limestone body, surrounded by argillite, chert and volcanic rock. Double Hill deposit #4, East Sound, NW Orcas Is. 48° 41.51', 122° 55.15'	fusulinids (Tethyan)	Early Permian (early Leonardian)	1, p. 155-156; 2, p. 496; 4 (#D9b)
D2†	limestone interbedded with pillow basalt. Deadman Bay, W. San Juan Is. 48° 30.86', 123° 8.92'	(a) algae (b) conodonts	Permian Early Permian (late? Leonardian)	1, p. 114; 2, p. 496; 4 (#D2a) 3 (GSC# C-103879)
D3	limestone interbedded with pillow basalt. Cowell Quarry, W. San Juan Is. 48° 31.09', 122° 8.86'	fusulinids (Tethyan)	Late Permian (early Guadalupian)	1, p. 109-111; 2, p. 496; 4 (#D2b)
D4	limestone interbedded in basalt sequence. Mitchell Bay, NW San Juan Is. 48° 34.23', 123° 10.35'	fusulinids, in part from limestone float (Tethyan)	Late Permian (early Guadalupian)	1, p. 118-119; 2, p. 496; 4 (#D3)
D5	small limestone lenses interbedded in pillow basalt and chert sequence. Judd Cove, Orcas Island 48° 41.17', 122° 55.13'	(a) fusulinids from limestone (Tethyan) (b) radiolaria from chert (2 samples)	Late Permian (early Guadalupian) Late Triassic	1, p.167-168; 2, p. 497; 4 (#D12a) 5 (#79J-141, 79812J-2)
D6	isolated limestone body, surrounded by chert and volcanic rocks. Fowler deposit #2. W. of Judd Cove, Orcas Island 48° 40.95', 122° 55.78'	fusulinids (Tethyan)	Late Permian (early Guadalupian)	1, p. 165; 2, p. 497; 4 (#D12b)

TABLE A-3. FOSSIL AGES FROM THE DEADMAN BAY VOLCANICS (continued)

No.	Geologic setting and location	Age-diagnostic† fossils	Age	References (sample no.)
D7	limestone interbedded in pillow basalt and chert sequence. Camp Indralaya deposit, S. of Judd Cove, Orcas Island 48° 40.94', 122° 54.91'	fusulinids (Tethyan)	Late Permian (early Guadalupian)	1, p. 169-171; 2, p. 497; 4 (#D12c)
D8	ribbon chert interbedded in pillow basalt sequence. S. of Smallpox Bay, W. San Juan Is. 48° 31.96', 123° 9.75'	(a) conodonts from chert (2 samples)	Early Permian (late Wolfcampian)	4 (#77-55D, -55B)
		(b) radiolaria from chert (6 samples)	Permian	4 (#77-55A, -55B, -55D, -55F, -55H, -55I)
		(c) radiolaria from chert (3 samples)	Triassic	4 (#77-55C, -55E, -55G)
D9	ribbon chert interbedded in pillow basalt sequence. S. of Smallpox Bay, W. San Juan Is. 48° 32.06', 123° 9.76'	radiolaria from chert	Permian	4 (#75-392)
D10	limestone lens in chert and volcanic rock; tentatively included with Deadman Bay unit. Young Hill, NW San Juan Is. 48° 35.02', 123° 8.31'	fusulinids from limestone float (Cosmopolitan or Tethyan)	Permian	1, p. 92; 4 (#D1)

†Paleontological report for D2b given in Table A-10.

‡Fusulinid faunal affinity is shown in parentheses where available.

References: (1) Danner, 1966; (2) Danner, 1977; (3) M. J. Orchard, written communication, 1985; (4) Whetten and others, 1978; (5) D. L. Jones, written communication, 1980.

TABLE A-4. FOSSIL AGES FROM THE ORCAS CHERT

No.	Geologic setting and location	Age and diagnostic fossils	References (sample no.)
<b>Localities on Northeast San Juan Island</b>			
O1	chert with tuff. W. of Limestone Point 48° 37.30', 123° 6.49'	probably E. Jurassic, radiolaria	1 (#76-100b)
O2	interbedded chert and pillow basalt. SE of Limestone Point 48° 37.18', 123° 6.09'	probably E. Jurassic, radiolaria	1 (#76-101)
O3	large limestone body surrounded by chert (see loc. O2 and O3). Limestone Point 48° 37.33', 123° 6.41'	Late Triassic (late Carnian), conodonts from limestone	2; supersedes age in ref. 3, p. 119-120 and ref. 1 (#D4)
O4	interbedded chert and basalt flows. S. of San Juan County Park. 48° 36.70', 123° 5.85'	M. or Lt. Triassic, radiolaria	1 (#76-104)
O5	ribbon chert with minor basalt and tuff. S. of O'Neal Is. 48° 35.78', 123° 5.50'	Triassic, radiolaria	1 (#77-14)
O6	highly faulted ribbon chert. Along coast W. of O'Neal Is. 48° 36.26', 123° 6.07'	Lt. Triassic-E. Jurassic, radiolaria	1 (#77-15a, -15b)
O7	interbedded chert, pillow basalt and minor limestone pods. SE of Davison Head 48° 37.20', 123° 8.13'	(a) Triassic, radiolaria	1 (#77-17a)
		(b) E. Jurassic, radiolaria (Pieinsbachian-Toarcian)	1 (#77-17c,d,e)
		(c) Jurassic, radiolaria (Toarcian-Tithonian)	1 (#77-17b)
<b>Localities on Northwest San Juan Island and Vicinity</b>			
O8	only ribbon chert. SW Pearl Is., N. of Roche Harbor 48° 36.95', 123° 10.02'	Triassic, radiolaria	1 (#77-44)
O9	disrupted sequence of chert and minor basalt. Opposite Pearl Is., N. of Roche Harbor 48° 36.87', 123° 9.31'	(a) Triassic?, radiolaria	1 (#77-43)
		(b) Lt. Triassic (Norian), conodonts and radiolaria	5 (#SJ-7)
O10	disrupted sequence of chert and basalt. N. of Roche Harbor 48° 36.71', 123° 8.99'	Lt. Triassic, radiolaria	5 (#SJ-3d, -4a)
O11	limestone, basalt and chert. SE of Roche Harbor Quarry 48° 36.04', 123° 8.90'	Lt. Triassic, radiolaria from chert	6 (#79J-26)
O12†	large limestone bodies in ribbon chert sequence (see p. 84-87 in ref. #3). Roche Harbor Quarry 48° 36.30', 123° 9.22'	(a) Triassic, radiolaria from chert	5 (#SJ-10)
		(b) Lt. Triassic (Carnian), conodonts from limestone	7; supersedes Paleozoic age in ref. 3, p. 87, and ref. 1 (#D5)

TABLE A-4. FOSSIL AGES FROM THE ORCAS CHERT (continued)

No.	Geologic setting and location	Age and diagnostic fossils	References (sample no.)
O13	chert and minor pillow basalt. White Point, SW of Roche Harbor Quarry 48° 35.45', 123° 10.19'	(a) Triassic, radiolaria (b) Mississippian, radiolaria (spurious age, see text)	1 (#77-42a, -42c) 1 (#77-42b)
O14	only ribbon chert. Yacht Haven 48° 35.14', 123° 10.09'	Lt. Triassic, radiolaria (lt. Norian)	5 (#SJ-100, -102)
O15	ribbon chert and minor basalt. SE Henry Island, SW of Roche Harbor 48° 35.79', 123° 12.09'	Triassic, radiolaria	1 (#77-40)
O16	ribbon chert and minor basalt. S. Henry Island, SW of Roche Harbor 48° 35.33', 123° 12.03'	Lt. Triassic-E. Jurassic, radiolaria	1 (#77-41)
O17	ribbon chert and minor basalt. Smuggler's Cove, S. of Roche Harbor 48° 33.88', 123° 10.46'	Lt. Triassic, conodonts (lt. Carnian-m. Norian)	5 (#SJ-106)
O18	ribbon chert and minor basalt. Smuggler's Cove, S. of Roche Harbor 48° 33.87', 123° 10.40'	E. Jurassic, radiolaria (probably Pleinsbachian)	5 (#SJ-107)
<b>Localities on Southwest San Juan Island</b>			
O19	only ribbon chert. Westside Rd., Deadman Bay area 48° 30.85', 123° 8.51'	probably Lt. Triassic, conodonts	5 (#SJ-210)
O20	fault slice of ribbon chert; may belong to Deadman Bay unit. N. side of beach of Deadman Bay 48° 30.80', 123° 8.80'	probably Lt. Triassic, conodonts	5 (#SJ-211)
O21	interbedded chert and basalt. S. of Deadman Bay 48° 30.35', 123° 8.47'	Triassic, radiolaria	1 (#77-54)
O22	ribbon chert (setting unknown) N. side of False Bay 48° 28.89', 123° 4.68'	Triassic, radiolaria	1 (#77-53)
O23	only ribbon chert. S. side of False Bay 48° 28.75', 123° 3.95'	Triassic, radiolaria	8 (#78F-4)
O24	only ribbon chert. Eagle Pt. 48° 27.55', 123° 2.18'	Triassic, radiolaria	8 (#78F-27)
<b>Localities on Shaw and Cliff Islands</b>			
O25	only ribbon chert. Neck Pt., Shaw Island 48° 35.17', 123° 0.79'	Triassic, radiolaria	1 (#77-56)
O26	only ribbon chert. NW Shaw Is. 48° 34.81', 123° 0.00'	probably E. Jurassic, radiolaria	6 (#79J-17)
O27	only ribbon chert, NW Shaw Is. 48° 34.81', 123° 0.12'	probably E. Jurassic, radiolaria	6 (#79J-19)
O28	minor chert interbedded in pillow basalt and limestone sequence. NW Cliff Island 48° 35.43', 123° 0.90'	Triassic, radiolaria from chert	1 (#77-57)

TABLE A-4. FOSSIL AGES FROM THE ORCAS CHERT (continued)

No.	Geologic setting and location	Age and diagnostic fossils	References (sample no.)
O29	minor chert interbedded in pillow basalt and limestone sequence. NE Cliff Island 48° 35.47', 123° 0.65'	Triassic, radiolaria from chert	1 (#77-95)
<b>Localities on Orcas Island</b>			
O30	interbedded limestone, chert and argillite. Four Winds deposit, West Sound, Orcas Island 48° 36.91', 122° 58.65'	Late Triassic, (lt. Carnian-lt. Norian), conodonts from limestone	4; see 3, p. 182 for description of locality
O31	only ribbon chert, SW Orcas Is. 48° 37.38', 122° 57.09'	Lt. Triassic-E. Jurassic, radiolaria	1 (#77-59)
O32	poorly exposed siliceous shale; unlike typical Orcas Chert, but tentatively included with the Orcas. S. of West Beach, NW Orcas Is. 48° 40.72', 122° 57.33'	Lt. Triassic-E. Jurassic, radiolaria	5 (#OC-9)

†Paleontological report for O12b given in Table A-10.

References: (1) Whetten and others, 1978; (2) Savage, 1983a; (3) Danner, 1966; (4) Savage, 1983b; (5) Igo and others, 1984; (6) D. L. Jones, written communication, 1980; (7) H. Igo, written communication, 1985; (8) D. L. Jones, personal communication, 1980 (see Brandon, 1980).

TABLE A-5. FOSSIL AGES FROM THE CONSTITUTION FORMATION

No.	Geologic setting and location	Age and diagnostic fossils	References (sample no.)
C1	ribbon chert interbedded with mudstone and sandstone in upper part of Constitution. Mulno Cove, San Juan Island 48° 29.52', 123° 0.98'	Lt. Jurassic-E. Cretaceous, radiolaria	1, 2 (#M-116) (figured on p. 21 of ref. 3)
C2†	ribbon chert interbedded in clastic sequence. Dinner Is., SE of San Juan Is. 48° 30.41', 123° 0.47'	Lt. Jurassic-E. Cretaceous, radiolaria	2 (#77-219); updated from report in ref. 1
C3	limestone slide block in mudstone and chert; separated from the main part of the Constitution by the Rosario thrust, but tentatively included with the Constitution (See Fig. 16 and text for discussion). Eagle Cove, SW San Juan Is. 48° 27.67', 123° 1.89'	Lt. Triassic (Carnian), conodonts	4 (figured on p. 75 of ref. 3)

†See Table A-10 for additional information.

References: (1) Whetten and others, 1978; (2) D. L. Jones, written communication, 1979; (3) Brandon, 1980; (4) Savage, 1984.

TABLE A-6. FOSSIL AGES AND ISOTOPIC DATES FROM THE LOPEX STRUCTURAL COMPLEX

No.	Geologic setting and location	Diagnostic fossils or dating method	Age	References (sample no.)
<b>Clastic Units</b>				
L1	chaotic mudstone sequence. Iceberg Pt., Lopez Is. 48° 25.61', 122° 52.98'	<i>Buchia pacifica</i>	E. Cretaceous (Valanginian)	1 (#76-69)
L2	chert interbedded with mudstone and siltstone. Iceberg Pt., Lopez Is. 48° 25.52', 122° 53.03'	radiolaria	Jurassic-Cretaceous	2 (#79L-1D)
<b>Jurassic Ocean-Floor Pillow Basalts of Johns Point</b>				
L3	chert interbedded with pillow basalts. Johns Pt., Lopez Is. 48° 25.97', 122° 52.72'	radiolaria	Jurassic	1 (#77L-130)
<b>Mid-Cretaceous Oceanic-Island? Pillow Basalts of Richardson</b>				
L4†	mudstone interbedded with pillow basalts. Town of Richardson, Lopez Is. 48° 26.82', 122° 53.88'	foraminifera	middle Cretaceous (latest Albian)	3; 1 (#77-46)
<b>Fault slices of Turtleback Complex (repeated from Table A-1)</b>				
T5	Turtleback tonalite. Cape San Juan, S. San Juan Is. 48° 28.10', 122° 57.95'	U/Pb zircon	early Paleozoic	1 (#75-92)
T6†	Turtleback tonalite. Iceberg Pt., S. Lopez Is. 48° 25.22', 122° 52.75'	U/Pb zircon	early Paleozoic	4 (#75-91)

†See Table A-10 for additional data.

References: (1) Whetten and others, 1978; (2) D. L. Jones, written communication, 1980; (3) W. V. Sliter, personal communication, 1986 (see Table A-10 for report); (4) R. E. Zartman, written communication, 1983.

TABLE A-7. FOSSIL AGES AND ISOTOPIC DATES FROM THE FIDALGO COMPLEX

No.	Geologic setting and location	Diagnostic fossils or dating method	Age or isotopic data	References (sample no.)
<b>Plutonic Rocks of the Fidalgo Complex</b>				
DF1	porphyritic tonalite intruding layered gabbro. Alexander Beach, Fidalgo Is. 48° 28.70', 122° 39.80'	(a) U/Pb zircon intercept date for tonalite; nearly concordant (n=4)  (b) K/Ar hornblende for gabbro  (c) fission-track zircon for tonalite	167 ± 3 Ma  157 ± 10 Ma  113 ± 16 Ma	1 (#75-374, -374A)  3 (#52-F84); 1 (#B-2)  1 (#75-374A)
DF2	hornblende-plagioclase tonalite intruding layered gabbro. E. Blakely Is. 48° 33.66', 122° 46.18'	(a) U/Pb zircon intercept date for tonalite; nearly concordant (n=2)  (b) fission-track zircon for tonalite	170 ± 3 Ma  145 ± 20 Ma	1 (#75-227)  1 (#75-227)
DF3	tonalite dikes associated with diabase and gabbro. E. Lopez Island 48° 28.81', 122° 51.02'	discordant U/Pb zircon analyses; no linear array present (n=4); date considered unreliable (see text for discussion)	age is less than 182 Ma	1 (#75-304)
DF4	tonalite apparently intruding gabbro. N. Lummi Island 48° 42.00', 122° 40.44'	concordant U/Pb zircon date (n=1)	160 ± 4 Ma	2 (#78-254); 4
DF5	hornblendite. Mount Erie, Fidalgo Is. (exact location not known)	K/Ar hornblende	162 ± 16 Ma	3 (#52-F35)
DF6	diorite. Mount Erie, Fidalgo Is. (exact location not known)	K/Ar hornblende	152 ± 15 Ma	3 (#52-F82)
<b>Pillow Basalt and Chert of the Fidalgo Complex</b>				
DF7	chert interbedded with pillow basalt. E. Lopez Is. 48° 27.68', 122° 51.60'	radiolaria	Jurassic	1 (#77L-104)
DF8	chert interbedded with pillow basalt. E. Lopez Is. 48° 27.92', 122° 51.35'	radiolaria	Late Jurassic	6 (#80-87); supersedes #77L-107 in ref. 1
DF9	chert interbedded with pillow basalt. Sunrise Cove, Lummi Is. 48° 41.85', 122° 39.56'	radiolaria	Middle Jurassic	4
DF10	chert interbedded with pillow basalt. N. of Reil Harbor, Lummi Is. 48° 40.19', 122° 37.00'	radiolaria	M.-Lt. Jurassic (lt. Bajocian-Kimmeridgian)	1; 4 (#PRC-23)
DF11	black siliceous mudstone interbedded with pillow basalt. Legoe Bay, Lummi Island 48° 42.80', 122° 41.89'	radiolaria	M.-Lt. Jurassic (lt. Bajocian-Kimmeridgian)	1; 4 (#PRC-64)
DF12	chert interbedded with pillow basalt. Deepwater Bay, Lummi Island 48° 40.33', 122° 37.14'	radiolaria	M. Jurassic or younger	1; 4 (#PRC-0)

TABLE A-7. FOSSIL AGES AND ISOTOPIC DATES FROM THE FIDALGO COMPLEX (continued)

No.	Geologic setting and location	Diagnostic fossils or dating method	Age or isotopic data	References (sample no.)
DF13	chert interbedded with pillow basalt. Migley Pt., Lummi Is. 48° 44.86', 122° 42.72'	radiolaria	Mesozoic	4
DF14	chert interbedded with pillow basalt. Rosario Head, Fidalgo Is. 48° 24.98', 122° 39.81'	radiolaria	Late Jurassic	6 (#80-77)
<b>Arc Volcanic Sequence of the Fidalgo Complex</b>				
DF15† and DF16†	tuffaceous argillite interbedded in arc-volcanic sequence. N. of Pass Lake, Fidalgo Is. 48° 25.40', 122° 38.13' 48° 25.75', 122° 38.37'	radiolaria	Late Jurassic (Oxfordian-lt. Tithonian)	5 (#66-M115) and -M154)
DF17† and DF18†	tuffaceous argillite (same area and setting as DF15). 48° 25.52', 122° 37.89' 48° 25.78', 122° 38.32'	radiolaria	Jurassic-E. Cret. (Toarcian-e. Hauterivian)	5 (#66-M123a and -M157)
DF19	siliceous argillite interbedded with siltstone and tuff. SW Trump Island 48° 30.11', 122° 50.28'	radiolaria	Late Jurassic (e. Tithonian)	1 (#75-62)
DF20†	siliceous argillite unconformably overlying plutonic rocks of the Fidalgo Complex. Marine Asphalt Quarry, Fidalgo Is. 48° 28.36', 122° 38.55'	radiolaria	Late Jurassic (lt. Kimmeridgian-e. Tithonian)	5 (#66-PT18); supersedes #B-1 in ref. 1
<b>Miscellaneous Sedimentary Rocks of the Fidalgo Complex</b>				
DF21	chert at base of Lummi turbidites. SW Lummi Is. 48° 39.11', 122° 38.01'	radiolaria	Lt. Jurassic-E. Cretaceous	4
DF22(§)	minor chert interbedded with clastic rocks. Probably at or near top of Fidalgo Complex. S. Orcas Island 48° 36.03', 122° 51.98'	radiolaria	Late Jurassic	1 (#77-61)
DF23(§)	same as DF22. 48° 35.81', 122° 52.15'	radiolaria	Lt. Jurassic-E. Cretaceous	1 (#77-60)
DF24(§)	same as DF22. 48° 36.06', 122° 51.81'	radiolaria	Jurassic-Cret.	1 (#77-64)

Note: Isotopic dates have been recalculated using new decay constants (e.g., Harland and others, 1982).

Errors for dates are estimated at the 95 percent confidence level ( $\pm$  two sigma).

†Lower intercept dates reported here are calculated for each locality, as opposed to Whetten and others (1978) who calculated a composite lower intercept date based on all analyses from DF1, DF2, and DF3.

‡Paleontological report given in Table A-10.

(§)DF22, DF23, and DF24, which were originally included in the Constitution Formation (Vance, 1975; Whetten and others, 1978), now are assigned to the Fidalgo Complex; see text for discussion.

References: (1) Whetten and others, 1978; (2) Whetten and others, 1980; (3) Brown, 1977, p. 70; (4) Carroll, 1980, p. 10; (5) Pessagno, personal communication, 1984; these localities are described in Gusey, 1978; ages here supersede those reported by Gusey, 1978 (see his p. 10, 33, 53); (6) Whetten and others, 1987.

TABLE A-8. FOSSIL AGES FROM THE LUMMI FORMATION

No.	Geologic setting and location	Age and diagnostic fossils	References (sample no.)
DL1	turbidite sequence. NE James Island (exact location not known)	Late Jurassic (it. Tithonian), <i>Buchia Piochii</i>	1
DL2 and DL3	turbidite sequence. Fauntleroy Pt. and Decatur Head, NE Decatur Is. (exact location not known)	Lt. Jurassic- E. Cretaceous, belemnite	2 (#75-42, -318)
DL4†	turbidite sequence containing abundant chert clasts. Watmough Head, SE Lopez Island 48° 25.65', 122° 48.13'	Lt. Jurassic- E. Cretaceous, belemnite	2 (#W-1)
DL5	mud-rich turbidite sequence. Dean's Corner, E. Fidalgo Island (exact location not known)	Jurassic or younger <i>Pinna</i> (clam)	3

†Originally included in the Lopez Complex by Whetten and others (1978); now assigned to the Lummi Formation. See text for discussion.  
References: (1) Garver, 1986; (3) Whetten and others, 1978; (3) Mulcahey, 1975.

TABLE A-9. FOSSIL AGES AND ISOTOPIC DATES FROM THE SPIEDEN GROUP AND HARO FORMATION

No.	Geologic setting and location	Diagnostic fossils or dating method	Age or isotopic data	References (sample no.)
<b>Haro Formation (northern San Juan Island)</b>				
H1 and H2	thin beds of coquina. Davison Head 48° 37.27', 123° 8.83' 48° 37.23', 123° 8.44'	<i>Halobia</i> cf. <i>H. inortissima</i>	Late Triassic (early Carnian-middle Norian)	1 (#H-1); 2
H3	shale interbedded in tuff breccia. Davison Head 48° 37.35', 123° 9.08'	radiolaria	Late Triassic (Carnian-Norian)	3 (#SJ-38)
H4	siliceous shale interbeds. Davison Head 48° 37.24', 123° 8.93'	radiolaria	Late Triassic-earliest Jurassic, (Norian-Pliensbachian)	3 (#SJ-16 to -31)
H5†	quartz albite porphyry; tentatively included with Haro Fm., but may be related to Spieden Group (see text). Barren Is., W. of Davison Head 48° 37.38', 123° 9.56'	K/Ar whole rock	141 ± 10 Ma	4
<b>Spieden Group (Splden Island)</b>				
S1	massive sandstone of the Spieden Bluff Fm. 48° 38.96', 123° 9.40'	<i>Buchia concentrica</i>	Late Jurassic (Oxfordian or Kimmeridgian)	1 (#75-51A); 5, p. 1698
S2†	andesite clast from conglomerate in the basal member of the Spieden Bluff Fm.; max. age of deposition. (exact location not known)	K/Ar hornblende	152 ± 4 Ma.	6; 5, p. 1697 (#SJ-513)
S3 and S4	massive sandstone of Sentinel Island Fm. 48° 38.95', 123° 9.47' 48° 38.26', 123° 6.86'	<i>Buchia crassicolis solida</i>	Early Cretaceous (Valanginian)	1 (#75-51B, -51D); 5, p. 1701
S5	massive sandstone of the Sentinel Island Fm. 48° 38.95', 123° 9.47'	<i>Inoceramus colonicus</i> or <i>ovitoides</i>	Early Cretaceous (Hautervian)	1 (#75-51C); 5, p. 1701
S6†	igneous clasts from conglomerate in the Sentinel Island Fm.; max. age of deposition. (exact location not known)	(a) K/Ar hornblende on dacite porphyry  (b) fission-track dates on dacite porphyry  (c) fission-track zircon date on granodiorite	145 ± 3 Ma  138 ± 16 Ma (zircon) 147 ± 22 Ma (apatite)  147 ± 20 Ma	6; 5, p. 1702 (#76-99)  5, p. 1702  5, p. 1702

†See Table A-10 for analytical data.

References: (1) Whetten and other, 1978; (2) Danner, 1966, p. 84, 121-122; (3) Igo and others, 1984; (4) Danner, 1977, p. 485, R. L. Armstrong, personal communication, 1986; (5) Johnson, 1981; (6) R. W. Tabor, written communication, 1986.

TABLE A-10. ADDITIONAL DATA FOR FOSSIL AGES AND ISOTOPIC DATES

**T2, Turtleback gabbro.** K/Ar hornblende date determined by Krueger Enterprises, Inc. (Cambridge, Massachusetts) (R. B. Forbes, written communication, 1980).

Sample no.	K (wt. %)	<sup>40</sup> Ar(rad) (10 <sup>-10</sup> mol/gr)	<sup>40</sup> Ar(rad)/ <sup>40</sup> Ar(tot) (n=2)	Date ± 2 sigma (Ma)
0-511	0.378 (n=3)	2.3382 (n=2)	85.0% (n=2)	332 ± 16

Note: "(n= )" indicates an average of n replicate measurements.

**T6, Turtleback tonalite.** U/Pb zircon date determined by R. E. Zartman (written communication, 1983) of the U.S. Geological Survey. Sample no. = 75-91.

Fraction	Mesh size	Concentration (ppm)			Pb isotopes (atom percent)			
		U	Th	Pb	<sup>204</sup> Pb	<sup>206</sup> Pb	<sup>207</sup> Pb	<sup>208</sup> Pb
A	-100+150	286.5	75.6	15.56	0.0549	85.16	5.422	9.364
B	-200+250	312.3	88.7	16.61	0.0276	85.99	5.060	8.922
Fraction		Date ± 2 sigma (Ma)						
		<sup>206</sup> Pb/ <sup>238</sup> U	<sup>207</sup> Pb/ <sup>235</sup> U	<sup>207</sup> Pb/ <sup>206</sup> Pb	<sup>208</sup> Pb/ <sup>232</sup> Th			
A		334 ± 5	340 ± 5	381 ± 10	337			
B		332 ± 5	338 ± 5	377 ± 10	332			

**T10, Dacite dike in Turtleback Complex.** Zircon fission-track date determined by J. A. Vance. Sample no. = JV-270. External method, 7 grains. Fossil tracks = 0.3135 x 10<sup>6</sup> tracks/cm<sup>2</sup> (1380 tracks). Induced tracks = 0.3772 x 10<sup>5</sup> tracks/cm<sup>2</sup> (166 tracks). Neutron flux = 0.101 x 10<sup>16</sup> neutrons/cm<sup>2</sup>. Date ± 2 sigma = 246 ± 41 Ma (error calculated using conventional error equation).

**D2b, Limestone from the Deadman Bay Volcanics.** Conodonts identified by Dr. M. Orchard (Geological Survey of Canada; report #C-103879, July 1985). Conodont taxa are: *Neogondoella* sp., *Neostreptognathodus* sp. indet., *Sweetognathodus* cf. *S. adjunctus* (Behnken). Age is Early Permian, late? Leonardian. Conodont alteration index is 3 to 4.

**O12b, Limestone in Orcas Chert.** Conodonts identified by Dr. Hisayoshi Igo, University of Tsukuba, Japan, (written communication, December 1985). His letter is quoted as follows: "Recently, we have found some Carnian conodonts from the pale gray foraminiferal limestone block embedded in the argillite-chert-graywacke sequence exposed at Roche Harbor Quarry. Conodonts are rather rare, but we found several fragments of ramiform elements and almost complete specimens of *Neogondoella tadopole* (Hayashi) from about 2.5 kg limestone sample. We also prepared many thin sections and checked the so-called Carboniferous *Eostaffella*-like foraminifers in these limestones. Identification of these foraminifers is still preliminary, but we discriminated several foraminifers which were recently reported from Upper Triassic limestone in Europe, such as, *Ophanthalmidium* spp., *Paraophthalmidium?* spp., *Turritelletta* sp., *Trochammina* spp., "*Nodosaria*" spp., *Endothyranella?* spp., *Agathammina?* sp."

**C2, Chert in Constitution Formation.** Radiolaria identified by Dr. D. L. Jones of the U.S. Geological Survey. Quoted is part of his letter dated 16 May 1979: "77-219 (= locality C2) is a little better preserved than M-116 (= locality C1) with a more diverse fauna, although it still is in bad shape. I think there's a possibility that this sample could be as young as Valanginian—I need more SEM pictures to be sure, but they won't be available for a while." His comment modifies the original age determination for C2 of "Late Jurassic" as reported in Whetten and others (1978) to "Late Jurassic or Early Cretaceous" as reported here.

TABLE A-10. ADDITIONAL DATA FOR FOSSIL AGES AND ISOTOPIC DATES (continued)

**L4, Mudstone from the basalts of Richardson.** Foraminifera identified by Dr. W. V. Sliter of the U.S. Geological Survey (personal communication, 1986). He identified *Planomalina buxtoffi* which is restricted to the lower half of the *P. buxtoffi* biozone of the latest Albian age. (Note: the *P. buxtoffi* biozone was previously called the *Rotalipora appenninica* zone in Sliter, 1984.) This biozone has an approximate absolute age of 101 to 98 Ma based on the Harland and others (1982) time scale (see Fig. 2 in Sliter, 1984).

**DF15-DF18, DF20, Argillite from the Fidalgo Complex.** Radiolaria identified by Dr. E. A. Pessagno, Jr., of the University of Texas at Dallas. These localities were originally reported by Gusey (1978, p. 10, 33, and 53). The revised determinations below are based on a reexamination of the original samples by Pessagno (personal communication, October 1984). The biozonation used is that of Pessagno's (see Pessagno and others, 1984, and references cited there).

DF15 (#66-M115) and DF16 (#66-M154): *Archaeodictyomitra* sp., *Eucrytidium? ptyctum* (Riedel and Sanfilippo). Upper part of Zone 1 into Zone 4; Oxfordian to late Tithonian.

DF17 (#66-M123a): *Parvacingula* sp., *Hsuum* sp. Base of Superzone 1 to top of Zone 5; Toarcian to late Valanginian or early Hauterivian.

DF18 (#66-M157): *Archaeodictyomitra* sp. Very poorly preserved, age indeterminate.

DF20 (#66-PT18): *Mirifusus* sp., *Rustola procera*, *Acanthocircus variabilis*, *Archaeodictyomitra rigida* (Pessagno), *Hsuum maxwelli* (Pessagno), *Praeococconocaryomma magnimamma* (Rust), *Parvacingula* sp.(?). Good preservation. Zone 2 or 3; late Kimmeridgian to early Tithonian. This sample supersedes #B1 of Whetten and others (1978) and #52-F108 of Gusey (1978, p. 10).

**H5, Barren Island porphyry, associated with Haro Formation.** K/Ar whole rock date determined by R. L. Armstrong of the University of British Columbia (personal communication, 1986).

K (wt. %)	<sup>40</sup> Ar(rad) (10 <sup>-10</sup> mol/gr)	<sup>40</sup> Ar(rad)/ <sup>40</sup> Ar(tot)	Date ± 2 sigma (Ma)
1.077	2.7444	40.9%	141.4 ± 10

**S2, S6a, Volcanic clasts in Spieden Group conglomerates.** K/Ar hornblende dates determined by Dr. R. W. Tabor of the U. S. Geological Survey (written communication, January 1986). For sample locality S2, two splits were dated (see below), resulting in two significantly different dates. The younger date of 133 Ma is rejected, because it is much younger than the age of the enclosing strata (Oxfordian or Kimmeridgian: 163-152 Ma; see S1 in Table A-9). Dates reported here are different than those reported by Johnson (1981), because of new decay constants and because he averaged the age of the two splits for S2.

Split	K (wt. %)	<sup>40</sup> Ar(rad) (wt. ppm)	<sup>40</sup> Ar(rad)/ <sup>40</sup> Ar(tot)	Date ± 2 sigma (Ma)
<b>S2 (#SJ-513): andesite clast</b>				
A	0.2341	0.6453	57.8%	152.3 ± 3.8
B	0.2341	0.5533	44.1%	133.4 ± 9.2
(n=2)				
<b>S6a (#76-99): dacite porphyry clast</b>				
	0.3146	0.7637	74.23%	145.1 ± 2.9
(n=4)				

## APPENDIX B SUMMARY OF GEOCHEMICAL ANALYSES

This appendix presents geochemical data for igneous rocks in the San Juan Islands. It contains a total of 69 analyses, 42 of which are new. Table B-1 and Figure B-1 give information on the location and geologic setting of the analyzed samples. The analyses are listed in Tables B-2 through B-8. In those cases where only total iron was determined, it is reported as  $\text{Fe}_2\text{O}_3$ , with FeO left blank. In cases where only total  $\text{H}_2\text{O}$  was determined, it is reported as  $\text{H}_2\text{O}^+$ , with  $\text{H}_2\text{O}^-$  left blank. “—” means not determined. Where an element or oxide is below the detection limit of the analytical method, the detection limit is reported as a maximum value (e.g., <56 ppm). Major elements are recalculated on a volatile-free basis, with an assumed ferrous/ferric ratio of  $\text{FeO} = 0.9 \times$  total FeO. All trace elements were determined on volatile-free samples. A brief description of the source of these data and the analytical methods used is given below.

Only a portion of the total analyses reported in Brown and others (1979) for Fidalgo Complex rocks are included here (ref. #6 in Table B-1), such as analyses of volcanic rocks and the more mafic diorite intrusions. The gabbro-diorites of Brown and others were not included because of uncertainties as to their affinity, whether they belong to the ophiolitic basement or the younger arc volcanics. Silicic intrusive rocks (trondhemite and albite granite of Brown and others) were also excluded because they are equivalent to, and therefore represented by, the dacite arc-volcanic rocks reported in Table B-7.

**Data Sources.** The analyses in this appendix come from six different sources. The list below is keyed to the numbered references in Table B-1.

(1) X-ray fluorescence (XRF) analyses published in Vance (1977). FeO determined by chemical method.

(2) Samples collected by J. T. Whetten and analyzed by the U.S. Geological Survey (reports no. RERR and 78-RE-NA0059). Analytical method for major elements and volatiles is described in Shapiro (1975). Trace elements were determined by instrumental neutron activation analysis (INAA) and generally have relative errors less than 5 to 10 percent.

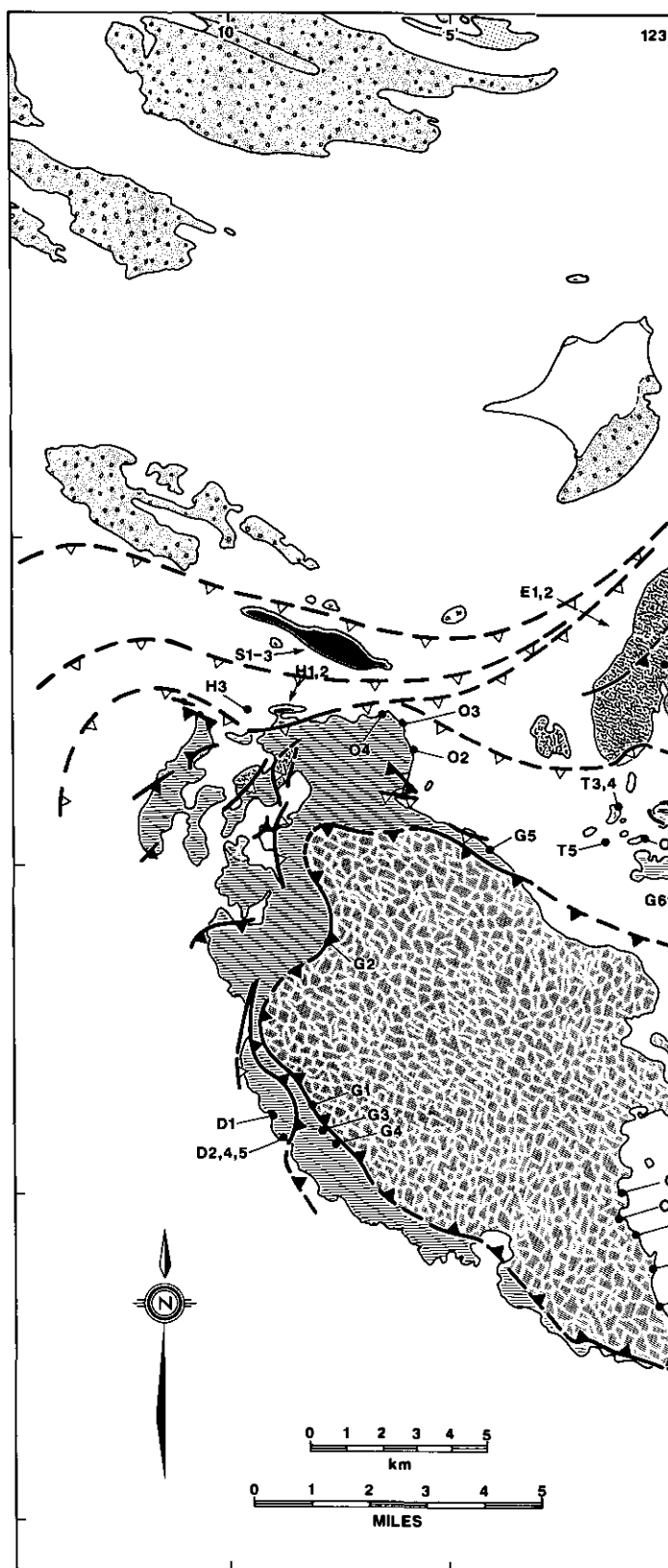
(3) XRF and INAA analyses published in Vance and others (1980; see their Appendix 1 on microfiche).

(4) Samples collected by Brandon and analyzed by the Analytical Chemistry Section of the Geological Survey of Canada (requisition no. 086-85). Major elements and most trace elements were analyzed by induction-coupled plasma spectrometry (ICP). Mo, Nb, Rb, Sr, Th, U, Y, and Zr were determined by energy-dispersive XRF, and FeO,  $\text{H}_2\text{O}$ ,  $\text{CO}_2$ , and S by chemical methods. Where included, REE, U, and Th were analyzed by XRay Assay Laboratories (Ontario, Canada) using INAA. Relative errors for the major elements are estimated at less than 2 percent, and for the trace elements at less than 5 percent for ICP and INAA analyses, and less than 10 percent for XRF analyses.

(5) Samples collected by Vance, and analyzed by XRF (FeO by chemical method) at the Università della Calabria, Italy.

(6) Selected analyses from Brown and others (1979), which were determined primarily by energy dispersive XRF. Brown and others estimated the relative error of their major-element analyses at less than 5 percent, except for  $\text{MgO}$  and  $\text{Na}_2\text{O}$ , which were less than 5 to 10 percent. Relative error for trace element analyses was estimated at less than about 15 percent, except for Rb and Sr at 5 percent.

Figure B-1. Location map for geochemical analyses listed in Appendix B. The first letter “G,” which precedes all geochemical locality numbers, is not included with the locality numbers shown on this map. Lines with an arrowhead indicate localities where the exact location is only approximately known.



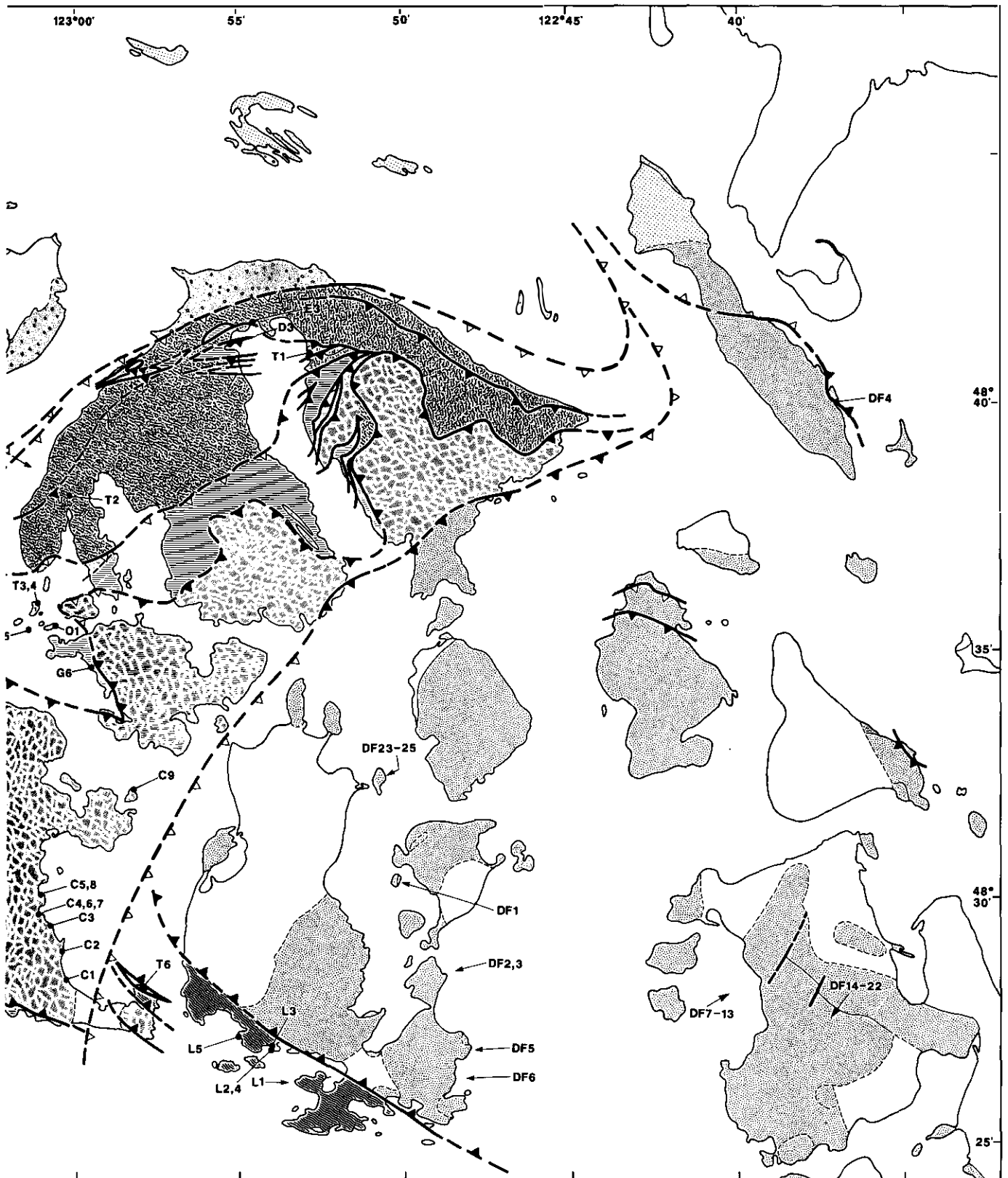


TABLE B-1. LOCATION DESCRIPTIONS AND ANALYTICAL METHODS FOR GEOCHEMICAL SAMPLES

Locality no.	Description and comments	Latitude, longitude	Data source and sample no.
<b>Turtleback complex</b>			
GT1	Cumulus gabbro from East Sound, Orcas Is.; collected near K/Ar locality T1.	48° 40.97', 122° 52.81'	1, #TBG
GT2	Tonalite from western Orcas Is.; collected from U/Pb zircon locality T3.	48° 38.10', 123° 0.13'	1, #O-466
GT3	Quartz diorite from McConnell Is., SW of Orcas Island.	48° 35.88', 123° 1.22'	2, #77-133
GT4	Quartz porphyry (tonalite), McConnell Is.	48° 35.88', 123° 1.22'	2, #77-134
GT5	Quartz diorite from Low Is., NW of Shaw Is.	48° 35.34', 123° 1.47'	2, #77-135
GT6	Tonalite from Cape San Juan, S. San Juan Is.; same as U/Pb zircon locality T5.	48° 28.10', 122° 57.94'	2, #77-139
<b>East Sound Group</b>			
GE1	Dacite from NW Orcas Island.	exact location not known	2, #77-131
GE2	Andesite from NW Orcas Island.	exact location not known	2, #77-132
GE3	Andesitic tuff breccia from near town of East Sound, NE Orcas Island.	48° 41.56', 122° 54.54'	1, #O-421
<b>Deadman Bay Volcanics</b>			
GD1	Pillow basalt from N. of Deadman Bay, W. San Juan Is.; collected near dated fossil locality D3.	48° 31.15', 123° 9.04'	2, #77-124
GD2	Pillow basalt from Deadman Bay; collected near dated fossil locality D2.	48° 30.81', 123° 8.88'	2, #77-123
GD3	Center of pillow basalt from Judd Cove, Orcas Is.; basalts are clearly interbedded with Late Permian, Tethyan fusulinid limestone and Late Triassic ribbon chert (see fossil locality D5 in Appendix A).	48° 41.17', 122° 55.13'	4, #79812J-1
GD4 and GD5	Pillow basalt from Deadman Bay.	exact locations not known	3, #SJ-21, #SJ-17
<b>Orcas Chert</b>			
GO1	Pillow basalt, Cliff Is., NW of Shaw Is.; collected near dated fossil locality O29	48° 35.41', 123° 0.65'	2, #77-136
GO2	Pillow basalt, San Juan Co. Park, NE San Juan Is.; collected near dated locality O4.	48° 36.73', 123° 5.82'	4, #79815J-1
GO3	Pillow basalt, NE San Juan Island; collected near dated fossil locality O2.	48° 37.15', 123° 6.05'	4, #79815J-2
GO4	Pillow basalt, Lonesome Cove, NE San Juan Is.; collected at dated fossil loc. O1, and near O3.	48° 37.30', 123° 6.49'	4, #79815J-3
<b>Garrison Schist</b>			
GG1	Amphibolite, Mt. Dallas, W. San Juan Is.	48° 31.31', 123° 8.15'	5, #S-75
GG2	Garnet-bearing amphibolite, W. of Mt. Cady, W. San Juan Island.	48° 33.81', 123° 7.75'	5, #S-108

**TABLE B-1. LOCATION DESCRIPTIONS AND ANALYTICAL METHODS FOR GEOCHEMICAL SAMPLES**  
(continued)

Locality no.	Description and comments	Latitude, longitude	Data source and sample no.
GG3	Coarse-grained amphibolite with minor blue amphibole, Mt. Dallas; collected at K/Ar locality G 1.	48° 30.96', 123° 7.93'	5, #S-161
GG4	Greenschist, Mt. Dallas	48° 30.72', 123° 7.62'	5, #S-95
GG5	Greenschist, NE San Juan Island	48° 35.23', 123° 4.09	5, #S-170
GG6	Greenschist, W. Shaw Island	48° 34.53', 122° 59.46'	5, #S-171
<b>Constitution Formation</b>			
GC1	Pillow basalt, Griffin Bay, SE San Juan Is.	48° 28.26', 123° 0.28'	4, #M-54
GC2	Pillow basalt, Low Pt., SE San Juan Is.	48° 28.83', 123° 0.40'	4, #M-64
GC3	Pillow basalt, Jensen Bay, SE San Juan Is.	48° 29.34', 123° 0.81'	4, #M-93
GC4	Pillow basalt, Mulno Cove, SE San Juan Is.	48° 29.60, 123° 1.18'	4, #M-106
GC5	Pillow basalt, Merrifield Cove, SE San Juan Island.	48° 30.00', 123° 1.13'	4, #M-35
GC6	Pillow basalt, Mulno Cove, SE San Juan Is.	48° 29.60', 123° 1.18'	2, #77-138
GC7	Pillow basalt, Mulno Cove, SE San Juan Is.	48° 29.60', 123° 1.18'	3, #S-165
GC8	Pillow basalt, Merrifield Cove, SE San Juan Island.	48° 30.00', 123° 1.13'	3, #S-166
GC9	Pillowed dacite, Turn Is., E. of San Juan Island.	48° 32.15', 122° 58.22'	2, #77-137
<b>Lopez Structural Complex</b>			
GL1	Pillow basalt, Johns Pt., S. Lopez Is.; contains interbedded Jur. chert (dated fossil locality L3). (Note: FeO for this sample incorrectly reported in ref #3).	exact location not known	3, #LOP24 and #L24
GL2	Pillow basalt, Richardson, S. Lopez Is.; part of the middle Cretaceous basalts of Richardson (collected near fossil loc. L4).	48° 26.82', 122° 53.90'	2, #77-140
GL3	Small gabbro intrusion associated with basalts at Richardson (see GL2).	48° 26.89', 122° 53.93'	3, #LOP27
GL4	Pillow basalt; Richardson (see GL2).	48° 26.82', 122° 53.90'	3, #LOP 25
GL5	Pillow basalt; east side of Davis Bay, S. Lopez Is.; westward continuation of middle Cretaceous basalts of Richardson	48° 27.09', 122° 55.00'	3, #LOP 28
<b>Fidalgo Igneous Complex: Ocean-floor basalts</b>			
GDF1	Pillow basalt, east side of Trump Is.	exact location not known	2, #77-144
GDF2, GDF3	Pillow basalt, Sperry Peninsula, SW Lopez Island.	exact locations not known	2, #77-143; 3, #LOP26
GDF4	Pillow basalt, Reil Harbor, E. Lopez Is.; basalts contain interbedded M.-Lt Jurassic chert (see fossil loc. DF10).	48° 40.02', 122° 36.95'	3, #LUM10
GDF5	Pillow basalt, Cape St. Mary, SW Lopez Is.	exact location not known	2, #77-141
GDF6	Pillow basalt, Chadwick Hill, SW Lopez Is.	exact location not known	2, #77-142

**TABLE B-1. LOCATION DESCRIPTIONS AND ANALYTICAL METHODS FOR GEOCHEMICAL SAMPLES**  
(continued)

Locality no.	Description and comments	Latitude, longitude	Data source and sample no.
<b>Fidalgo Igneous Complex: Arc-related basalts and diorites</b>			
GDF7, GDF8	Pyroxene basalt, N. Fidalgo Is.	exact locations not known	6, #6A, #9A
GDF9	Diorite, N. Fidalgo Is.	exact location not known	6, #3B
GDF10 - GDF13	Quartz diorite, N. Fidalgo Is.	exact locations not known	6, #3C, #10B, #28A, #25A
GDF14	Basalt, near Mt. Erie, Fidalgo Is.	exact location not known	6, #3H and 3, #52F3H
GDF15- GDF18	Basalt, near Mt. Erie, Fidalgo Is.	exact locations not known	3, #52F7G; 6, #76, #98, #103G
<b>Fidalgo Igneous Complex: Arc-related dacites</b>			
GDF19- GDF22	Dacite, near Mt. Erie, Fidalgo Is.; (called keratophyre by Brown and others, 1979).	exact locations not known	6, #99, #102A, #102B, #103D
<b>Fidalgo Igneous Complex: Arc-related dikes</b>			
GDF23	Mafic dike, Frost Is.	exact location not known	2, #77-145
GDF24, GDF25	Silicic dikes, Frost Is.	exact locations not known	2, #77-146, #77-147
<b>Haro Formation</b>			
GH1, GH2	Volcanic clasts in conglomerate, Davison Head, N. San Juan Island (near dated fossil localities H1-H4).	exact locations not known	2, #77-126, #77-127
GH3	Quartz albite porphyry, Barren Is., W. of Davison Head; tentatively included with Haro Fm., but may be related to Spieden Grp.; this locality yielded a Lt. Jurassic K/Ar date (see H5 in Appendix A).	48° 37.38', 123° 9.57'	2, #77-125
<b>Spieden Group</b>			
GS1 - GS3	Volcanic clasts from conglomerate, Spieden Island; isotopic dates (S2 and S6) indicate a Lt. Jurassic age for the clasts.	exact locations not known	2, #77-128, #77-129, #77-130

TABLE B-2. ANALYSES FROM THE TURTLEBACK COMPLEX AND EAST SOUND GROUP

Locality	Turtleback Complex						East Sound Group		
	GT1	GT2	GT3	GT4	GT5	GT6	GE1	GE2	GE3
<b>Major Elements (oxide wt. %)</b>									
SiO <sub>2</sub>	44.30	70.67	55.80	71.60	59.70	72.10	65.70	58.40	60.09
TiO <sub>2</sub>	0.42	0.34	1.90	0.30	0.87	0.28	0.53	0.88	0.93
Al <sub>2</sub> O <sub>3</sub>	15.90	14.67	13.90	13.30	17.20	13.70	13.70	15.10	15.51
Fe <sub>2</sub> O <sub>3</sub>	1.39	1.67	3.30	1.60	1.10	1.20	1.20	1.80	2.21
FeO	4.28	1.65	7.60	2.20	1.00	1.40	3.60	6.10	4.40
MnO	0.09	0.05	0.24	0.08	0.06	0.05	0.09	0.16	0.11
MgO	12.52	0.77	3.50	2.90	2.70	1.10	2.70	4.50	2.37
CaO	16.04	2.80	5.90	0.81	4.20	2.40	2.60	2.80	4.85
Na <sub>2</sub> O	0.84	4.47	4.50	4.50	6.40	4.00	5.40	5.10	3.37
K <sub>2</sub> O	0.15	0.85	0.41	0.72	1.80	0.93	0.52	0.41	1.57
P <sub>2</sub> O <sub>5</sub>	0.01	0.07	0.43	0.05	0.25	0.04	0.17	0.18	0.17
<b>Volatiles (wt. %)</b>									
H <sub>2</sub> O+	—	—	2.20	2.00	1.50	1.40	2.00	3.40	—
H <sub>2</sub> O-	—	—	0.14	0.07	0.20	0.42	0.09	0.20	—
CO <sub>2</sub>	0.38	—	0.21	0.02	2.20	0.02	1.10	0.73	—
S	0.11	—	—	—	—	—	—	—	—
Total	96.43	98.01	100.03	100.15	99.18	99.04	99.40	99.76	95.58
<b>Recalculated Major Elements (oxide wt. %)</b>									
SiO <sub>2</sub>	46.21	72.20	53.37	73.11	62.72	74.25	68.34	61.26	62.97
TiO <sub>2</sub>	0.44	0.35	1.95	0.31	0.91	0.29	0.55	0.92	0.97
Al <sub>2</sub> O <sub>3</sub>	16.59	14.99	14.29	13.58	18.07	14.11	14.25	15.84	16.25
Fe <sub>2</sub> O <sub>3</sub>	0.64	0.36	1.21	0.41	0.23	0.28	0.54	0.90	0.74
FeO	5.19	2.90	9.78	3.34	1.88	2.30	4.38	7.29	6.03
MnO	0.09	0.05	0.25	0.08	0.06	0.05	0.09	0.17	0.12
MgO	13.06	0.79	3.60	2.96	2.84	1.13	2.81	4.72	2.48
CaO	16.73	2.86	6.07	0.83	4.41	2.47	2.70	2.94	5.08
Na <sub>2</sub> O	0.88	4.57	4.63	4.59	6.72	4.12	5.62	5.35	3.53
K <sub>2</sub> O	0.16	0.87	0.42	0.74	1.89	0.96	0.54	0.43	1.65
P <sub>2</sub> O <sub>5</sub>	0.01	0.07	0.44	0.05	0.26	0.04	0.18	0.19	0.18
Total	100.00	100.00	100.00	100.00	100.00	100.00	100.00	100.00	100.00
<b>Trace Elements (element wt. ppm)</b>									
Ba	—	—	241	201	499	237	129	163	—
Co	—	—	21.9	6.2	2.9	4.7	8.7	15.8	—
Cr	—	—	7.4	7.5	13.2	2.4	34.5	13.5	—
Cs	—	—	<1.6	<1.0	<1.3	0.3	<1.2	<1.5	—
Hf	—	—	4.4	2.5	3.1	3.7	2	1.5	—
Mo	—	—	—	—	—	—	—	—	—
Nb	—	—	—	—	—	—	—	—	—
Ni	—	—	—	—	—	—	—	—	—
Rb	—	—	<39	16	44	22	<30	<37	—
Sc	—	—	30.15	11.33	22.28	8.47	16.59	27.57	—
Sr	—	—	—	—	—	—	—	—	—
Ta	—	—	0.97	1.49	0.49	0.34	1.4	1.01	—
Th	—	—	0.9	2.2	3.6	3.9	1.5	1	—
U	—	—	<1.3	0.9	1.7	1.4	<1.4	<1.8	—
V	—	—	—	—	—	—	—	—	—
Y	—	—	—	—	—	—	—	—	—
Zr	—	—	—	—	—	—	—	—	—
<b>REE Elements (element wt. ppm)</b>									
La	—	—	11	5	14	11	5	6	—
Ce	—	—	28	12	30	22	14	12	—
Nd	—	—	21	6	18	11	9	8	—
Sm	—	—	7	2.2	5	2.9	2.8	2.4	—
Eu	—	—	2.13	0.35	1.11	0.61	0.64	0.85	—
Gd	—	—	5	4.1	6.2	2.9	3.3	<5.1	—
Tb	—	—	1.44	0.5	0.8	0.63	0.59	0.61	—
Ho	—	—	0.9	<0.6	<0.9	<0.8	0.9	<1.8	—
Tm	—	—	0.84	0.48	<0.5	0.5	0.4	<0.5	—
Yb	—	—	4.8	2.4	2.7	2.7	2.6	2.1	—
Lu	—	—	0.73	0.4	0.39	0.44	0.43	0.36	—

TABLE B-3. ANALYSES FROM THE DEADMAN BAY VOLCANICS AND ORCAS CHERT

Locality	Deadman Bay Volcanics					Orcas Chert			
	GD1	GD2	GD3	GD4	GD5	GO1	GO2	GO3	GO4
<b>Major Elements (oxide wt. %)</b>									
SiO <sub>2</sub>	52.80	46.20	47.40	—	—	49.10	49.00	50.50	50.60
TiO <sub>2</sub>	1.00	2.60	2.33	—	—	1.90	2.38	2.44	2.20
Al <sub>2</sub> O <sub>3</sub>	15.40	15.30	15.90	—	—	14.60	15.70	14.00	13.90
Fe <sub>2</sub> O <sub>3</sub>	3.00	6.50	3.00	9.44	6.11	2.40	3.60	4.60	4.10
FeO	2.60	5.40	6.20	—	—	5.70	6.30	7.10	6.10
MnO	0.09	0.16	0.14	—	—	0.13	0.23	0.20	0.16
MgO	2.60	7.30	8.68	—	—	7.10	5.82	5.15	4.62
CaO	10.90	6.10	7.18	—	—	9.70	4.52	6.07	8.43
Na <sub>2</sub> O	6.10	3.30	3.94	—	—	4.20	5.62	4.40	5.53
K <sub>2</sub> O	0.31	2.10	0.51	—	—	0.72	1.10	0.63	0.34
P <sub>2</sub> O <sub>5</sub>	0.29	0.50	0.53	—	—	0.36	0.75	0.51	0.31
<b>Volatiles (wt. %)</b>									
H <sub>2</sub> O+	1.90	3.80	5.20	—	—	2.70	3.50	3.40	2.80
H <sub>2</sub> O-	0.38	0.71	—	—	—	0.90	—	—	—
CO <sub>2</sub>	2.30	0.58	0.80	—	—	1.60	2.00	1.10	1.70
S	—	—	0.03	—	—	—	0.12	0.12	0.10
Total	99.67	100.55	101.84	—	—	101.11	100.64	100.22	100.89
<b>Recalculated Major Elements (oxide wt. %)</b>									
SiO <sub>2</sub>	55.67	48.66	49.58	—	—	51.28	51.71	53.01	52.71
TiO <sub>2</sub>	1.05	2.74	2.44	—	—	1.98	2.51	2.56	2.29
Al <sub>2</sub> O <sub>3</sub>	16.24	16.12	16.63	—	—	15.25	16.57	14.70	14.48
Fe <sub>2</sub> O <sub>3</sub>	0.62	1.32	1.03	—	—	0.91	1.12	1.31	1.13
FeO	5.03	10.67	8.38	—	—	7.39	9.06	10.62	9.18
MnO	0.09	0.17	0.15	—	—	0.14	0.24	0.21	0.17
MgO	2.74	7.69	9.08	—	—	7.41	6.14	5.41	4.81
CaO	11.49	6.43	7.51	—	—	10.13	4.77	6.37	8.78
Na <sub>2</sub> O	6.43	3.48	4.12	—	—	4.39	5.93	4.62	5.76
K <sub>2</sub> O	0.33	2.21	0.53	—	—	0.75	1.16	0.66	0.35
P <sub>2</sub> O <sub>5</sub>	0.31	0.53	0.55	—	—	0.38	0.79	0.54	0.32
Total	100.00	100.00	100.00	—	—	100.00	100.00	100.00	100.00
<b>Trace Elements (element wt. ppm)</b>									
Ba	272	253	160	—	—	242	3600	1500	540
Co	16.3	49.4	38	—	—	37.7	31	36	39
Cr	4.2	303.9	310	105	5	329.2	90	65	220
Cs	<1.3	1.2	—	—	—	0.7	—	—	—
Hf	7.4	4.8	—	5.6	9.1	3.8	—	—	—
Mo	—	—	<10	—	—	—	—	—	—
Nb	—	—	29	22.5	59	—	53	25	18
Ni	—	—	190	64	—	—	150	140	160
Rb	<38	41	<10	18	8.4	18	<10	<10	<10
Sc	12.08	20.65	—	17	11	28.81	—	—	—
Sr	—	—	130	770	333	—	530	280	550
Ta	3.97	2.28	—	—	—	2.11	—	—	—
Th	5.7	1.9	2	1.8	6.2	2.6	4	2	2
U	1.3	<1.3	0.8	—	—	1.2	1.5	0.5	0.6
V	—	—	180	—	—	—	180	270	260
Y	—	—	22	25.2	34	—	26	24	35
Zr	—	—	210	213	352	—	320	150	190
<b>REE Elements (element wt. ppm)</b>									
La	46	23	25	21.1	52.9	25	40	24	19
Ce	87	51	40	49.2	102.3	52	65	40	35
Nd	36	28	—	—	—	28	—	—	—
Sm	6.8	7.1	6.5	7.32	7.18	5.7	7.6	6.4	6.4
Eu	1.4	2.14	4	2.65	1.44	1.56	3	3	3
Gd	6.4	5.1	—	—	—	5.3	—	—	—
Tb	1.09	0.99	<1	1.08	1.18	0.73	<1	<1	<1
Ho	<1.7	<0.9	—	—	—	<1.0	—	—	—
Tm	0.88	0.34	—	—	—	0.5	—	—	—
Yb	2.9	2.2	2	1.79	3.4	2.1	3	3	4
Lu	0.42	0.29	0.3	0.253	0.494	0.34	0.3	0.4	0.6

TABLE B-4. ANALYSES OF THE MAFIC ROCKS FROM THE GARRISON SCHIST

Locality	amphibolites			greenschists		
	GG1	GG2	GG3	GG4	GG5	GG6
<b>Major Elements (oxide wt. %)</b>						
SiO <sub>2</sub>	48.43	47.92	49.93	46.54	44.98	49.24
TiO <sub>2</sub>	2.07	2.08	1.42	1.28	2.12	2.01
Al <sub>2</sub> O <sub>3</sub>	11.50	12.12	14.05	13.42	13.93	10.34
Fe <sub>2</sub> O <sub>3</sub>	6.12	6.38	6.61	8.36	6.15	6.73
FeO	9.20	8.46	4.91	2.21	5.00	4.85
MnO	0.19	0.22	0.20	0.21	0.14	0.16
MgO	7.04	6.98	5.50	8.35	9.60	8.10
CaO	10.41	10.71	10.71	11.74	10.49	11.30
Na <sub>2</sub> O	2.35	2.52	4.10	2.29	2.44	2.21
K <sub>2</sub> O	0.15	0.14	0.39	0.99	0.47	0.23
P <sub>2</sub> O <sub>5</sub>	0.17	0.18	0.15	0.11	0.35	0.22
<b>Volatiles (wt. %)</b>						
H <sub>2</sub> O+	—	—	—	—	—	—
H <sub>2</sub> O-	—	—	—	—	—	—
CO <sub>2</sub>	—	—	—	—	—	—
S	—	—	—	—	—	—
Total	97.63	97.71	97.97	95.50	95.67	95.39
<b>Recalculated Major Elements (oxide wt. %)</b>						
SiO <sub>2</sub>	49.83	49.29	51.25	49.11	47.26	51.92
TiO <sub>2</sub>	2.13	2.14	1.46	1.35	2.23	2.12
Al <sub>2</sub> O <sub>3</sub>	11.83	12.47	14.42	14.16	14.64	10.90
Fe <sub>2</sub> O <sub>3</sub>	1.68	1.62	1.24	1.14	1.23	1.28
FeO	13.62	13.15	10.03	9.24	9.96	10.35
MnO	0.20	0.23	0.21	0.22	0.15	0.17
MgO	7.24	7.18	5.65	8.81	10.09	8.54
CaO	10.71	11.02	10.99	12.39	11.02	11.92
Na <sub>2</sub> O	2.42	2.59	4.21	2.42	2.56	2.33
K <sub>2</sub> O	0.15	0.14	0.40	1.04	0.49	0.24
P <sub>2</sub> O <sub>5</sub>	0.17	0.19	0.15	0.12	0.37	0.23
Total	100.00	100.00	100.00	100.00	100.00	100.00
<b>Trace Elements (element wt. ppm)</b>						
Ba	64	51	566	81	265	126
Co	—	—	—	—	—	—
Cr	133	133	379	737	310	803
Cs	—	—	—	—	—	—
Hf	—	—	—	—	—	—
Mo	—	—	—	—	—	—
Nb	11	4	4	4	19	15
Ni	61	62	73	164	157	213
Rb	4	0	8	21	10	3
Sc	—	—	—	—	—	—
Sr	241	198	634	623	437	439
Ta	—	—	—	—	—	—
Th	—	—	—	—	—	—
U	—	—	—	—	—	—
V	571	551	301	280	255	257
Y	56	55	42	28	31	21
Zr	119	112	76	58	166	142
<b>REE Elements (element wt. ppm)</b>						
La	<3	<3	<5	<3	9	15
Ce	<3	<5	<5	<5	24	33
Nd	—	—	—	—	—	—
Sm	—	—	—	—	—	—
Eu	—	—	—	—	—	—
Gd	—	—	—	—	—	—
Tb	—	—	—	—	—	—
Ho	—	—	—	—	—	—
Tm	—	—	—	—	—	—
Yb	—	—	—	—	—	—
Lu	—	—	—	—	—	—

TABLE B-5. ANALYSES OF PILLOWED VOLCANICS FROM THE CONSTITUTION FORMATION

Locality	pillow basalts								-dacite- GC9
	GC1	GC2	GC3	GC4	GC5	GC6	GC7	GC8	
<b>Major Elements (oxide wt. %)</b>									
SiO <sub>2</sub>	51.20	50.00	50.70	48.40	49.90	50.10	44.49	—	61.10
TiO <sub>2</sub>	1.40	1.43	1.08	1.71	1.35	1.20	1.69	—	0.55
Al <sub>2</sub> O <sub>3</sub>	15.30	14.40	15.90	13.00	14.60	12.80	17.36	—	15.70
Fe <sub>2</sub> O <sub>3</sub>	2.20	2.70	4.40	2.70	2.30	2.30	12.15	14.00	6.80
FeO	6.40	7.00	4.80	6.40	6.90	6.20	—	—	1.80
MnO	0.17	0.18	0.21	0.18	0.17	0.14	0.19	—	0.12
MgO	6.37	7.95	4.20	7.42	7.27	6.40	5.70	—	0.82
CaO	7.73	9.15	12.90	11.90	10.30	12.80	11.55	—	1.80
Na <sub>2</sub> O	4.17	4.31	1.94	3.00	4.22	3.90	2.16	—	4.70
K <sub>2</sub> O	0.09	0.15	0.15	0.12	0.17	0.41	0.13	—	6.20
P <sub>2</sub> O <sub>5</sub>	0.14	0.14	0.13	0.17	0.15	0.11	0.19	—	0.05
<b>Volatiles (wt. %)</b>									
H <sub>2</sub> O+	4.00	3.50	4.40	3.90	3.10	2.00	—	—	1.60
H <sub>2</sub> O-	—	—	—	—	—	0.27	—	—	0.21
CO <sub>2</sub>	1.90	1.20	0.40	2.80	0.80	2.50	—	—	0.01
S	0.04	0.06	0.00	0.10	0.07	—	—	—	—
Total	101.11	102.17	101.21	101.80	101.30	101.13	95.61	—	101.46
<b>Recalculated Major Elements (oxide wt. %)</b>									
SiO <sub>2</sub>	53.87	51.42	52.78	51.04	51.34	52.07	47.07	—	61.69
TiO <sub>2</sub>	1.47	1.47	1.12	1.80	1.39	1.25	1.79	—	0.56
Al <sub>2</sub> O <sub>3</sub>	16.10	14.81	16.55	13.71	15.02	13.30	18.37	—	15.85
Fe <sub>2</sub> O <sub>3</sub>	0.98	1.08	1.01	1.03	1.03	0.95	1.29	—	0.89
FeO	7.94	8.73	8.21	8.38	8.31	7.74	10.41	—	7.20
MnO	0.18	0.19	0.22	0.19	0.17	0.15	0.20	—	0.12
MgO	6.70	8.18	4.37	7.82	7.48	6.65	6.03	—	0.83
CaO	8.13	9.41	13.43	12.55	10.60	13.30	12.22	—	1.82
Na <sub>2</sub> O	4.39	4.43	2.02	3.16	4.34	4.05	2.29	—	4.75
K <sub>2</sub> O	0.09	0.15	0.16	0.13	0.17	0.43	0.14	—	6.26
P <sub>2</sub> O <sub>5</sub>	0.15	0.14	0.14	0.18	0.15	0.11	0.20	—	0.05
Total	100.00	100.00	100.00	100.00	100.00	100.00	100.00	—	100.00
<b>Trace Elements (element wt. ppm)</b>									
Ba	100	80	100	30	50	<274	—	—	344
Co	49	40	51	38	45	38.8	—	—	0.4
Cr	240	210	110	130	210	282.9	160	210	3.1
Cs	—	—	—	—	—	<1.7	—	—	0.7
Hf	—	—	—	—	—	1.7	3.3	2.4	17.4
Mo	<10	<10	<10	<10	<10	—	—	—	—
Nb	<10	<10	<10	<10	<10	—	—	—	—
Ni	120	49	63	56	60	—	70	70	—
Rb	<10	<10	<10	<10	<10	<37	—	—	87
Sc	—	—	—	—	—	37.54	45	50.1	4.11
Sr	420	180	260	170	130	—	—	—	—
Ta	—	—	—	—	—	0.64	—	—	9.17
Th	<30	<30	<30	<30	<30	<1.0	0.4	0.5	11.1
U	<30	<30	<30	<30	<30	<1.3	—	—	<1.4
V	310	260	270	280	240	—	—	—	—
Y	32	29	18	26	29	—	—	—	—
Zr	79	93	73	120	85	—	—	—	—
<b>REE Elements (element wt. ppm)</b>									
La	<10	<10	<10	<10	<10	4	5.68	2.6	95
Ce	—	—	—	—	—	10	16.1	8.1	187
Nd	—	—	—	—	—	10	—	—	84
Sm	—	—	—	—	—	2.6	4.2	3.54	17.7
Eu	—	—	—	—	—	0.88	1.51	1.33	2.9
Gd	—	—	—	—	—	3	—	—	14
Tb	—	—	—	—	—	0.65	1	0.9	2.83
Ho	—	—	—	—	—	0.7	—	—	1.9
Tm	—	—	—	—	—	0.44	—	—	1.28
Yb	2.9	2.2	1.8	2.5	2.2	1.9	3.31	3.75	7.5
Lu	—	—	—	—	—	0.29	0.53	0.62	1.06

TABLE B-6. ANALYSES OF BASALTS FROM THE LOPEZ COMPLEX

Locality	Jurassic basalt	mid-Cretaceous basalts			
	GL1	GL2	GL3	GL4	GL5
<b>Major Elements (oxide wt. %)</b>					
SiO <sub>2</sub>	51.97	49.30	—	—	—
TiO <sub>2</sub>	1.09	2.60	—	—	—
Al <sub>2</sub> O <sub>3</sub>	14.63	12.60	—	—	—
Fe <sub>2</sub> O <sub>3</sub>	7.88	3.80	14.40	8.33	8.67
FeO	—	5.50	—	—	—
MnO	0.14	0.12	—	—	—
MgO	5.72	4.20	—	—	—
CaO	10.99	11.50	—	—	—
Na <sub>2</sub> O	3.35	3.30	—	—	—
K <sub>2</sub> O	0.41	0.10	—	—	—
P <sub>2</sub> O <sub>5</sub>	0.11	0.38	—	—	—
<b>Volatiles (wt. %)</b>					
H <sub>2</sub> O+	—	3.20	—	—	—
H <sub>2</sub> O-	—	0.52	—	—	—
CO <sub>2</sub>	—	3.20	—	—	—
S	—	—	—	—	—
Total	96.29	100.32	—	—	—
<b>Recalculated Major Elements (oxide wt. %)</b>					
SiO <sub>2</sub>	54.37	52.94	—	—	—
TiO <sub>2</sub>	1.14	2.79	—	—	—
Al <sub>2</sub> O <sub>3</sub>	15.31	13.53	—	—	—
Fe <sub>2</sub> O <sub>3</sub>	0.82	1.06	—	—	—
FeO	6.68	8.62	—	—	—
MnO	0.15	0.13	—	—	—
MgO	5.98	4.51	—	—	—
CaO	11.50	12.35	—	—	—
Na <sub>2</sub> O	3.50	3.54	—	—	—
K <sub>2</sub> O	0.43	0.11	—	—	—
P <sub>2</sub> O <sub>5</sub>	0.12	0.41	—	—	—
Total	100.00	100.00	—	—	—
<b>Trace Elements (element wt. ppm)</b>					
Ba	—	332	—	—	—
Co	—	41.7	—	—	—
Cr	515	86.4	10	90	110
Cs	—	<1.7	—	—	—
Hf	1.5	4.3	1.6	4.8	4.2
Mo	—	—	—	—	—
Nb	0.6	—	—	16	—
Ni	175	—	—	44	54
Rb	0.9	<40	—	1	—
Sc	31	28.94	44	27	27.8
Sr	108	—	—	185	—
Ta	—	1.38	—	—	—
Th	0.17	1.3	6.6	1.3	1.2
U	—	3.5	—	—	—
V	—	—	—	—	—
Y	20.1	—	—	31	—
Zr	60	—	—	185	—
<b>REE Elements (element wt. ppm)</b>					
La	2.71	14	15.6	12.65	11.33
Ce	7.3	32	38.3	31.9	29.7
Nd	—	21	—	—	—
Sm	2.36	6.4	8	6.24	5.9
Eu	1	1.92	2.5	1.96	1.35
Gd	—	5.8	—	—	—
Tb	0.55	1.08	1.4	1.18	1
Ho	—	0.9	—	—	—
Tm	—	0.59	—	—	—
Yb	2.1	2.5	3.48	2.48	2.43
Lu	0.302	0.36	0.51	0.423	0.35

TABLE B-7. ANALYSES FROM THE FIDALGO IGNEOUS COMPLEX

Locality	ocean-floor pillow basalts					
	GDF1	GDF2	GDF3	GDF4	GDF5	GDF6
<b>Major Elements (oxide wt. %)</b>						
SiO <sub>2</sub>	44.00	50.00	—	49.97	46.80	44.40
TiO <sub>2</sub>	1.10	1.30	—	1.59	1.00	1.50
Al <sub>2</sub> O <sub>3</sub>	18.90	13.50	—	13.55	17.90	16.50
Fe <sub>2</sub> O <sub>3</sub>	2.40	2.60	11.20	10.20	1.90	2.30
FeO	6.40	6.50	—	—	4.90	5.80
MnO	0.26	0.14	—	0.18	0.11	0.12
MgO	3.10	6.70	—	6.96	3.80	4.20
CaO	14.20	11.60	—	9.91	12.10	12.50
Na <sub>2</sub> O	2.50	3.40	—	2.62	3.10	3.90
K <sub>2</sub> O	0.21	0.10	—	0.99	1.30	0.31
P <sub>2</sub> O <sub>5</sub>	0.11	0.12	—	0.14	0.09	0.15
<b>Volatiles (wt. %)</b>						
H <sub>2</sub> O+	4.40	2.60	—	—	2.80	2.90
H <sub>2</sub> O-	0.53	0.47	—	—	0.41	0.32
CO <sub>2</sub>	2.10	1.30	—	—	2.40	4.20
S	—	—	—	—	—	—
Total	100.21	100.33	—	96.11	98.61	99.10
<b>Recalculated Major Elements (oxide wt. %)</b>						
SiO <sub>2</sub>	47.29	52.19	—	52.49	50.39	48.50
TiO <sub>2</sub>	1.18	1.36	—	1.67	1.08	1.64
Al <sub>2</sub> O <sub>3</sub>	20.31	14.09	—	14.23	19.27	18.03
Fe <sub>2</sub> O <sub>3</sub>	1.02	1.03	—	1.07	0.79	0.96
FeO	8.28	8.30	—	8.68	6.40	7.74
MnO	0.28	0.15	—	0.19	0.12	0.13
MgO	3.33	6.99	—	7.31	4.09	4.59
CaO	15.26	12.11	—	10.41	13.03	13.66
Na <sub>2</sub> O	2.69	3.55	—	2.75	3.34	4.26
K <sub>2</sub> O	0.23	0.10	—	1.04	1.40	0.34
P <sub>2</sub> O <sub>5</sub>	0.12	0.13	—	0.15	0.10	0.16
Total	100.00	100.00	—	100.00	100.00	100.00
<b>Trace Elements (element wt. ppm)</b>						
Ba	155	157	—	—	<249	<323
Co	46.8	37.8	—	—	46.2	33.1
Cr	346.1	153	210	155	252.7	142
Cs	<1.6	<1.7	—	—	0.8	<1.7
Hf	1.6	2	2.6	2.8	1.4	2.2
Mo	—	—	—	—	—	—
Nb	—	—	—	3.5	—	—
Ni	—	—	—	17	—	—
Rb	<38	<39	—	18.8	25	<41
Sc	30.63	38.4	45.5	43	28.87	34.56
Sr	—	—	—	58.5	—	—
Ta	<0.84	0.71	—	—	1.51	2.94
Th	0.4	0.5	0.4	0.28	<0.9	<1.2
U	<1.3	<1.4	—	—	<1.3	<1.8
V	—	—	—	—	—	—
Y	—	—	—	31.5	—	—
Zr	—	—	—	92	—	—
<b>REE Elements (element wt. ppm)</b>						
La	2	5	4.7	3.93	3	5
Ce	5	12	12.2	10.8	8	10
Nd	8	7	—	—	8	10
Sm	2.7	3.1	3.5	3.41	2.4	3.3
Eu	1.01	1.05	1.35	1.19	0.84	1.05
Gd	<5.0	3.8	—	—	<4.8	<5.9
Tb	0.67	0.52	0.8	0.94	0.58	0.83
Ho	0.9	<1.1	—	—	<0.9	<1.3
Tm	0.43	<0.57	—	—	<0.52	<0.6
Yb	1.9	2	2.9	3.29	1.7	2
Lu	0.33	0.35	0.44	0.52	0.27	0.34

TABLE B-7. ANALYSES FROM THE FIDALGO IGNEOUS COMPLEX (continued)

Locality	arc-related basalts and diorites								
	GDF7	GDF8	GDF9	GDF10	GDF11	GDF12	GDF13	GDF14	GDF15
<b>Major Elements (oxide wt. %)</b>									
SiO <sub>2</sub>	48.40	51.00	50.70	56.60	58.70	59.70	58.20	54.80	—
TiO <sub>2</sub>	1.04	1.03	0.75	0.50	0.49	0.37	0.46	0.51	—
Al <sub>2</sub> O <sub>3</sub>	15.00	15.50	15.00	16.50	13.40	14.90	14.00	14.50	—
Fe <sub>2</sub> O <sub>3</sub>	11.40	12.00	10.70	8.19	8.51	8.51	8.29	8.82	9.55
FeO	—	—	—	—	—	—	—	—	—
MnO	0.16	0.18	0.18	0.12	0.15	0.16	0.14	0.13	—
MgO	8.23	7.03	9.40	4.70	7.90	5.09	6.63	8.40	—
CaO	9.29	9.09	9.80	7.50	7.25	8.70	9.10	5.40	—
Na <sub>2</sub> O	3.97	3.46	2.54	3.23	2.98	3.26	4.15	3.04	—
K <sub>2</sub> O	0.38	0.18	0.17	0.68	0.82	0.41	0.24	1.90	—
P <sub>2</sub> O <sub>5</sub>	—	—	—	—	—	—	—	—	—
<b>Volatiles (wt. %)</b>									
H <sub>2</sub> O+	—	—	—	—	—	—	—	—	—
H <sub>2</sub> O-	—	—	—	—	—	—	—	—	—
CO <sub>2</sub>	—	—	—	—	—	—	—	—	—
S	—	—	—	—	—	—	—	—	—
Total	97.87	99.47	99.24	98.02	100.20	101.10	101.21	97.50	—
<b>Recalculated Major Elements (oxide wt. %)</b>									
SiO <sub>2</sub>	49.98	51.83	51.59	58.18	59.03	59.50	57.93	56.67	—
TiO <sub>2</sub>	1.07	1.05	0.76	0.51	0.49	0.37	0.46	0.53	—
Al <sub>2</sub> O <sub>3</sub>	15.49	15.75	15.26	16.96	13.48	14.85	13.94	14.99	—
Fe <sub>2</sub> O <sub>3</sub>	1.18	1.22	1.09	0.84	0.86	0.85	0.83	0.91	—
FeO	9.53	9.88	8.82	6.82	6.93	6.87	6.68	7.39	—
MnO	0.17	0.18	0.18	0.12	0.15	0.16	0.14	0.13	—
MgO	8.50	7.15	9.56	4.83	7.94	5.07	6.60	8.69	—
CaO	9.59	9.24	9.97	7.71	7.29	8.67	9.06	5.58	—
Na <sub>2</sub> O	4.10	3.52	2.58	3.32	3.00	3.25	4.13	3.14	—
K <sub>2</sub> O	0.39	0.18	0.17	0.70	0.82	0.41	0.24	1.96	—
P <sub>2</sub> O <sub>5</sub>	0.00	0.00	0.00	0.00	0.00	0.00	0.00	0.00	—
Total	100.00	100.00	100.00	100.00	100.00	100.00	100.00	100.00	100.00
<b>Trace Elements (element wt. ppm)</b>									
Ba	—	—	—	—	—	—	—	—	—
Co	—	—	—	—	—	—	—	—	—
Cr	130	185	110	73	520	71	239	275	190
Cs	—	—	—	—	—	—	—	—	—
Hf	—	—	—	—	—	—	—	1.57	1.3
Mo	—	—	—	—	—	—	—	—	—
Nb	—	—	—	—	—	—	—	—	—
Ni	78	73	—	40	—	37	87	110	90
Rb	0	0	0	—	7	—	—	18	—
Sc	—	—	—	—	—	—	—	29.9	31.6
Sr	138	208	205	—	178	—	—	172	—
Ta	—	—	—	—	—	—	—	—	—
Th	—	—	—	—	—	—	—	0.46	0.36
U	—	—	—	—	—	—	—	—	—
V	—	—	—	—	—	—	—	—	—
Y	18	18	17	—	9	—	—	13	—
Zr	43	53	38	55	41	40	50	54	—
<b>REE Elements (element wt. ppm)</b>									
La	—	—	—	—	—	—	—	3.82	3.85
Ce	—	—	—	—	—	—	—	9.3	9.35
Nd	—	—	—	—	—	—	—	—	—
Sm	—	—	—	—	—	—	—	1.91	1.71
Eu	—	—	—	—	—	—	—	0.63	0.58
Gd	—	—	—	—	—	—	—	—	—
Tb	—	—	—	—	—	—	—	0.45	0.34
Ho	—	—	—	—	—	—	—	—	—
Tm	—	—	—	—	—	—	—	—	—
Yb	—	—	—	—	—	—	—	1.44	1.33
Lu	—	—	—	—	—	—	—	0.22	0.2

TABLE B-7. ANALYSES FROM THE FIDALGO IGNEOUS COMPLEX (continued)

Locality	arc-related basalts and diorites			arc-related dacites				arc-related dikes		
	GDF16	GDF17	GDF18	GDF19	GDF20	GDF21	GDF22	GDF23	GDF24	GDF25
<b>Major Elements (oxide wt. %)</b>										
SiO <sub>2</sub>	48.30	58.00	54.50	64.70	68.30	74.00	65.90	47.00	66.30	74.20
TiO <sub>2</sub>	0.55	0.68	0.81	0.34	0.39	0.30	0.47	0.72	0.61	0.41
Al <sub>2</sub> O <sub>3</sub>	14.30	15.50	15.70	13.90	14.10	12.10	14.10	16.10	15.60	13.00
Fe <sub>2</sub> O <sub>3</sub>	11.20	9.84	10.40	6.41	4.69	3.22	5.81	3.10	2.00	1.90
FeO	—	—	—	—	—	—	—	6.20	2.70	0.68
MnO	0.18	0.15	0.17	0.07	0.10	0.03	0.13	0.18	0.08	0.05
MgO	7.76	6.31	6.00	2.80	1.50	0.82	2.25	8.40	2.00	0.94
CaO	11.30	2.58	3.40	4.10	1.04	0.84	1.63	9.90	3.50	3.00
Na <sub>2</sub> O	2.97	4.45	4.64	3.73	5.56	5.09	5.72	3.50	6.10	5.40
K <sub>2</sub> O	0.33	0.38	1.52	0.26	0.11	1.72	0.61	0.31	0.31	0.10
P <sub>2</sub> O <sub>5</sub>	—	—	—	—	—	—	—	0.10	0.20	0.10
<b>Volatiles (wt. %)</b>										
H <sub>2</sub> O+	—	—	—	—	—	—	—	3.60	1.20	0.54
H <sub>2</sub> O-	—	—	—	—	—	—	—	0.03	0.13	0.08
CO <sub>2</sub>	—	—	—	—	—	—	—	0.55	0.03	0.08
S	—	—	—	—	—	—	—	—	—	—
Total	96.89	97.89	97.14	96.31	95.79	98.12	96.62	99.69	100.76	100.48
<b>Recalculated Major Elements (oxide wt. %)</b>										
SiO <sub>2</sub>	50.37	59.79	56.65	67.58	71.62	75.64	68.58	49.32	66.80	74.49
TiO <sub>2</sub>	0.57	0.70	0.84	0.36	0.41	0.31	0.49	0.76	0.61	0.41
Al <sub>2</sub> O <sub>3</sub>	14.91	15.98	16.32	14.52	14.78	12.37	14.67	16.89	15.72	13.05
Fe <sub>2</sub> O <sub>3</sub>	1.17	1.01	1.08	0.67	0.49	0.33	0.60	1.05	0.50	0.27
FeO	9.46	8.22	8.76	5.42	3.98	2.67	4.90	8.49	4.08	2.16
MnO	0.19	0.15	0.18	0.07	0.10	0.03	0.14	0.19	0.08	0.05
MgO	8.09	6.50	6.24	2.92	1.57	0.84	2.34	8.81	2.02	0.94
CaO	11.79	2.66	3.53	4.28	1.09	0.86	1.70	10.39	3.53	3.01
Na <sub>2</sub> O	3.10	4.59	4.82	3.90	5.83	5.20	5.95	3.67	6.15	5.42
K <sub>2</sub> O	0.34	0.39	1.58	0.27	0.12	1.76	0.63	0.33	0.31	0.10
P <sub>2</sub> O <sub>5</sub>	0.00	0.00	0.00	0.00	0.00	0.00	0.00	0.10	0.20	0.10
Total	100.00	100.00	100.00	100.00	100.00	100.00	100.00	100.00	100.00	100.00
<b>Trace Elements (element wt. ppm)</b>										
Ba	—	—	—	—	—	—	—	<280	191	161
Co	—	—	—	—	—	—	—	35.7	8.5	4.8
Cr	—	—	—	—	—	—	—	67.8	<6.3	2.6
Cs	—	—	—	—	—	—	—	<1.7	<1.1	<0.8
Hf	—	—	—	—	—	—	—	1.1	3.4	3.8
Mo	—	—	—	—	—	—	—	—	—	—
Nb	—	—	—	—	—	—	—	—	—	—
Ni	—	—	—	—	—	—	—	—	—	—
Rb	—	—	—	—	—	—	—	—	—	—
Sc	—	—	—	—	—	—	—	<38	<27	<20
Sr	—	—	—	—	—	—	—	41.23	11.69	6.89
Ta	—	—	—	—	—	—	—	<0.87	0.54	0.51
Th	—	—	—	—	—	—	—	<1.0	1.5	2.2
U	—	—	—	—	—	—	—	<1.4	<1.2	<1.0
V	—	—	—	—	—	—	—	—	—	—
Y	—	—	—	—	—	—	—	—	—	—
Zr	—	—	—	—	—	—	—	—	—	—
<b>REE Elements (element wt. ppm)</b>										
La	—	—	—	—	—	—	—	4	13	11
Ce	—	—	—	—	—	—	—	8	28	25
Nd	—	—	—	—	—	—	—	7	18	15
Sm	—	—	—	—	—	—	—	2.1	5.1	3.8
Eu	—	—	—	—	—	—	—	0.68	1.29	0.93
Gd	—	—	—	—	—	—	—	<5.3	2.1	3.9
Tb	—	—	—	—	—	—	—	0.39	0.88	0.7
Ho	—	—	—	—	—	—	—	<1.0	<1.1	<0.9
Tm	—	—	—	—	—	—	—	<0.55	0.43	0.4
Yb	—	—	—	—	—	—	—	0.8	3.1	2.6
Lu	—	—	—	—	—	—	—	0.21	0.5	0.44

TABLE B-8. ANALYSES FROM THE HARO FORMATION AND SPIEDEN GROUP

Locality	Haro		- intrusive - GH3	Spieden		
	— volc. clasts — GH1	GH2		GS1	volcanic clasts GS2	GS3
<b>Major Elements (oxide wt. %)</b>						
SiO <sub>2</sub>	77.10	65.10	78.60	72.80	62.30	62.00
TiO <sub>2</sub>	0.21	0.44	0.20	0.38	0.40	0.47
Al <sub>2</sub> O <sub>3</sub>	11.10	14.70	11.20	13.10	16.10	16.30
Fe <sub>2</sub> O <sub>3</sub>	0.85	1.70	0.81	2.00	2.50	2.40
FeO	1.40	4.00	0.76	1.60	2.50	2.80
MnO	0.08	0.05	0.02	0.05	0.18	0.12
MgO	0.71	3.10	0.47	0.82	2.70	2.90
CaO	1.50	2.80	1.00	1.60	4.10	4.60
Na <sub>2</sub> O	5.10	3.70	4.20	5.80	4.10	3.50
K <sub>2</sub> O	0.41	0.72	2.10	0.83	1.50	2.20
P <sub>2</sub> O <sub>5</sub>	0.03	0.09	0.04	0.08	0.17	0.13
<b>Volatiles (wt. %)</b>						
H <sub>2</sub> O+	0.78	2.40	0.92	1.10	0.97	1.20
H <sub>2</sub> O-	0.27	0.82	0.38	0.09	1.30	0.20
CO <sub>2</sub>	0.68	0.24	0.12	0.02	0.71	0.11
S	—	—	—	—	—	—
Total	100.22	99.86	100.82	100.27	99.53	98.93
<b>Recalculated Major Elements (oxide wt. %)</b>						
SiO <sub>2</sub>	78.33	67.61	79.13	73.61	64.66	63.76
TiO <sub>2</sub>	0.21	0.46	0.20	0.38	0.42	0.48
Al <sub>2</sub> O <sub>3</sub>	11.28	15.27	11.27	13.25	16.71	16.76
Fe <sub>2</sub> O <sub>3</sub>	0.24	0.64	0.17	0.38	0.55	0.57
FeO	1.98	5.17	1.35	3.09	4.44	4.59
MnO	0.08	0.05	0.02	0.05	0.19	0.12
MgO	0.72	3.22	0.47	0.83	2.80	2.98
CaO	1.52	2.91	1.01	1.62	4.26	4.73
Na <sub>2</sub> O	5.18	3.84	4.23	5.86	4.26	3.60
K <sub>2</sub> O	0.42	0.75	2.11	0.84	1.56	2.26
P <sub>2</sub> O <sub>5</sub>	0.03	0.09	0.04	0.08	0.18	0.13
Total	100.00	100.00	100.00	100.00	100.00	100.00
<b>Trace Elements (element wt. ppm)</b>						
Ba	143	1178	691	207	1153	930
Co	1.5	4.3	0.9	2.7	11	13
Cr	3	25	13.7	4.4	9	6.7
Cs	<1.1	<1.5	0.4	<1.1	<1.0	<1.3
Hf	1.6	0.9	1.1	3.1	1.9	1.6
Mo	—	—	—	—	—	—
Nb	—	—	—	—	—	—
Ni	—	—	—	—	—	—
Rb	<25	<32	24	<29	23	35
Sc	13.78	29.77	13	11.38	11.5	18.46
Sr	—	—	—	—	—	—
Ta	1.45	<0.78	<0.81	0.42	0.92	2.8
Th	1	<0.9	0.7	3.3	1.6	1.8
U	<1.3	<1.5	<1.5	1.5	<1.1	<1.5
V	—	—	—	—	—	—
Y	—	—	—	—	—	—
Zr	—	—	—	—	—	—
<b>REE Elements (element wt. ppm)</b>						
La	4	3	6	15	14	11
Ce	10	6	13	30	25	20
Nd	8	<25	9	18	12	10
Sm	2	1.3	2.4	4.7	2.6	2.2
Eu	0.48	0.42	0.75	1.09	0.78	0.67
Gd	<3.6	<4.7	<4.0	4.3	2.3	2.4
Tb	0.51	0.42	0.48	0.88	0.39	0.32
Ho	<1.2	<1.4	<1.4	<1.6	<0.9	<1.5
Tm	0.36	<0.49	<0.43	0.61	<0.36	<0.44
Yb	2.8	1.1	1	3.6	1.4	1.2
Lu	0.43	0.17	0.15	0.55	0.24	0.22

## REFERENCES CITED

- Ando, C. J., Irwin, W. P., Jones, D. L., and Saleeby, J. B., 1983, The ophiolitic North Fork terrane in the Salmon River region, central Klamath Mountains, California: *Geological Society of America Bulletin*, v. 94, p. 236-252.
- Armstrong, R. L., 1988, Mesozoic and early Cenozoic magmatic evolution of the Canadian Cordillera: *Geological Society of America Special Paper 218* (John Rodgers Symposium volume) (in press).
- Armstrong, R. L., Bernardi, M. L., and Rady, P. M., 1983, Late Paleozoic high-pressure metamorphic rocks in northwestern Washington and southwestern British Columbia; The Vedder Complex: *Geological Society of America Bulletin*, v. 94, p. 451-458.
- Arthur, A., 1986, Stratigraphy along the west side of Harrison Lake, southwestern British Columbia: *Geological Survey of Canada, Paper 86-1B*, p. 715-720.
- Beck, M. E., Jr., Burmester, R. F., and Schoonover, R., 1981, Paleomagnetism and tectonics of the Cretaceous Mt. Stuart Batholith of Washington; Translation or tilt? *Earth and Planetary Science Letters*, v. 56, p. 336-342.
- Bloomer, S. H., 1983, Distribution and origin of igneous rocks from the landward slopes of the Mariana trench; Implications for its structure and evolution: *Journal of Geophysical Research*, v. 88, p. 7411-7428.
- Boettcher, A. L., and Wyllie, P. J., 1968, The calcite-aragonite transition measured in the system  $\text{CaO-CO}_2\text{-H}_2\text{O}$ : *Journal of Geology*, v. 76, p. 314-330.
- Boyer, S. E., and Elliott, D., 1982, Thrust systems: *American Association of Petroleum Geologists Bulletin*, v. 66, p. 1196-1230.
- Brandon, M. T., 1980, Structural geology of middle Cretaceous thrust faulting on southern San Juan Island, Washington [M.S. thesis]: Seattle, University of Washington, 130 p.
- , 1982, Mid-Cretaceous high-pressure regional metamorphic event in the San Juan Islands, Washington; Evidence for rapid structural burial and uplift: *Geological Society of America Abstracts with Programs*, v. 14, p. 152.
- , 1985, Mesozoic melange of the Pacific Rim Complex, western Vancouver Island, in Tempelman-Kluit, D., ed., *Field guides to geology and mineral deposits in the southern Canadian Cordillera* (Geological Society of America Cordilleran section meeting): Vancouver, British Columbia, Geological Survey of Canada, p. 7.1-7.28.
- Brandon, M. T., and Cowan, D. S., 1985, The Late Cretaceous San Juan Islands-northwestern Cascades thrust system [abs.]: *Geological Society of America Abstracts with Programs*, v. 17, p. 343.
- Brandon, M. T., Orchard, M. J., Parrish, R. R., Sutherland Brown, A., and Yorath, C. J., 1986, Fossil ages and isotopic dates from the Paleozoic Sicker Group and associated intrusive rocks, Vancouver Island, British Columbia: *Geological Survey of Canada Paper 86-1A*, p. 683-696.
- Brown, E. H., 1977, Ophiolite on Fidalgo Island, Washington, in Coleman, R. G., and Irwin, W. P., eds., *North American ophiolites*: Oregon Department of Geology and Mineral Industries Bulletin 95, p. 67-73.
- Brown, E. H., Bradshaw, J. Y., and Mustoe, G. E., 1979, Plagiogranite and keratophyre in ophiolite on Fidalgo Island, Washington: *Geological Society of America Bulletin, Part I*, v. 90, p. 493-507.
- Brown, E. H., Bernardi, M. L., Christenson, B. W., Cruver, J. R., Haugerud, R. A., Rady, P. M., and Sondergaard, J. N., 1981, Metamorphic facies and tectonics in part of the Cascade Range and Puget Lowland, northwestern Washington: *Geological Society of America Bulletin*, v. 92, p. 170-178.
- Bruns, T. R., 1983, Model for the origin of the Yakutat block, an accreting terrane in the northern Gulf of Alaska: *Geology*, v. 11, p. 718-721.
- Carlson, W. D., and Rosenfeld, J. L., 1981, Optical determination of topotactic aragonite-calcite growth kinetics; metamorphic implications: *Journal of Geology*, v. 89, p. 615-638.
- Carroll, P. R., 1980, Petrology and structure of the pre-Tertiary rocks of Lummi and Eliza Island, Washington [M.S. thesis]: Seattle, University of Washington, 78 p.
- Champion, D. E., Howell, D. G., and Gromme, C. S., 1984, Paleomagnetic and geologic data indicating 2,500 km of northward displacement for the Salinian and related terranes, California: *Journal of Geophysical Research*, v. 89, p. 7736-7752.
- Clowes, R. M., Brandon, M. T., Green, A. G., Yorath, C. J., Sutherland Brown, A., Kanasevich, E. R., and Spencer, C., 1987, LITHOPROBE-southern Vancouver Island; Cenozoic subduction complex imaged by deep seismic reflections: *Canadian Journal of Earth Sciences*, v. 24, p. 31-51.
- Cowan, D. S., 1985, Structural styles in Mesozoic and Cenozoic melanges in the western Cordillera of North America: *Geological Society of America Bulletin*, v. 96, p. 451-462.
- Cowan, D. S., and Miller, R. B., 1981, Deformational styles in two Mesozoic fault zones, western Washington, U.S.A., in McClay, K. R., and Price, N. J., eds., *Thrust and nappe tectonics*: Geological Society of London Special Publication no. 9, p. 483-490.
- Cowan, D. S., and Whetten, J. T., 1977, Geology of Lopez and San Juan Islands, in Brown, E. H., and Ellis, R. C., eds., *Geological excursions in the Pacific Northwest*: Bellingham, Western Washington University, p. 321-338.
- Crawford, W. A., and Hoersch, A. L., 1972, Calcite-aragonite equilibrium from 50°C to 150°C: *American Mineralogist*, v. 57, p. 995-998.
- Curry, J. R., and Moore, D. G., 1971, Growth of the Bengal deep-sea fan and denudation in the Himalayas: *Geological Society of America Bulletin*, v. 82, p. 563-572.
- Dailey, A. D., 1985, Chemical and physical fluid characterization during low grade metamorphism [M.S. thesis]: Seattle, University of Washington, 80 p.
- Danner, W. R., 1957, Stratigraphic reconnaissance in the northwestern Cascade Mountains and San Juan Islands of Washington State [Ph.D. thesis]: Seattle, University of Washington, 562 p.
- , 1966, Limestone resources of western Washington: *Washington Division of Mines and Geology Bulletin*, v. 52, 474 p.
- , 1977, Paleozoic rocks of northwest Washington and adjacent parts of British Columbia, in Stewart, J. H., Stevens, C. H., and Fritsche, A. E., eds., *Paleozoic paleogeography of the western United States*: Society of Economic Paleontologists and Mineralogists, Pacific Section, p. 481-502.
- Davis, D., Suppe, J., and Dahlen, F. A., 1983, Mechanics of fold-and-thrust belts and accretionary wedges: *Journal of Geophysical Research*, v. 88, p. 1153-1172.
- Davis, G. A., Monger, J. W. H., and Burchfiel, B. C., 1978, Mesozoic construction of the Cordilleran "collage," central British Columbia to central California, in Howell, D. G., and McDougall, K. A., eds., *Mesozoic paleogeography of the western United States*: Society of Economic Paleontologists and Mineralogists, Pacific Section, p. 1-32.
- Dickinson, W. R., 1976, Sedimentary basins developed during the evolution of Mesozoic-Cenozoic arc-trench system in western North America: *Canadian Journal of Earth Sciences*, v. 13, p. 1268-1287.
- Dickinson, W. R., and Suzcek, C. A., 1979, Plate tectonics and sandstone compositions: *American Association of Petroleum Geologists Bulletin*, v. 63, p. 2164-2182.
- Dickinson, W. R., and Thayer, T. P., 1978, Paleogeographic and paleotectonic implications of Mesozoic stratigraphy and structure in the John Day inlier of central Oregon, in Howell, D. G., and McDougall, K. A., eds., *Mesozoic paleogeography of the western United States*: Society of Economic Paleontologists and Mineralogists, Pacific Section, p. 147-161.
- Draper, G., and Bone, R., 1981, Denudation rates, thermal evolution, and preservation of blueschist terrains: *Journal of Geology*, v. 89, p. 601-613.
- Einsele, G., and 18 others, 1980, Intrusion of basaltic sills into highly porous sediments, and resulting hydrothermal activity: *Nature*, v. 283, p. 441-445.
- Ernst, W. G., 1971, Petrologic reconnaissance of Franciscan metagraywackes from the Diablo Range, Central California Coast Ranges: *Journal of Petrology*, v. 12, p. 413-437.
- , ed., 1981, *The geotectonic development of California*: Englewood Cliffs, New Jersey, Prentice-Hall, Inc., 706 p.
- Fairchild, L. H., and Cowan, D. S., 1982, Structure, petrology, and tectonic history of the Leech River complex northwest of Victoria, Vancouver Island: *Canadian Journal of Earth Sciences*, v. 19, p. 1817-1835.

- Floyd, P. A., and Winchester, J. A., 1975, Magma type and tectonic setting discrimination using immobile elements: *Earth and Planetary Science Letters*, v. 27, p. 211-218.
- Garcia, M. O., 1978, Criteria for the identification of ancient volcanic arcs: *Earth Science Reviews*, v. 14, p. 147-165.
- Garver, J. I., 1985, Sedimentology and tectonic significance of the Tithonian to (?)Neocomian clastic sequence of the Decatur terrane, San Juan Islands, Washington: *Geological Society of America Abstracts with Programs*, v. 17, p. 356.
- , 1986, Great Valley Group/Coast Range Ophiolite fragment in the San Juan Islands of Washington: *Geological Society of America Abstracts with Programs*, v. 18, p. 109.
- , 1988, Stratigraphy, depositional setting, and tectonic significance of the clastic cover to the Fidalgo Ophiolite, San Juan Islands, Washington: *Canadian Journal of Earth Sciences* (in press).
- Gill, J. B., 1981, *Orogenic andesites and plate tectonics*: New York, Springer-Verlag, 390 p.
- Glassley, W. E., Whetten, J. T., Cowan, D. S., and Vance, J. A., 1976, Significance of coexisting lawsonite, prehnite, and aragonite in the San Juan Islands, Washington: *Geology*, v. 4, p. 301-302.
- Gleadow, A. J. W., and Brooks, C. K., 1979, Fission track dating, thermal histories, and tectonics of igneous intrusions in East Greenland: *Contributions to Mineralogy and Petrology*, v. 71, p. 45-60.
- Gusey, D. L., 1978, The geology of southwestern Fidalgo Island [M.S. thesis]: Bellingham, Western Washington University, 85 p.
- Hamilton, W., 1978, Mesozoic tectonics of the western United States in Howell, D. G., and McDougall, K. A., eds., *Mesozoic paleogeography of the western United States*: Society of Economic Paleontologists and Mineralogists, Pacific Section, p. 33-70.
- Harland, W. B., Cox, A. V., Llewellyn, P. G., Pickerton, C. A. G., Smith, A. G., and Walters, R., 1982, *A geologic time scale*: Cambridge, Cambridge University Press, 131 p.
- Harper, G. D., 1984, The Josephine ophiolite, northwestern California: *Geological Society of America Bulletin*, v. 95, p. 1009-1026.
- Haskin, L. A., Haskin, M. A., Frey, F. A., and Wilderman, T. R., 1968, Relative and absolute terrestrial abundances of the rare earths, in Ahrens, L. H., ed., *Origin and distribution of the elements*: Oxford, Pergamon Press, p. 889-912.
- Haugerud, R. A., 1985, Geology of the Hozameen Group and the Ross Lake shear zone, Maselanik area, North Cascades, southwest British Columbia [Ph.D. thesis]: Seattle, University of Washington, 263 p.
- Hopson, C. A., Mattinson, J. M., and Pessagno, E. A., Jr., 1981, Coast Range ophiolite, western California, in Ernst, W. G., ed., *The geotectonic development of California*: Englewood Cliffs, New Jersey, Prentice-Hall, Inc., p. 418-510.
- Hotz, P. E., Lanphere, M. A., and Swanson, D. A., 1977, Triassic blueschist from northern California and north-central Oregon: *Geology*, v. 5, p. 659-663.
- Igo, H., Koike, T., Igo, H., Sashida, K., Hisada, K., and Isozaki, Y., 1984, On the occurrence of conodonts and radiolarians from the San Juan Islands, Washington, and Vancouver Islands, British Columbia: *Annual Report of the Institute of Geoscience, the University of Tsukuba*, no. 10, p. 86-91.
- Irving, E., Woodsworth, G. J., Wynne, P. J., and Morrison, A., 1985a, Paleomagnetic evidence for displacement from the south of the Coast Plutonic Complex, British Columbia: *Canadian Journal of Earth Sciences*, v. 22, p. 584-598.
- Irving, E., Woodsworth, G. J., and Wynne, P. J., 1985b, Paleomagnetic evidence for northward motion of the western Cordillera in latest Cretaceous to early Tertiary times [abs.]: *Geological Society of America Abstracts with Programs*, v. 17, p. 363.
- Irwin, W. P., 1981, Tectonic accretion in the Klamath Mountains, in Ernst, W. G., ed., *The geotectonic development of California*: Englewood Cliffs, New Jersey, Prentice-Hall, Inc., p. 29-49.
- Isachsen, C. E., 1984, Geology, geochemistry and geochronology of the West-coast Crystalline Complex and related rocks, Vancouver Island, British Columbia [M.S. thesis]: Vancouver, University of British Columbia, 144 p.
- Jakeš, P., and Gill, J., 1970, Rare earth elements and the island arc tholeiitic series: *Earth and Planetary Science Letters*, v. 9, p. 17-28.
- Johnson, S. Y., 1978, *Sedimentology, petrology, and structure of Mesozoic strata in the northwestern San Juan Islands, Washington* [M.S. thesis]: Seattle, University of Washington, 106 p.
- , 1981, The Spieden Group; An anomalous piece of the Cordilleran paleogeographic puzzle: *Canadian Journal of Earth Sciences*, v. 14, p. 2565-2577.
- , 1984a, Stratigraphy, age, and paleogeography of the Eocene Chuckanut Formation, northwest Washington: *Canadian Journal of Earth Sciences*, v. 21, p. 92-106.
- , 1984b, Cyclic fluvial sedimentation in a rapidly subsiding basin, northwest Washington: *Sedimentary Geology*, v. 38, p. 361-391.
- , 1984c, Evidence for a margin-truncating transcurrent fault (pre-Late Eocene) in western Washington: *Geology*, v. 12, p. 538-541.
- Johnson, S. Y., Zimmerman, R. A., and Naeser, C. W., 1986, Fission-track dating of the tectonic development of the San Juan Islands, Washington: *Canadian Journal of Earth Sciences*, v. 23, p. 1318-1330.
- Jones, D. L., Silberling, N. J., and Hillhouse, J., 1977, Wrangellia; A displaced terrane in northwestern North America: *Canadian Journal of Earth Sciences*, v. 14, p. 2565-2577.
- Jones, D. L., Silberling, N. J., Berg, H. C., and Plafker, G., 1981, Map showing tectonostratigraphic terranes of Alaska, columnar sections, and summary of descriptions of terranes: *United States Geological Survey Open-File Report* no. 81-792, 20 p.
- Jones, D. L., Howell, D. G., Coney, P. J., and Monger, J. W. H., 1983, Recognition, character, and analysis of tectonostratigraphic terranes in western North America, in Hashimoto, M., and Uyeda, S., eds., *Accretion tectonics in the circum-Pacific regions*: Tokyo, Terra Scientific Publishing Company, p. 21-35.
- Karig, D. E., 1983, Deformation in the forearc; Implication for mountain belts, in Hsü, K. J., ed., *Mountain building processes*: New York, Academic Press, p. 59-71.
- Karl, S. M., 1982, Geochemical and depositional environments of upper Mesozoic radiolarian cherts from the northeastern Pacific Rim and from Pacific DSDP cores [Ph.D. thesis]: Stanford, California, Stanford University, 245 p.
- Kay, R. W., 1984, Elemental abundances relevant to identification of magma sources: *Philosophical Transactions of the Royal Society of London, Series A*, v. 310, p. 535-547.
- Kent, D. V., and Gradstein, F. M., 1985, A Cretaceous and Jurassic geochronology: *Geological Society of America Bulletin*, v. 96, p. 1419-1427.
- Li, Y. H., 1976, Denudation of Taiwan Island since the Pliocene Epoch: *Geology*, v. 4, p. 105-107.
- Liou, J. G., 1971, P-T stabilities of laumontite, wairakite, lawsonite, and related minerals in the system  $\text{CaAl}_2\text{Si}_2\text{O}_8\text{-SiO}_2\text{-H}_2\text{O}$ : *Journal of Petrology*, v. 12, p. 379-411.
- Massey, N. W. D., 1986, The Metchosis Igneous Complex, southern Vancouver Island; Ophiolite stratigraphy developed in an emergent island setting: *Geology*, v. 14, p. 602-605.
- Mattinson, J. M., 1972, Ages of zircons from the northern Cascade Mountains, Washington: *Geological Society of America Bulletin*, v. 83, p. 3769-3783.
- McLellan, R. D., 1924, The Devonian Orcas Group of Washington: *American Journal of Science*, v. 208, p. 217-222.
- , 1927, The geology of the San Juan Islands: Seattle, University of Washington Publication in Geology no. 2, 185 p.
- Miller, R. B., 1985, The ophiolitic Ingalls Complex, north-central Cascade Mountains, Washington: *Geological Society of America Bulletin*, v. 96, p. 27-42.
- Misch, P., 1966, Tectonic evolution of the northern Cascades of Washington State; A west-Cordilleran case history: *Canadian Institute of Mining and Metallurgy Special Volume 8*, p. 101-148.
- , 1971, Metamorphic facies types in North Cascades [abs.]: *Geological Association of Canada, Cordilleran Section Meeting, Program and Abstracts*, p. 22-23.
- , 1977, Bedrock geology of the North Cascades, in Brown, E. H., and Ellis, R. C., eds., *Geological excursions in the Pacific Northwest*: Bellingham, Western Washington University, p. 1-62.

- Miyashiro, A., 1975, Volcanic rock series and tectonic setting: *Annual Reviews of Earth and Planetary Sciences*, v. 3, p. 251-269.
- Miyashiro, A., and Shido, F., 1975, Tholeiitic and calc-alkalic series in relation to the behaviors of titanium, vanadium, chromium, and nickel: *American Journal of Science*, v. 275, p. 265-277.
- Monger, J.W.H., 1970, Hope map area, west half, British Columbia: *Geological Survey of Canada Paper* 69-47, 75 p.
- , 1977, Upper Paleozoic rocks of the western Canadian Cordillera and their bearing on Cordilleran evolution: *Canadian Journal of Earth Sciences*, v. 14, p. 1832-1859.
- , 1986, Geology between Harrison Lake and Fraser River, Hope map area, southwestern British Columbia: *Geological Survey of Canada, Paper* 86-1B, p. 699-706.
- Monger, J.W.H., and Berg, H. C., 1984, Lithotectonic terrane map of western Canada and southeastern Alaska, in Silberling, N.J., and Jones, D. L., eds., *Lithotectonic terrane maps of the North American Cordillera*: U.S. Geological Survey Open-File Report 84-523, Part B, scale 1:2,500,000.
- Monger, J.W.H., and Ross, C. A., 1971, Distribution of fusulinaceans in the western Canadian Cordillera: *Canadian Journal of Earth Sciences*, v. 8, p. 259-278.
- Monger, J.W.H., Price, R. A., and Tempelman-Kluit, D. J., 1982, Tectonic accretion and the origin of two major metamorphic and plutonic belts in the Canadian Cordillera: *Geology*, v. 10, p. 70-75.
- Mulcahey, M. T., 1975, The geology of Fidalgo Island and vicinity, Skagit County, Washington [M.S. thesis]: Seattle, University of Washington, 49 p.
- Muller, J. E., 1977, Evolution of the Pacific margin, Vancouver Island, and adjacent regions: *Canadian Journal of Earth Sciences*, v. 14, p. 2062-2085.
- , 1980, The Paleozoic Sicker Group of Vancouver Island, British Columbia: *Geological Survey of Canada Paper* 79-30, 23 p.
- , 1983, Geology, Victoria, British Columbia: *Geological Survey of Canada Map* 1553A, scale 1:100,000.
- Muller, J. E., and Jeletsky, J. A., 1970, Geology of the Upper Cretaceous Nanaimo Group, Vancouver Island and Gulf Islands, British Columbia: *Geological Survey of Canada Paper* 69-27, 77 p.
- Muller, J. E., Northcote, K. E., and Carlisle, D., 1974, Geology and mineral deposits of Alert-Cape Scott map area, Vancouver Island, British Columbia: *Geological Survey of Canada Paper* 74-8, 77 p.
- Muller, J. E., Cameron, B.E.B., and Northcote, K. E., 1981, Geology and mineral deposits of Nootka Sound map area, Vancouver Island, British Columbia: *Geological Survey of Canada Paper* 80-16, 53 p.
- Mutti, E., and Ricci-Lucchi, F., 1978, Turbidites of the northern Apennines; Introduction to facies analysis: *International Geological Review*, v. 20, p. 125-166 (English translation from original Italian paper published in 1972).
- Newton, R. C., Goldsmith, J. R., and Smith, J. V., 1969, Aragonite crystallization from strained calcite at reduced pressures and its bearing on aragonite in low-grade metamorphism: *Contributions to Mineralogy and Petrology*, v. 22, p. 335-348.
- Nitsch, K. H., 1968, Die stabilität von lawsonit: *Naturwissenschaften*, v. 55, p. 388.
- North American Commission of Stratigraphic Nomenclature, 1983, North American stratigraphic code: *American Association of Petroleum Geologists Bulletin*, v. 67, p. 841-875.
- Pacht, J. A., 1984, Petrologic evolution and paleogeography of the Late Cretaceous Nanaimo Basin, Washington and British Columbia; Implications for Cretaceous tectonics: *Geological Society of America Bulletin*, v. 95, p. 766-778.
- Page, B. M., 1982, Migration of Salinian composite block, California, and disappearance of fragments: *American Journal of Science*, v. 282, p. 1694-1734.
- Paterson, I. A., and Harakal, J. E., 1974, Potassium-argon dating of blueschists from Pinchi Lake, central British Columbia: *Canadian Journal of Earth Sciences*, v. 11, p. 1007-1011.
- Pearce, J. A., 1975, Basalt geochemistry used to investigate past tectonic environments on Cyprus: *Tectonophysics*, v. 25, p. 41-67.
- Pearce, J. A., and Cann, J. R., 1971, Ophiolite origin investigated by discriminant analysis using Ti, Zr, and Y: *Earth and Planetary Science Letters*, v. 12, p. 339-349.
- , 1973, Tectonic setting of basic volcanic rocks determined using trace element analyses: *Earth and Planetary Science Letters*, v. 19, p. 290-300.
- Perkins, D., III, Westrum, E. F., Jr., and Essene, E. J., 1980, The thermodynamic properties and phase relations of some minerals in the system CaO-Al<sub>2</sub>O<sub>3</sub>-SiO<sub>2</sub>-H<sub>2</sub>O: *Geochimica et Cosmochimica Acta*, v. 44, p. 61-84.
- Pessagno, E. A., Jr., Blome, C. D., and Longoria, J. F., 1984, A revised radiolarian zonation for the Upper Jurassic of western North America: *Bulletins of American Paleontology*, v. 87, no. 320, 51 p.
- Pitcher, W. S., 1982, Granite type and tectonic environment, in Hsü, K. J., ed., *Mountain building processes*: New York, Academic Press, p. 19-40.
- Potter, C. J., 1983, Geology of the Bridge River Complex, southern Shulaps Range, British Columbia; A record of Mesozoic convergent tectonics: Seattle, University of Washington, 192 p.
- Ray, G. E., 1986, The Hozameen fault system and related Coquihalla serpentine belt of southwestern British Columbia: *Canadian Journal of Earth Sciences*, v. 23, p. 1022-1041.
- Ross, C. A., 1967, Development of fusulinid (Foraminifera) faunal realms: *Journal of Paleontology*, v. 41, p. 1341-1354.
- , 1979, Late Paleozoic collision of North and South America: *Geology*, v. 7, p. 41-44.
- Rusmore, M. E., and Cowan, D. S., 1985, Jurassic-Cretaceous rock units along the southern edge of the Wrangellia terrane on Vancouver Island: *Canadian Journal of Earth Sciences*, v. 22, p. 1223-1232.
- Saleeby, J. B., 1983, Accretionary tectonics of the North American Cordillera: *Annual Reviews of Earth and Planetary Sciences*, v. 15, p. 45-73.
- Savage, N. M., 1983a, Late Triassic (Karnian) conodonts from northern San Juan Island, Washington: *Journal of Paleontology*, v. 57, p. 804-808.
- , 1983b, Late Triassic (Karnian to Norian) conodonts from Orcas Island, northwest Washington: *Journal of Paleontology*, v. 57, p. 870-872.
- , 1984, Devonian conodonts from Jones Island, northwest Washington: *Canadian Journal of Earth Sciences*, v. 21, p. 1339-1343.
- Schweickert, R. A., 1981, Tectonic evolution of the Sierra Nevada Range, in Ernst, W. G., ed., *The geotectonic development of California*: Englewood Cliffs, New Jersey, Prentice-Hall, Inc., p. 87-131.
- Shapiro, L., 1975, Rapid analysis of silicate, carbonate, and phosphate rocks; Revised edition: U.S. Geological Survey Bulletin 1401, 76 p.
- Shervais, J. W., 1982, Ti-V plots and the petrogenesis of modern and ophiolitic lavas: *Earth and Planetary Science Letters*, v. 59, p. 101-118.
- Shervais, J. W., and Kimbrough, D. L., 1985, Geochemical evidence for the tectonic setting of the Coast Range ophiolite; A composite island arc-oceanic crust terrane in western California: *Geology*, v. 13, p. 35-38.
- Sliter, W. V., 1984, Foraminifers from Cretaceous limestone of the Franciscan Complex, northern California, in Blake, M. C., Jr., ed., *Franciscan geology of northern California*: Society of Economic Paleontologists and Mineralogists, Pacific Section, v. 43, p. 149-162.
- Stevenson, A. J., Scholl, D. W., and Vallier, T. L., 1983, Tectonic and geologic implications of the Zodiac fan, Aleutian Abyssal Plain, northeast Pacific: *Geological Society of America Bulletin*, v. 94, p. 259-273.
- Stewart, R. J., and Page, R. J., 1974, Zeolite facies metamorphism of the Late Cretaceous Nanaimo Group, Vancouver Island and Gulf Islands, British Columbia: *Canadian Journal of Earth Sciences*, v. 11, p. 280-284.
- Strecheisen, A. L. (chairman), 1973, Plutonic rocks; Classification and nomenclature recommended by the IUGS Subcommission on the Systematics of Igneous Rocks: *Geotimes*, October, p. 26-30.
- Suppe, J., 1981, Mechanics of mountain building and metamorphism in Taiwan: *Geological Society of China Memoir* 4, p. 67-89.
- Sutherland Brown, A., 1968, Geology of the Queen Charlotte Islands, British Columbia: British Columbia Department of Mines and Petroleum Resources Bulletin 54, 226 p.
- Tabor, R. W., and Cady, W. M., 1978, The structure of the Olympic Mountains, Washington; Analysis of a subduction zone: U.S. Geological Survey Profes-

- sional Paper 1033, 38 p.
- Tipper, H. W., Woodsworth, G. J., and Gabrielse, H., 1981, Tectonic assemblage map of the Canadian Cordillera and adjacent parts of the United States of America: Geological Survey of Canada Map 1505A, scale 1:2,000,000.
- Vallier, T. L., Brooks, H. C., and Thayer, T. P., 1977, Paleozoic rocks of eastern Oregon and western Idaho, in Howell, D. G., and McDougall, K. A., eds., Paleozoic paleogeography of the western United States: Society of Economic Paleontologists and Mineralogists, Pacific Section, p. 455-466.
- Vance, J. A., 1968, Metamorphic aragonite in the prehnite-pumpellyite facies, northwest Washington: American Journal of Science, v. 266, p. 299-315.
- , 1975, Bedrock geology of San Juan County, in Russell, R. H., ed., Geology and water resources of the San Juan Islands: Washington Department of Ecology Water Supply Bulletin 46, p. 3-19.
- , 1977, The stratigraphy and structure of Orcas Island, San Juan Islands, in Brown, E. H., and Ellis, R. C., eds., Geological excursions in the Pacific Northwest: Bellingham, Western Washington University, p. 170-203.
- Vance, J. A., Dungan, M. A., Blanchard, D. P., and Rhodes, J. A., 1980, Tectonic setting and trace element geochemistry of Mesozoic ophiolitic rocks in western Washington: American Journal of Science, v. 280-A, p. 359-388.
- von Huene, R., 1984, Tectonic processes along the front of modern convergent margins; Research of the past decade: Annual Reviews of Earth and Planetary Sciences, v. 12, p. 359-381.
- Ward, P. D., 1978, Revisions to the stratigraphy and biochronology of the Upper Cretaceous Nanaimo Group, British Columbia and Washington State: Canadian Journal of Earth Sciences, v. 15, p. 405-423.
- Ward, P. D., and Stanley, K. O., 1982, The Haslam Formation; A late Santonian-early Campanian forearc basin deposit in the Insular Belt of southwestern British Columbia and adjacent Washington: Journal of Sedimentary Petrology, v. 52, p. 975-990.
- Ward, P. D., Verosub, K. L., and Haggart, J. W., 1983, Marine magnetic anomaly 33-34 identified in the Upper Cretaceous Great Valley Sequence of California: Geology, v. 11, p. 90-93.
- Whetten, J. T., 1975, The geology of the southeastern San Juan Islands, in Russell, R. H., ed., Geology and water resources of the San Juan Islands: Washington Department of Ecology Water Supply Bulletin 46, p. 341-357.
- Whetten, J. T., Jones, D. L., Cowan, D. S., and Zartman, R. E., 1978, Ages of Mesozoic terranes in the San Juan Islands, Washington, in Howell, D. G., and McDougall, K. A., eds., Mesozoic paleogeography of the western United States: Society of Economic Paleontologists and Mineralogists, Pacific Section, p. 117-132.
- Whetten, J. T., Zartman, R. E., Blakely, R. J., and Jones, D. L., 1980, Allochthonous Jurassic ophiolite in northwest Washington: Geological Society of America Bulletin, Part I, v. 91, p. 359-368.
- Whetten, J. T., Gower, H. D., Carroll, P. R., and Brown, E. H., 1987, Bedrock geologic map of the Port Townsend Quadrangle, Washington: U.S. Geological Survey Miscellaneous Investigations Series Map 1-1198G, scale 1:100,000 (in press).
- Wilson, M., and Davidson, J. P., 1984, The relative roles of crust and upper mantle in the generation of oceanic island arc magmas: Philosophical Transactions of the Royal Society of London, Series A, v. 310, p. 667-674.
- Woodsworth, G. J., 1979, Metamorphism, deformation, and plutonism in the Mount Raleigh pendant, Coast Mountains, British Columbia: Geological Survey Bulletin 295, 58 p.
- Wright, J. E., 1982, Permo-Triassic accretionary subduction complex, southwestern Klamath Mountains, Northern California: Journal of Geophysical Research, v. 87, p. 3805-3818.
- Yule, R. W., and Irving, E., 1980, Displacement of Vancouver Island; Paleomagnetic evidence from the Karmutsen Formation: Canadian Journal of Earth Sciences, v. 17, p. 1210-1228.

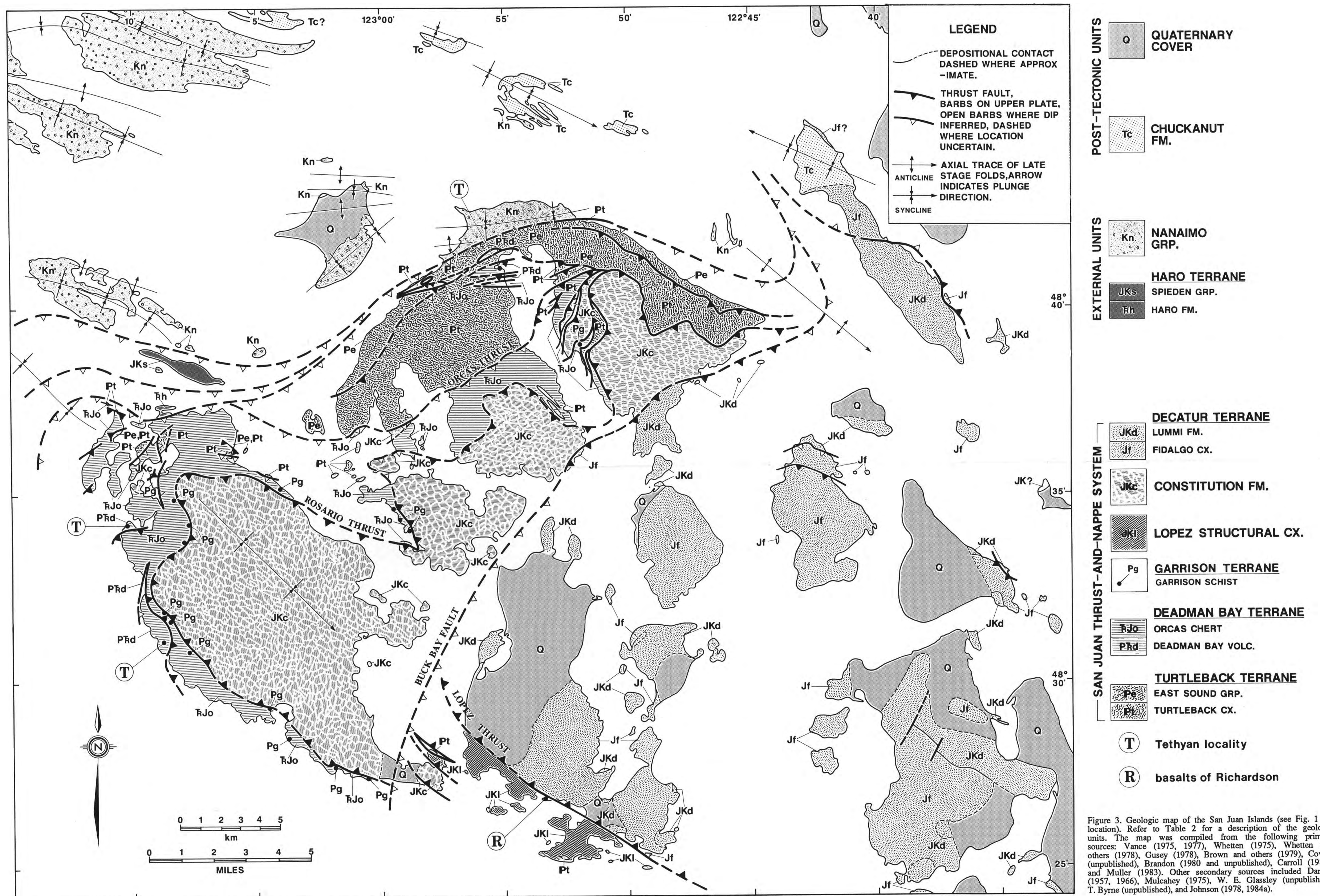


Figure 3. Geologic map of the San Juan Islands (see Fig. 1 for location). Refer to Table 2 for a description of the geologic units. The map was compiled from the following primary sources: Vance (1975, 1977), Whetten (1975), Whetten and others (1978), Gusey (1978), Brown and others (1979), Cowan (unpublished), Brandon (1980 and unpublished), Carroll (1980), and Muller (1983). Other secondary sources included Danner (1957, 1966), Mulcahey (1975), W. E. Glassley (unpublished), T. Byrne (unpublished), and Johnson (1978, 1984a).